Abstract

WANG, ZHIJIAN. A Dual Measurement System for Radioactive Tracer Pebble Tracking in PBRs. (Under direction of Professor Robin P. Gardner.)

The pebble motion measurements are needed to validate the dynamic simulations that are necessary for pebble bed reactor core burn up calculations and critical safety analysis. To date, the relevant data is limited, and particularly in the expected environmental high temperature condition is almost non-existent.

A dual measurement system that has been developed includes one system that has three collimated detectors that can be moved to determine the maximum counting rates in the height and two horizontal positions to determine the position of the radioactive tracer pebble. A parabolic interpolation of the last three measurements is used that include a maximum counting rate. The measurement is moving with increasing counting rate until a decreasing counting rate is obtained. This system can only measure the position of one slowly moving tracer pebble at a time, but is fast enough for pebble motion in Pebble Bed Reactor (PBR).

A patch was developed into MCNP5 to generate DRF's with a significant accuracy and efficiency improvements for gamma ray up to energy of 3.1 Mev. This approach accounts for NaI scintillation efficiency nonlinearity and the variable flat continua part of the DRF's with a speed-up feature with a factor up to 200. This accurate and efficient generator just makes some cases of Monte Carlo Library Least Square (MCLLS) method

for inverse analysis for parameters which are sensitive to gamma ray spectrum possible. With this DRF's generator from modified MCNP5, a new multiple radioactive particles tracking system with only six 2"X2" NaI un-collimated detectors system was developed and used to study the pebble flow pattern in a modeling PBR, working with the benchmark purpose collimated detectors system.

A Dual Measurement System for Radioactive Tracer Pebble Tracking in PBRs

by
Zhijian Wang

A dissertation submitted to the Graduate Faculty of
North Carolina State University
in partial fulfillment of the
requirements for the Degree of
Doctor of Philosophy

Nuclear Engineering

Raleigh, North Carolina

2011

APPROVED BY：

_____	_____
Dr. Yousry Y. Azmy	Dr. Man-Sung Yim
_____	_____
Prof. Peter Bloomfield	Prof. Robin P. Gardner, Chair

BIOGRAPHY

Zhijian Wang was born as the last kid of five in his family in April 4, 1977. His first name in Chinese “zhi” means “wisdom”, and “jian” means “healthy”. He has three sisters and one brother. His father is Wang Kangrong, and his mother is Zhou er. Zhanjiang, Guangdong, China is his hometown.

Zhijian graduated from Fudan University in Shanghai in 1999, received his Science Bachelor’s Degree from Department of Materials Science. His thesis was about the mechanics of the boundary diffusion of crystals, under supervision of Dr. Jin Li.

After his graduation, he entered the China Customs through a nationwide qualify exam, and one year later, in 2000, he was selected with full funding support to continue his study in Tsinghua University in Beijing. He received his second Bachelor’s Degree in Engineering from the Engineering Physics Department in 2002. His thesis was about the optimization of the linear electron accelerator system for x-ray source in cargo monitor. His advisor was Prof. Dechun Tong.

He serviced in the China Customs in Guangdong for two and half years for a new arrangement of cargo monitor system after graduated from Tsinghua University, and resigned in 2005. He worked as a journalist in Shanghai Education Television Station for

two months and as an assistant manager in a public relationship company Zenith for three months before his arrival to USA.

He began his graduate study in the Nuclear Engineering Department at North Carolina State University from fall, 2005, worked as a research assistant under Prof. Robin P. Gardner's advisory.

Zhijian married with Xia Cai in Dec. 2005. His son Cuntas Wang was born in Oct. 2010.

ACKNOWLEDGEMENTS

First of all, I am deeply grateful to the chair of my advisory committee - Dr Robin P. Gardner with my full heart. He not only shared his insight understanding in the area of our research which guided me through this work, but also set me a model of researcher with enthusiasm which will guide me in the future.

I would also like to extend my warmest thanks to other members of my committee: DR. Yousry Y. Azmy, Dr. Man-Sung Yim, Dr. Peter Bloomfield and Dr. Charles Proctor for helping me to achieve such an important milestone in my life. Appreciation is also extended to other professors and staff in the Department of Nuclear Engineering.

I would like to express my special thanks to previous colleagues: Dr. Xiaogang Han, Libai Xu, Fusheng Li, Dr. Xuanyun Ai and Huawei Yu for their sincere help and support, and of course, to our team members in CEAR especially to: Jiaxin Wang, Kyoung O. Lee, and Adan Calderon as well. I am also grateful for the NERIC Contract from DOE for financial support.

Finally, my parents are my sources of strength; my sister Jinglan is all about love; my brother Zhichun is all about encouragement and ambition to me; and my wife Xia and my son Cuntas are my sources of happiness.

TABLE OF CONTENTS

LIST OF FIGURES……..……..viii

LIST OF TABLES……...…...xii

1 INTRODUCTION…….……..1

1.1 Overview…….…..…1

1.2 Pebble Bed Reactor (PBR)……...…4

1.3 Pertinent Radiation detection and measurement techniques ……...…7

2 TECHNOLOGY REVIEWS FOR PARTICLE TRACKING RELATED TO PBRs……...……10

3 **COLLIMATED DETECTORS SYSTEM**……....…….15

3.1 Theory of collimated detectors system ……..…..….15

3.2 Experimental arrangement……...…….17

3.3 System optimization…….....20

3.4 Electronics and Software I……..…..….23

3.5 Scanning technique……..…...26

4 **THE MODELING SCALED PEBBLE BED REACTOR**……...…28

4.1 Vessel……...…...30

4.2 Pebbles…….…….…32

4.3 Pebble packing……..…....33

4.4 Extractor and pebble flow rate…….34

4.5 Radioactive Particles……..…….....34

5 **EXPERIMENTS AND RESULTS I**……..…….....36

5.1 Benchmark experimental results…….……..36

5.2 Experimental results with PBR…….……37

6 **UN-COLLIMATED DETECTOR SYSTEM**…….……40

6.1 Overview……...……....40

6.2 Development of DRF's in MCNP5…….……...…44

6.3 Monte Carlo Library Least Squares approach…….…...…..58

6.4 Un-collimated detectors system arrangements……....……..63

6.4.1 Detectors and configuration……..…….……63

6.4.2 Electronics and software II……..……..….63

7 **EXPERIMENTS AND RESULTS II**……..…….....…71

7.1 Benchmark experimental results……..……..…...71

7.2 Particle tracking testing……...……79

7.2.1 The testing experimental results for single particle……..……82

7.2.2 The testing experimental results for two particles ....…….....86

7.3 Particle tracking experiments and results……..90

7.3.1 Experiment description……....…90

7.3.2 The arrangement of the library packages……....96

7.3.3 The analysis for the position for the positions of the sources……..…98

7.3.4 The experiment results.……....100

7.4 Summary……..110

8 **RELATED CRITICAL TOPICS**……...113

8.1 The safety feature of PBR……..……..113

8.2 Spectrum stripping……...……115

8.3 Dead time……..……118

8.4 Peak analysis by PEAKSI……119

8.5 Variance reduction techniques……..…122

8.5.1 Weight window…….……122

8.5.2 Energy cutoff……...….123

8.5.3 Correlated Sampling…….....124

8.6 Computer cluster……..128

9 **CONCLUSIONS AND DISCUSSION**……...…129

10 **FUTURE WORKS**……....131

11 **REFERENCES**…….....133

LIST OF FIGURES

Figure 1.1 Nuclear Reactors worldwide……..…….4

Figure 1.2 Generations of Reactors…….….5

Figure 1.3 Common PBR and pebble fuel design……7

Figure 2.1 Gatt's Experimental arrangements……..……11

Figure 2.2 Gatt's Particle Tracking System……..….12

Figure 2.3 Visible Tracking in MIT……..…….13

Figure 2.4 Top view (left) and Longitudinal view of 3D Exp.....14

Figure 3.1 Detector responses as a function of the angular position of the detector…….17

Figure 3.2 Configuration of the detectors for collimated detectors system…….…....18

Figure 3.3 X, Y Measurement System……..…....18

Figure 3.4 A schematic of the slot opening portion of the collimator……...……20

Figure 3.5 A comparison between responses of two different sets of collimators…...….22

Figure 3.6 Component of the collimated system hard wares…….……...…24

Figure 3.7 Flow Chart of Automatic Control……..…….27

Figure 4.1 Detective areas for center detector…….…….31

Figure 4.2 Modeling PBR design…….……..…….…..32

Figure 5.1 A comparison of the predetermined and measured positions……..…….36

Figure 5.2 Single particle tracking with collimated detectors system.....…...38

Figure 6.1 Mass attenuation for Si.....…..42

Figure 6.2 NaI scintillation efficiency nonlinearity……...…...46

Figure 6.3 Cs137 Benchmark Results……...…….…...48

Figure 6.4 S37 for nonlinearity benchmark results…….….51

Figure 6.5 Heath Experimental arrangements…….…52

Figure 6.6 Geometrical in put in MCNP5 for Heath experiments…….…..…52

Figure 6.7 the Cs137 for efficiency in MCNP5.....…...56

Figure 6.8 Cubic cells Library……...59

Figure 6.9 Illustration of the spectrum stripping deconvolution of multiple radioactive particles……...……..……61

Figure 6.10 Comparison for NaI and BGO for Resolution and Sensitivity……....……64

Figure 6.11 Effect of Size of Resolution and Sensitivity……..……..……66

Figure 6.12 Peak-to-total Ratio for Various Sizes Detectors……..……..67

Figure 6.13 Motion plane ABCDEF…….…….……..…..68

Figure 6.14 Un-collimated detectors tracking system.....…...69

Figure 6.15 Electronics set up for un-collimated detectors system.....…...70

Figure 6.16 Electronics flow chart in un-collimated detectors system……..……..70

Figure 7.1 The lead shielding cave with detector; the details of the 2”X2”NaI detector..72

Figure 7.2 Cs137 benchmark experiment for 2”X2 NaI in Cave…….….73

Figure 7.3 The MCNP5 input plot in simulation.....…...74

Figure 7.4 Cs 137 benchmark experiment in PBR……..…….76

Figure 7.5 Benchmark results for detectors #4 and #5……....…….78

Figure 7.6 Square elements for libraries……..……..80

Figure 7.7 Square element libraries relationship……81

Figure 7.8 Triangular elements…….……..……82

Figure 7.9 Elements in testing experiment.....…...84

Figure 7.10 Multiple Source spectra with Cs137 and Co60……..…87

Figure 7.11 Spectrum for multiple source treating process.....…...88

Figure 7.12 The fitting results of Co60…….……...…….89

Figure 7.13 Measurement examples for "Cs1301" The total view……...……92

Figure 7.14 Spatial configuration of library…….....…….97

Figure 7.15 Down ward searching schemes…….....……99

Figure 7.16 Initial guess and regions……..……..101

Figure 7.17 Output information for position search…….…….…..102

Figure 7.18 Fitting results Vs measured spectrum……...…104

Figure 7.19 Residual plot of fitting…….……..…104

Figure 7.20 Pebble paths plot.....105

Figure 7.21 Multiple tracking with Cs137 and Co60…….……....…106

Figure 7.22 Dual measurement system comparisons…….…....107

Figure 7.23 The motion fluctuation at -11cm off axis……..……109

Figure 7.24 The rotation effect of the detector…….....…...111

Figure 7.25 Library error effect……...……111

Figure 8.1 Peak behaviors with nonlinearity with Cs137……....120

Figure 8.2 PEAKSI and maximum point for peak channel with Cs137……..……121

Figure 8.3 The Energy cut off effects Cs137 in detector #4……124

LIST OF TABLES

Table 4.1 Nature of the Problem for modeling PBR…….……35

Table 6.1 The flat continua factors…….……...49

Table 6.2 Speed-up methods efficiency.....…...56

Table 7.1 The side length of square elements……80

Table 7.2 The search of the minimum Chi-square…….83

Table 7.3 The searching results with original MCNP5”…….....86

Table 7.4 Iterations depended on off axis position for Cs137……...…….96

Table 7.5 The interpretation of the output…….…...103

INTRODUCTION

1.1 Overview

Multiphase flow systems involving two or more phases are common in areas from the processing of fuels and chemicals to the production of foods, and specialty materials. Despite widely used, the multiphase systems were designed largely by intuition and rule of thumb rather than on first principles. The main reason for this state of affairs is that the local flow structure is extremely complex and the link between the micro and macro-scale has not been clearly established. The lack of detailed structural and dynamic information at micro-scale, and the mathematical difficulties associated with the methods for handling the randomness of the multiphase materials are the prime reasons for the inability to treat these flows purely from a theoretical aspect. Successfully modeling the complex flows requires reliable data, which in turn depends on the implementation of sophisticated measuring techniques capable of non-invasive investigation and the ability to provide the required information over the entire region of interest. The data of the flow pattern of the multiphase systems are crucial in order to establish the models for computational fluid dynamics, residence time distribution, flow characterization etc., and would finally used to develop an optimal system design.

Engineers very early realized the merits of using nuclear radiations for probing and

measuring the process characteristics non-invasively. There are two major advantages of using nuclear methods. One is the strong penetrating ability of the nuclear radiations-high energy photons from X-ray to Gamma ray, and neutron. Other fact is the characteristic features of nuclear radiations-X-ray fluorescence and neutron prompt gamma ray.

In a Pebble Bed Reactor (PBR), spherical fueled pebbles enter at the top of the reactor vessel and pass through the bed and out through the base of the vessel via an extractor. The reactor is cooled by an inert or semi-inert gas such as helium, nitrogen or carbon dioxide. PBR is a typical multiphase system. Pebble pathway and relative velocity are of special importance to the basic reactor design calculations, optimization of fuel cycle and burn-up calculation, core operation simulation and safety analysis. The extreme case would be the permanent fixation of a given pebble or group of pebbles in a region of the vessel which could result in severe irradiation and thermal damage to the pebble with possible leaking of fission products.

To track the fueled pebbles in the real PBR is impossible. The large scale and safety shielding materials of PBR make the radioactive particles informatively un-measurable. And the homogeneous fueled pebbles cannot be indentified by the outside detectors. The most feasible experimental technique for accurate flow characterization and studying the dynamics of the pebbles in a PBR is to tracking pebbles in a simulated scaled PBR. In this case the simulated pebbles would be dummy (without fuel), and one or several pebbles

that under studying would be tagged with radiotracers.

The research in scaled down PBR for tracking the pebble motion is also very limited. In early 1970's Gatt (1970, 1972, 1973) proposed and test a three collimated detectors method in tracking a single tracer particle in the scaled down PBR. But his experiment was not automatic tracking; the searching of the particle was highly depended on the fact that you have already known where the particle rough is before hand. The most recent methods were proposed by Andrew C. Kadak and Martin Z. Bazant (2004) offering a half model method which used a method of visible tracking on a plane cut cross the axis of the modeling PBR. They also used two collimated detectors in verifying the tracer pebble motion in a streamline in the upper area in the PBR which technically is not a real tracking. These two experiments will be reviewed in details in Chapter 2.

In this dissertation, the author provided a dual measurement system with a collimated detectors system and an un-collimated detectors system to track the radioactive tracer pebbles in a scaled down modeling PBR. The focus in this research is the development of new feasible tracking methods for pebble tracking in PBR.

1.2 Pebble bed reactor

Electricity was generated for the first time by a nuclear reactor on Dec., 20, 1951 at

the experimental station near Arco Idaho, which initially produced about 100KW. Today, about 14% of the world electricity comes from nuclear power. There are 436 reactors operating in 31 countries and areas around the world (IAEA, 2000):

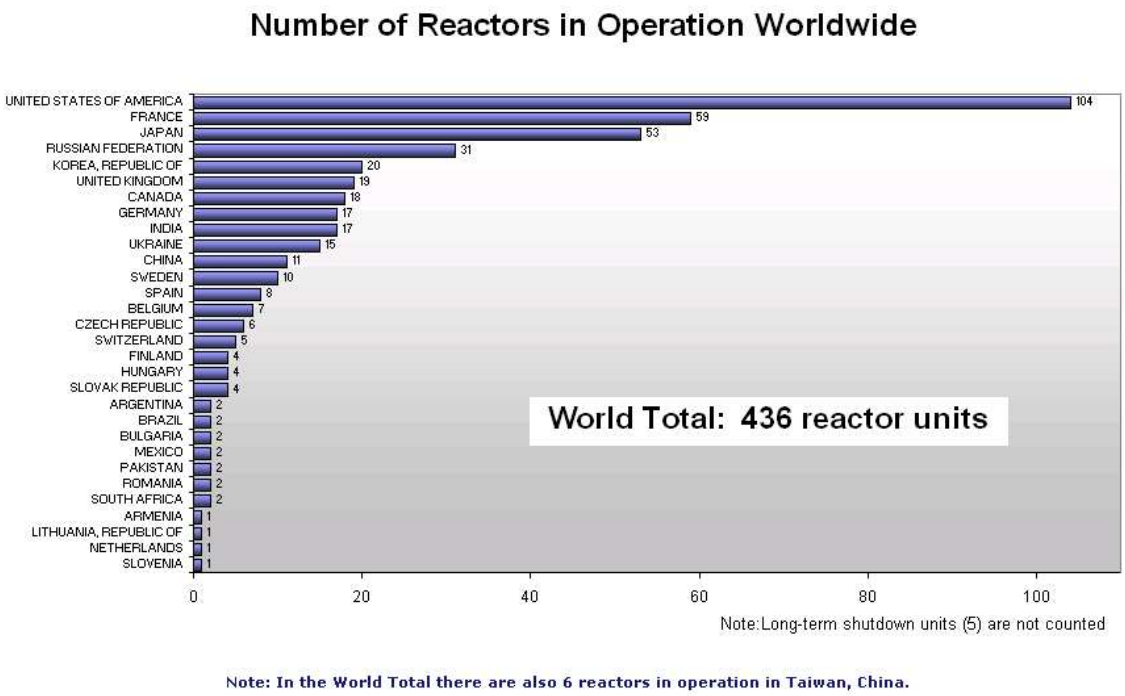

Figure 1.1 Nuclear Reactors worldwide

Yet, debates on nuclear power never stop. Arguments of economics and safety are used by both sides of the debates. In the United States the outcome of the debates is that no new nuclear reactor has been constructed from 1980s. Why? Among the 104 operating reactors in the United States, 69 units are "Pressurized Water Reactors (PWRs), the other 35 are "Boiling Water Reactors (BWRs). They are both falling into the category of Generation II power reactors.

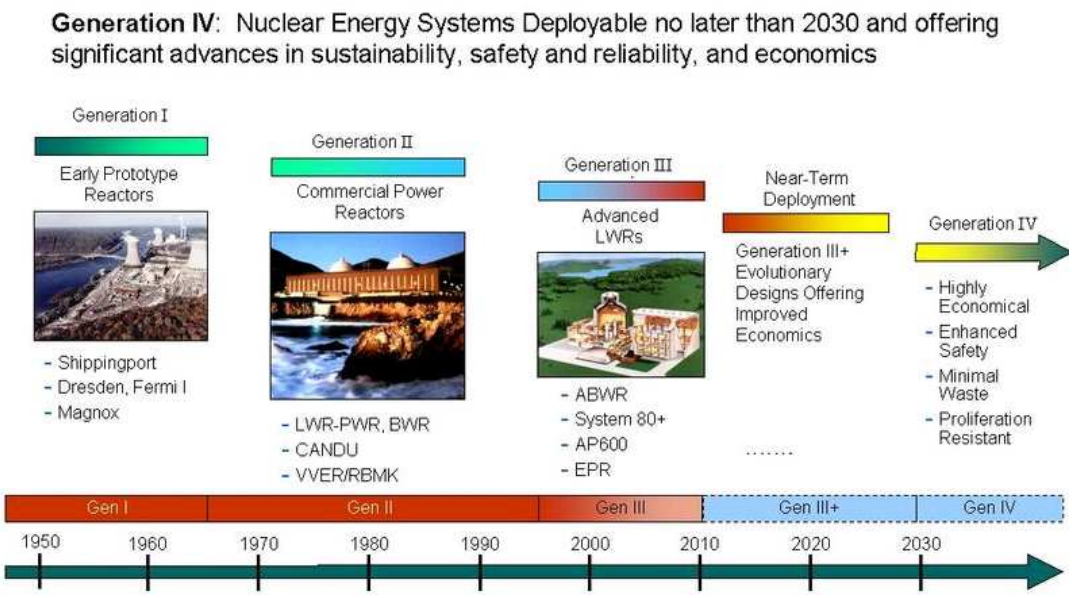

Figure 1.2 Generations of Reactors

The shortcomings that limit their desirability as the type of nuclear plant for the future are: the size and complexity of the various integrated support systems which have driven up capital costs, staffing requirements and regulatory requirement. And the high demand for management attention is a serious deterrent to new orders.

The generation IV reactor, especially the Pebble Bed Reactor (PBR) is believed would be the trigger for a "renaissance" of the nuclear power. Pebble Bed Reactor, or called Pebble Bed Modular Reactor (PBMR), is one type of the High Temperature Gas-cooled Reactor (HTGR), which uses helium gas as coolant. The main unique feature of PBR is the pebble-like fuel flowing from the top of the container core and exiting from the bottom. In Jan. 1998, MIT, A project targeted on the possible future nuclear power plant

design advised by Ronald Ballinger and Andrew Kadak (2004) reviewed eight likely options:

1. Westinghouse AP600 advanced pressurized Light Water Reactor. (LWR)
2. ABB System 80+ LWR
3. GE Advanced Boiling Water Reactor (ABWR)
4. General Atomics High Temperature Gas Reactor (HTGR)
5. German AVR pilot Pebble Bed Reactor (PBR)
6. Lead bismuth reactor
7. Thorium breeder reactor
8. Liquid metal breeder reactor

Their evaluation process considered 26 criteria such as safety, economics, construction time, modularity, efficiency, and life time. The process selected the small, modular PBR. Here are some unique features the PBR identified: inherent safety, high efficiency, short construction time, small size, etc.

PBR is one type of VHTR, named after its unique core design. The 6cm diameter pebble-like fuels are filled in the core to reach the critical volume. It works in a simple pattern that fuel pebbles flow through the core from the top to the bottom, shown in Figure 2.1:

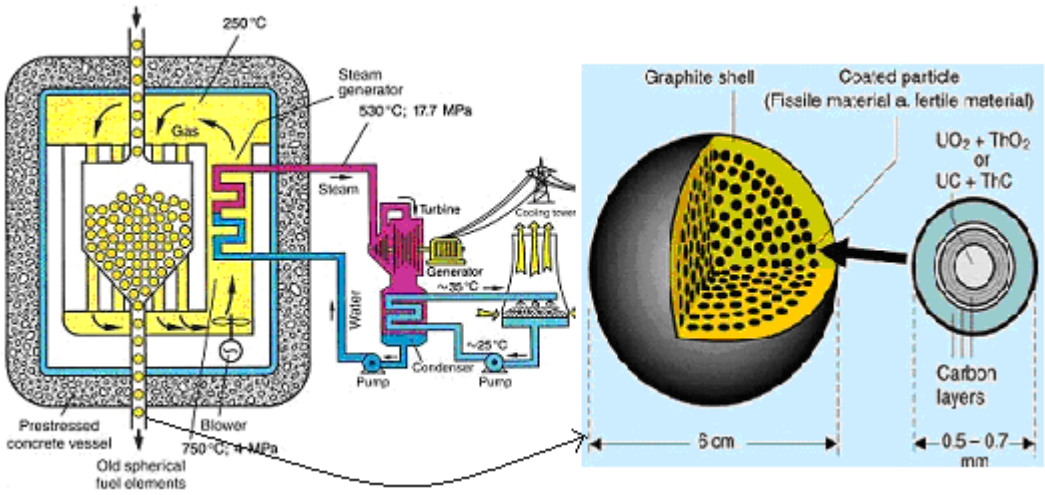

Figure 1.3 Common PBR and pebble fuel design

In 1950's Rudolf Schulten initially came up with the PBR ideas in Germany. Later on, testing reactors AVR and THTR PBRs were built and operated in Germany in the 1960's and 1980's (AGE 1990). Currently there are several countries around the world active in PBR research: the test reactor HTTR in Japan (Takakazu, 2005); the test reactor HTR-10 in China (Yuliang 2007); PBMR at South Africa (Closed Sep. 2010); the US Energy Policy Act of 2005 authorizing $1.25 billion on PBR project.

1.3 Radiation detection and measurement techniques in CEAR

One of the most important critical parameters is the pebble motion in the core, which will direct the core's design and heat distribution. In order to acquire this information for PBR, The researches are done for the existed and under developing model PBR, and a

modeling PBR is built in a size within the tracking system's capability. This modeling PBR has the capability of self-standing, automatically recycling features.

Radiation detection technique is long term developed in the Center of Applications of Radioisotopes (CEAR) in Nuclear Engineering department of North Carolina State University back to very early 1960's. Recently a 3D Single Particle Tracking (SPT) system was developed in CEAR, which used three collimated NaI detectors on a moving plate to locate the position of a radiation particle (Ashraf, 2005). This system was verified in very slow motion case. As the pebble flow in the PBR is comparably slow, this system is suitably used for studying the motion of the pebbles in the PBR.

CEAR pioneers in the area of Detector Response Functions (DRF's). Monte Carlo-Library Least Squares (MCLLS) approach is a very powerful method in inverse analysis with DRF's, which was successfully applied in Prompt Gamma Neutron Activation Analysis (PGNAA) (Han, 2006) and Energy-Dispersive X-ray Fluorescence (EDXRF) (Li, 2008). The author has initially developed an accurate DRF's from the general-purpose Monte Carlo simulation code which was developed at the Los Alamos National Lab. This new version of MCNP5 takes into account of the flat continua and scintillation detector's efficiency nonlinearity. And for the first time that the MCLLS method was used to inverse analyze the positions of the sources.

Some other detail supporting techniques turned out to be very critical via the

development of the dual measurement system. For example, the PEAKSI technique used in determining the exact peak channel; the Gaussian broadening factors decided from the experiments; the measuring spectrum peak drifting phenomenon and understanding; The spectrum stripping technique used in measured spectrum and analysis processing spectrum; the comprehensive techniques used in Monte Carlo simulating process, etc. all these techniques are important in improving the accuracy of the measurement of the system. Some of them just make this system feasible.

2. TECHNOLOGY REVIEWS FOR PARTICLES TRACKING RELATED TO PBR

Leesment and Stephenson (1964), Deutsch (1967), Szomanski and Tingate (1967) found that the recirculation rates had not significant affect on the pebble flow pattern in

certain range. This range can be one per two minutes to 50,000 per minute.

From late 1960's to early 1970's F.C. Gatt (1968, 1970, 1972, and 1973) carried out a comprehensive experiment to study the behaviors of the pebbles while passing through the vessel. The experiment focus on the effect of the changing conditions:

1) base angle
2) base shape
3) extractor position
4) pebble diameter
5) pebble shape
6) pebble specific gravity
7) pebble bed height, and
8) the radius position of the pebble

Diameters of 1.0 and 0.75 in. pebbles were studied in a 30 in. diameter, 60 in. height cylindrical vessel with core angle varying in 15, 25, 35, and 45 degrees respectively. The interested pebbles were marked in the experiment, so, no detectors were involved. The experiments described in Figure 2.1:

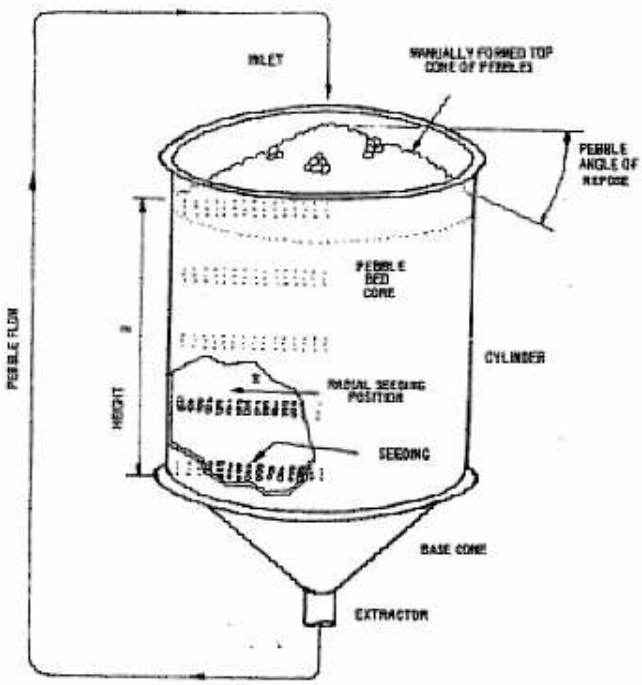

Figure 2.1 Gatt's Experimental Set-up

Gatt reported that the optimum reactor configuration for these sizes of pebbles is 27.5 in. in height and 25 or 45 degrees for conical base angle. The optimum condition is the minimum transit number (a variable indicates how fast the pebbles passing through the vessel) mean and standard deviation.

Later after the previous experiment Gatt continued his research in this area by using a tracking system to study the individual pebble flow path. Three collimated detectors were mounted on a platform whose height could be varied. The axial detector is used to establish the vertical position of the radiation pebble (Co60 tagged), and then the outer pairs rotate until both are aligned with it. Its location is then defined by the height of the

platform and the angular positions of the outer detectors:

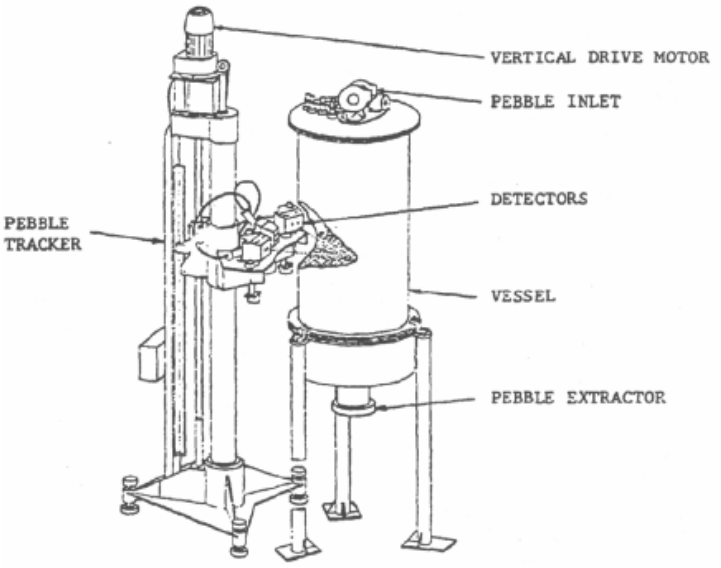

Figure 2.2 Gatt's Particle Tracking System

Very little interference or crossing between pebble path were reported, and very little or no effect of the extractor on the pebble motion as well. But the automatic controlling and data recording capability heavily limit the tracking ability. It is not able for real time tracking and position reporting.

Andrew C. Kadak and Martin Z. Bazant (2004) conducted a series of one-to-ten-scale of the real reactor experiments to study the pebble flow in the core of the PBR. They used 6mm diameter plastic pebble, cylindrical container with 28.cm in diameter and 81cm in height. The tracking techniques are visible and invisible with detectors. In the visible one they used half-model with a transparent plane, and then hand recorded the positions of the

pebbles or recorded the marked pebbles path, shown in Figure 2.3:

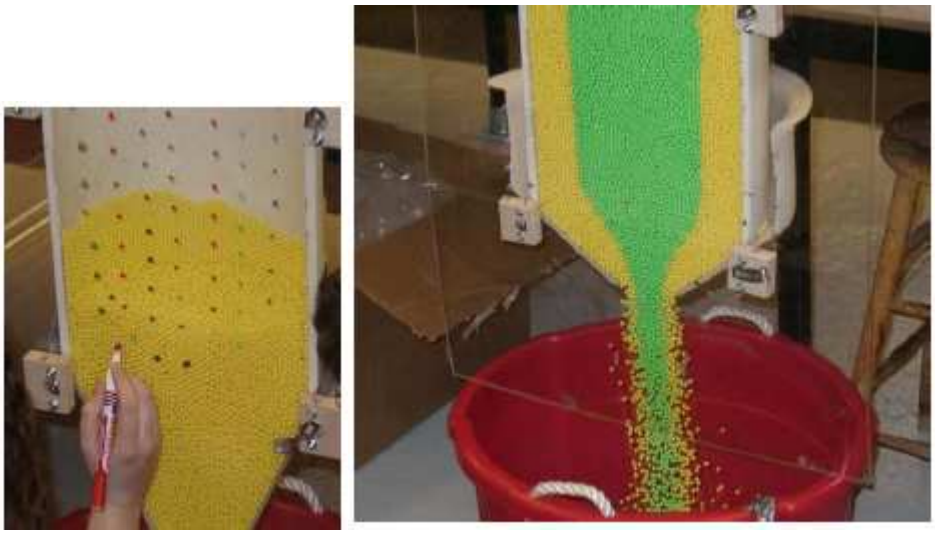

Figure 2.3 Visible Tracking in MIT

In the invisible three dimensions model, Sodium 24 tracer pebble was used. But the configuration was not commented. From the output of the results, they only tracked the pebble to verify that pebble moves in a streamline:

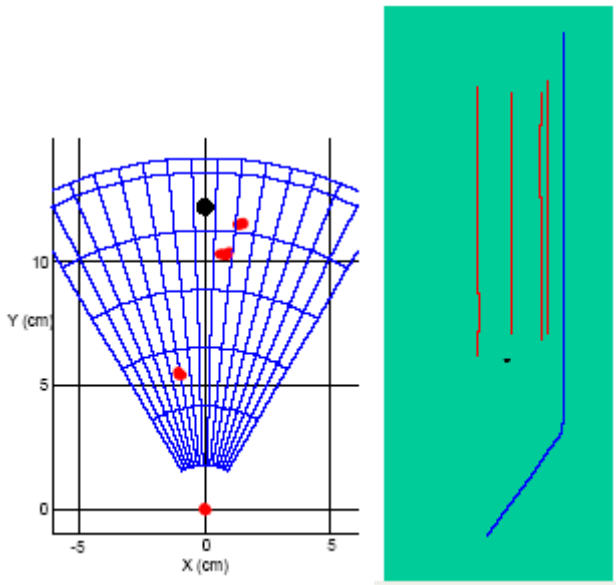

Figure 3.4 Top view (left) and Longitudinal view of 3D Exp.

All their experiments indicated pebbles move in a streamlined manner on the upper end of the container. But the nature of the experimental arrangement is not accurate. The half-model is not the real situation by inducing a new plane. The 3D model can not track the pebble positions.

3. COLLIMATED DETECTORS SYSTEM

3.1 Theory of collimated detectors system

In principle, the collimated detectors radioactive particle tracking system is based on using radioactive nuclides that release their energy by emission of gamma rays. The highly penetrating photons can travel substantial distance to a location where a detector may be placed. The counting rate (number of photon registered) depends on the distance

between the radioactive particle and the detector, the intensity of the source, the detector properties and the material that gamma rays must travel through. All these factors can be divided into two categories “external” and “inherent” factors (Gardner and Ely 1967). The external factors include the factors: Geometry, Absorption, Scattering and statistical fluctuations counting rate. The inherent factors include the factors: Detector resolving time, detector Efficiency. The counting rate in the detector is decided:

$$R=YI \tag{3-1}$$

where R is the detector counting rate in counts per second, I is the radiation source emission rate in radiations emitted per second, and Y is the counting yield of the detector in counts per radiation emitted.

It is assumed here that the counting yield can be treated as the product of six separate factors as soon as the measurement experiment is installed.

$$Y = f_G f_A f_S f_T f_E f_D \tag{3-2}$$

where the factors f_G , f_A etc. represent Geometry, Absorption (between source and detector), Scattering (between source and detector), detector resolving Time, detector Efficiency, and other parameters of the Detector, respectively. Most of the factors

(except f_S) vary from zero to unity.

The optimal system for radiation particle tracking is to reduce the factors that affect the counting rate, best only one factor left and this factor should be very sensitive to the position of the source. Using a stable detector can eliminate the inherent factors effect. And a concept of collimation can make the geometry factor dominate all other external factors, so that the detectors' responses will be maxima when the collimated detectors are oriented in a way that the slot is directly facing (on line of light) the radioactive particle, demonstrated in Figure 3.1:

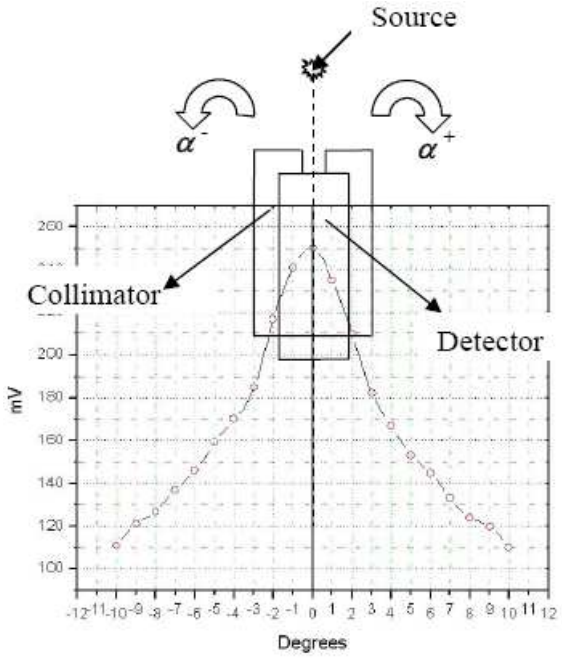

Figure 3.1 Detector responses as a function of the angular position of the detector

3.2 Experimental arrangement

Similar to Gatt's 3-D particle tracking system, three well collimated 2"X2" NaI detectors, deciding the three coordinates simultaneously, are mounted on a movable platform. The platform can be moved to track the radiation particle vertically via a collimated detector that has a horizontal slot opening. The other two collimated detectors with vertical slot openings can be rotated to track the radioactive particle in the planer domain and deduce the particle polar coordinates. (Ashraf & Gardner 2006), (Ashraf, 2005), shown in Figure 3.2:

Figure 3.2 Configurations of Detectors for Collimated detectors system

On the horizontal axis of a two-dimensional Cartesian coordinate system, let Z to be the horizontal axis, then the Z position is the platform position when the centre detector reach it maximum counting rate. X, Y are defined in this way:

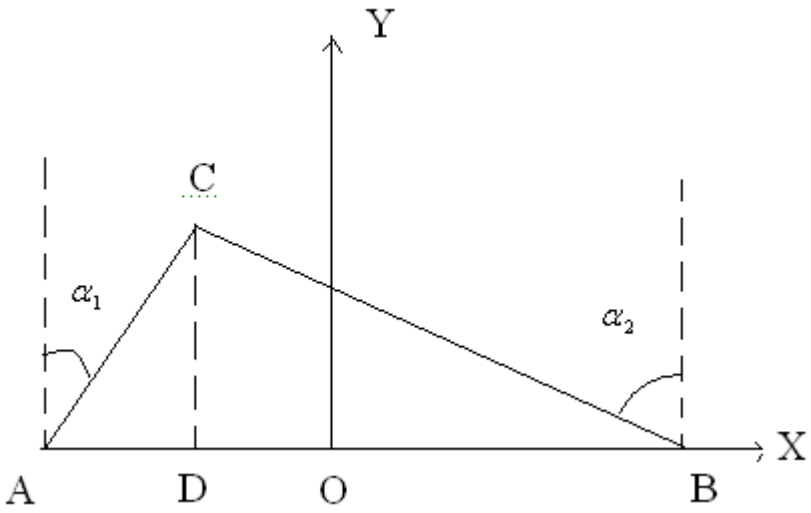

Figure3.3 X, Y Measurement System

where A and B are the positions of the rotated detectors for angular measuring when the counting rate of the detectors reach the maximum, which define the angular of α_1 and α_2 respectively (AB=L is known). C is the tracer position.

$$L=AD+BD=CD\tan\alpha_1+CD\tan\alpha_2=CD(\tan\alpha_1+\tan\alpha_2) \qquad (3\text{-}3)$$

$$\text{So} \quad CD=\frac{L}{\tan\alpha_1+\tan\alpha_2}=Y \qquad (3\text{-}4)$$

And

$$OD=BD-OB=CD\tan\alpha_1-\frac{1}{2}L=\frac{L}{\tan\alpha_1+\tan\alpha_2}\tan\alpha_1-\frac{1}{2}L=X \qquad (3\text{-}5)$$

This is the principle of the how this tracking system works.

For a real time particle tracking, the measured signal of the detectors should be translated into positions simultaneously. In order to achieve this capability, the collimated feature of the detectors required to be moved to the right position to make the measurement for any unknown position. So, the obvious assumptions are:

1) The original position of the particle is known, or will lose the tracking before the system can find it.
2) The speed of searching is faster than the velocity of the particle, or system will fail in tracking.

3.3 Optimization of the system

As mentioned before, the key point in measuring precisely any given angular position of the detector is the identification of the angle corresponding to the maximum counting rate. In order to investigate the effect of the different design parameters of the collimator, a series of analytical and experimental studies were conducted. The slot width and slot depth were found to be of greatest effect:

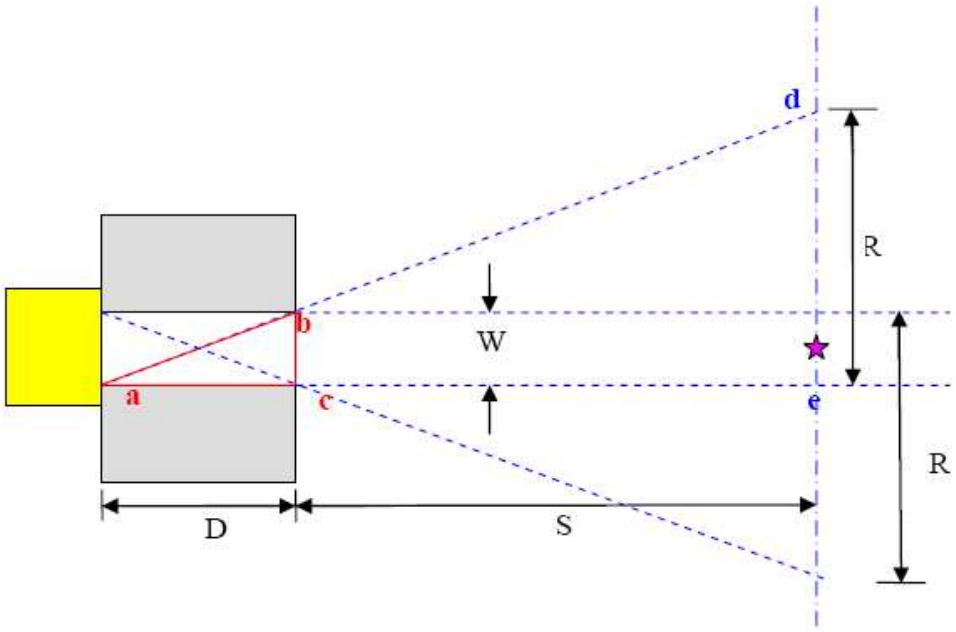

Figure 3.4 A schematic of the slot opening portion of the collimator

where W is the collimator's slot width, and D is the collimator's slot depth. Assuming the source is placed at a distance S from the outer side of the collimator. From the geometry in the figure it can be seen that the collimator has a Range of View "ROV":

$$\text{Range of View (ROV)} = (R - W/2) + (R - W/2) = 2R - W \qquad (3\text{-}6)$$

In figure 2.4, it can be shown that triangles abc are similar to ade. Thus:

$$\frac{W}{D} = \frac{R}{S + D} \qquad (3\text{-}7)$$

$$\text{So,} \quad R = \frac{W}{D}(S + D) \qquad (3\text{-}8)$$

Now carry on with the algebra:

$$
\begin{aligned}
ROV &= 2R - W \\
&= \frac{2W}{D}(S + D) - W \\
&= \frac{2WS}{D} + 2W - W \\
&= \frac{2WS}{D} + W
\end{aligned}
\qquad (3\text{-}9)
$$

Therefore, if we are to maximize the resolution of the position of the source we have to minimize ROV. Minimum ROV would require a minimum W, as well as a maximum D. To verify the above analysis regarding collimator' resolution, two different sets of design parameters had been optimized by a series of Monte Carlo simulations of the response of the collimated detectors. The first collimator used in the center detector has a slot width W of 3mm and a slot depth D of 25.4mm. According to the Eq(2-9), the ROV of the collimator is 26.6mm for a source located at a distance S of 100 mm. The second collimator used has a value of W of 1 mm and a value of D of 50.8 mm. In this case, for a source located at distance of 100 mm, the ROV is equal to 4.94 mm. The response of the detector with these two sets of collimators is compared:

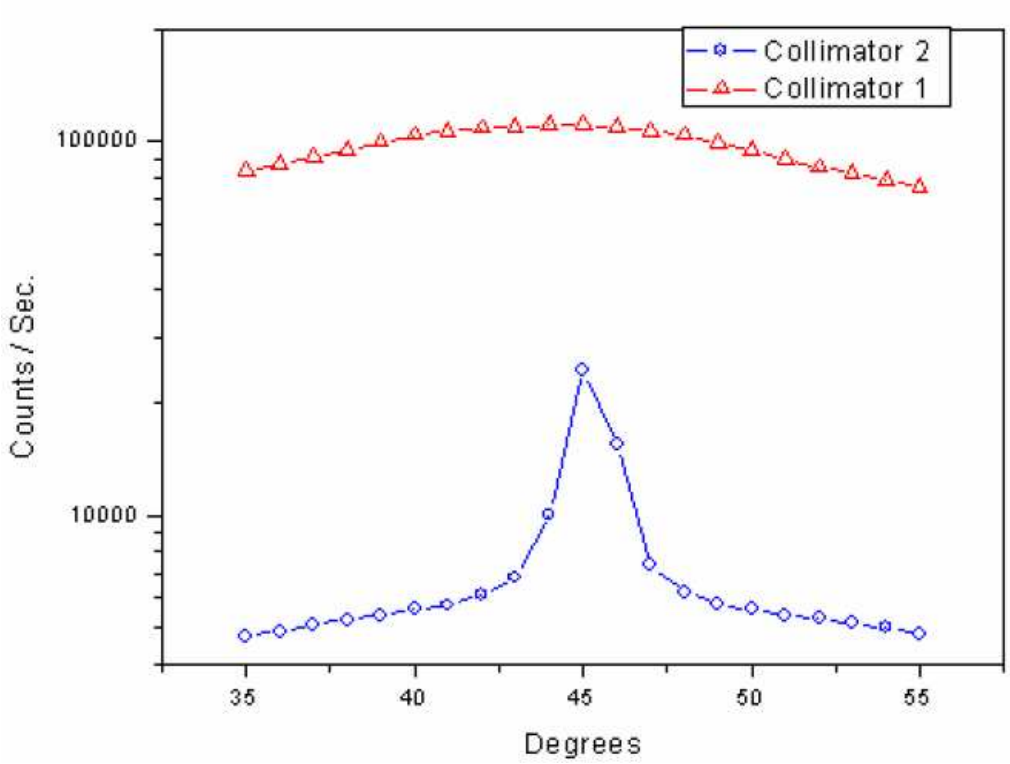

Figure 3.5 A comparison between responses of two different sets of collimated detectors

It is clear from the figure 2.5 that the degree of enhancement of the resolution of the observed maxima. But it also clearly shows an almost two orders of magnitude reduction in the counting rate. So, a tradeoff compromise must be considered that would also include the source activity to obtain a good resolution as well as reasonable signal strength to avoid worsening the statistics of the counting rate.

3.4 Electronics and software

There are two major processes to fulfill a single radioactive particle tracking with the collimated detectors system. One is the detectors signals acquiring process. Another is the signals analysis for the position of the particle.

The first process includes high voltage supplies to supply high voltage to the detectors, linear amplifiers to magnify signals produced from the detectors, and single channel analyzers used to discriminate against low level pulses.

The second process is working simultaneously with the signals acquiring process. This system is required to be fully automated and computer controlled with minimal intrusion during the course of a tracing process. For this purpose a computer is used to perform control of the motion and running the motors to accurately locate each detector to the appropriate position. Three stepper motors are used to drive the motors for their advantages. Firstly the stepper motors are very easily controlled by digital computers. In fact, the control and operation of the stepper motors is based on the logical pulse train of zeros and ones produced by a digital microcontroller or a computer. Secondly, the stepper motors are moved step by step, and each step is identical in the amount of displacement in a particular axis of motion the step produces. There for, the number of the steps the stepper motor moved will be corresponding to a specific position the axis of motion will be at. Tracking the detectors' position is keeping tracking the number of steps the stepper motor has moved relative to the initial reference point.

The main components are showed in Figure 3.6 below:

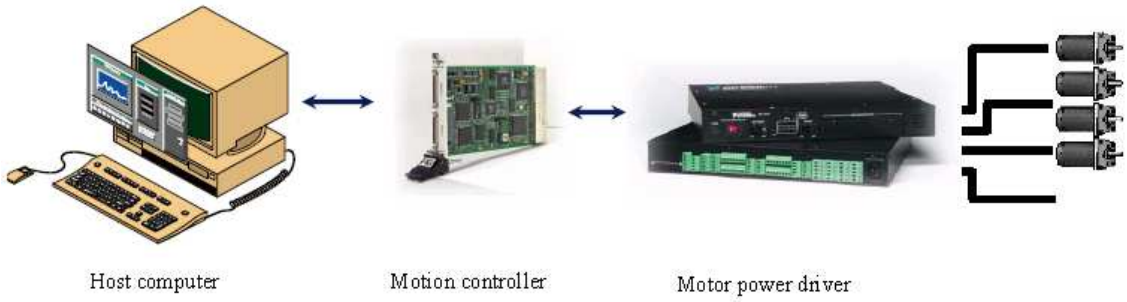

Figure 3.6 Component of the collimated system hard-wares

A host computer with motion control software is interfaced with a motion controller. The motion controller is to convert the motion logic produce by the motion software into a logic pulse train that convey the targeted position in terms of a number of steps and direction of the motion. Then a motor power driver is used to receive the logic signal and direction pulse from the motion controller and amplify that signal into a power signal with a current that can drive the stepper motor the required number of steps in required direction. The motion controller used is a National Instruments four axis stepper and servo PCI controller. The motor driver is also a National Instruments four axis external stepper driver. A National Instruments data acquisition PCI board is used as well to acquire the amplified signals produced by the detectors.

National Instrument LABVIEW is the program language used to develop the automation and control program needed for the tracking system. LABVIEW stands for Laboratory Virtual Instrument Engineering Workbench. The main features of the language are the development environment based on graphical programming concept. LABVIEW

uses terminology, icons, and relies on graphical symbols rather than textual language to describe programming actions. It offers unrivaled integration with thousands of hardware devices and provides hundreds of build-in libraries for advanced analysis and data visualization- all for creating virtual instrumentation. The LABVIEW platform is scalable across multiple targets and Operation Systems, and, since its introduction in 1986, it has become an industry leader. The Multiple Particles Tracking system described in later part of this dissertation is also controlled under LABVIEW program.

LABVIEW has been adapted to carry out motion control of the stepper motors, data acquisition of detectors' signals, perform a rate meter function to produce a counting rate proportional parameter, carry out the counting rates maximum detection algorithms, and present the tracking results both graphically and in data form.

3.5 Scanning technique

Suppose that at one instant that tracking system has located the radioactive particle. Assume that the particle will move in a presumably unknown direction. The dynamic electromechanical tracker we have should start moving accordingly to fellow the tracer particle. But lacking of the information about the direction the source will move to, the system has no way to know the direction to follow. So, if the detector happens to move to the wrong direction, it would completely lose the track of the particle. The logic used to resolve this problem is based on a so called Scanning Technique. In this technique, the

detector would move in an oscillating way around the pre-located position of the particle. It scans a range of angular or vertical positions, and the acquired detector response would have a distribution over the range. The maximum of the distribution is then corresponding to the position where the particle is located. The range that the detector will oscillate around the particle is based on the previously established particle position, and each established position will be used to update the oscillation range for the next cycle of oscillation.

A flow chart like description is reported for a radioactive particle in an unknown position:

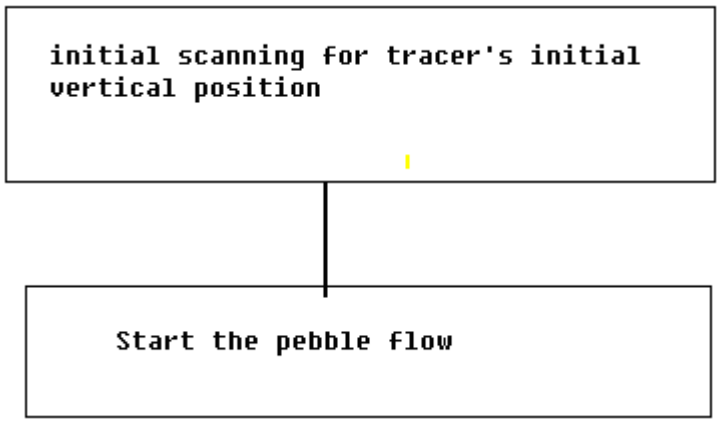

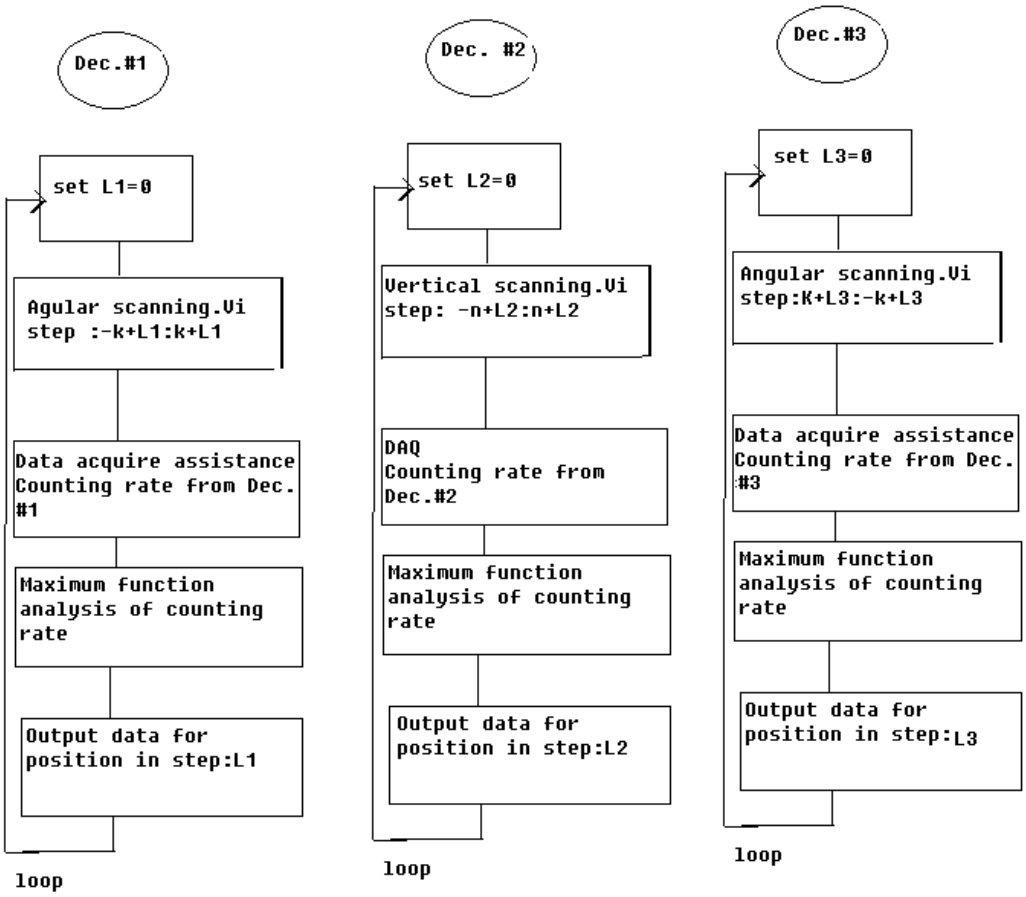

Figure 3.7 Flow chats for scanning technique

Note the three detectors are simultaneously performing the scanning action, where k, n and L are the step ranges for stepper motors motions.

4. THE MODELING SCALED PEBBLE BED REACTOR

The Pebble Bed Reactor (PBR) is the result of some initial interest in ultra-safe reactors by engineering in order to provide for future electricity production that includes nuclear as an option when coal supplies dwindle, as well as environmental concerns that coal–fired generation engenders. After operating experience is gained from the early model PBR, improvements reach an acceptance of high-temperature alloys for use in gas-cooled reactors (Koster, Matzie and Matzer, 2004).

One of the licensing issues for PBRs is the perception that the stochastic nature of the

pebble distribution permits the collection of relatively reactive pebbles in regions of high neutron flux, so that the local power density could become excessive either in normal operation or in accident scenarios. Some rough estimates of the probabilities associated with this phenomenon were performed and indicated that this risks are very small. However, a more rigorous analysis is warranted to develop flow models for pebbles and all possible regions in the PBR.

The HTR-10 pebble bed reactor in the People's Republic of China can provide core physics benchmark data resulting various startup core physics experiment. But the experimental data of the pebbles in a PBR HTR core is almost non-existent. This information is crucial to address important outstanding issues like local fuel clustering and bed or reflector interface effects.

To measure the pebble flow data in a real operating PBR is impossible. The scale of the bed diameter is several meters itself, including the shielding wall of the reactor, that will not have strong radioactive particles to be measured by the outside detectors for analysis purpose, and actually, not allowed to for safety reason. And the TRISO fuel particles are all the same in size and in physical properties. It is not possible to follow some of the particles in side the bed.

Some factors limit the design of the model PBR. One is the applied design of real PBR. Another is the capability of the Lab conditions. Technically, the shape should be the same

as a real PBR, while the size should be within the tracking capability of the tracking system.

4.1 Vessel

The same ratio of shape design comes from Gatt's experiments; a cylindrical vessel with a core angle of 25 degrees corn is set. MIT experimental conclusions are considered. MIT reported a streamlined motion on the top of the PBR area, so, it may reasonable to cut this part off. Other than in ratio of D:H:d=30:60:1, a ratio of D:H:d=30:30:1 is applied, where D is the diameter of the cylindrical vessel, H is the height of the cylindrical vessel, and d is the diameter of the pebbles.

As the centre detector has a horizontal collimated window with 6cm in width 2.54cm in depth, the detective area would be limited to those area that can be "seen" from this window.

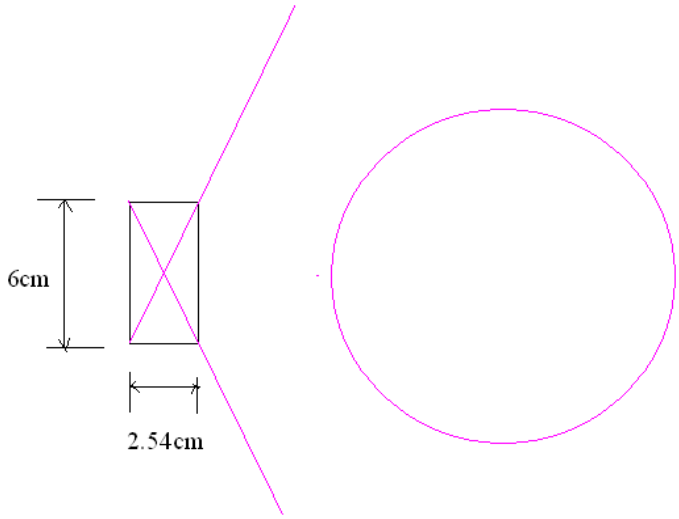

Figure 4.1 Detective areas for center detector

And in order to acquire as higher counting rate as possible, the PBR should de smaller and in the center to avoid blind point for the detector.

The collimated detectors system tracking speed is mostly limited by the velocity of the platform, which is mounting three lead collimated detectors. It is driven by a step motor, in a stable speed of 1000step per second, which mean 2.75cm/ minute or 0.0458cm/sec. Due to the Scanning Technique in particle position locating process, the tracer' velocity in Z direction can only be half or less of the that speed. This called tracking speed limit around 1.37cm/minute (0.0279cm/sec). All of these shape the design as (cm) is shown in Figure 4.2:

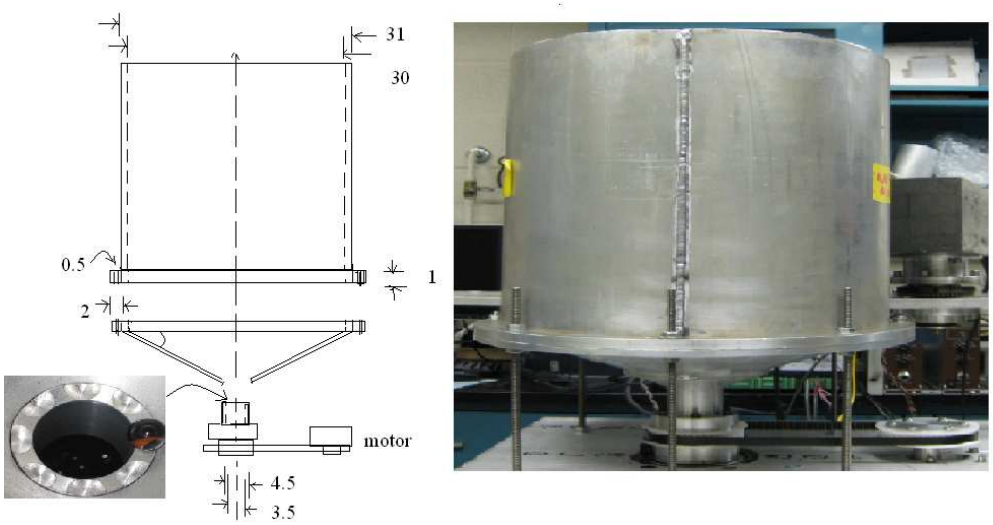

Figure 4.2 Modeling PBR design

4.2 Pebbles

For economic concern, the easiest to get pebble in the market to mimic the pebbles in the PBR is glass pebbles. 18,000 marbles with a size of 1.2 cm in diameter without radiation are used for dummy pebbles, which have a variation in diameter of 0.15 cm as indicated by product description-around 12.5 percent of the diameter of the marbles

4.3 Pebble packing

The void fraction can vary dramatically in different types of packing. When applied a random packing style, the void fraction is around 0.4 (Cerlsmith, 1962) in PBR. The real PBR is also working in a random packing style as we applied in our case.

4.4 Extractor and pebble flow rate

A too large outlet under the bottom of the vessel will result in a too fast flow rate. And the tracking capability of the tracking system will lose the track of the radioactive particles. A too small outlet, on the opposite, will result in the jamming condition that the flow will stop. An extractor was design to agitate the marbles to let the marble flow continue, but not affect the marble inside the bed with a small catch design in the same size of the marbles. This extractor is controlled by a stepper motor working in selected

speeds. The outlet is designed to easily get jamming when the motor driver stops. So, the flow rate of the pebble can work in continue constant or stop and go styles with a maximum flow rate of 60-100 pebbles per minute. In addition, Edwards (1965) has found that a variation in flow rate of from 0.5 to 3800 pebbles per minute has no noticeable effect on the flow profile.

4.5 Radioactive particles

The tagged radioactive tracer particle should have the same shape, diameter, specific gravity and surface finish as those dummy pebbles in the PBR. But as the glass is very easily been broken, aluminum ball with drilled hole was used to hold the radioactive source with the same shape, diameter and weight instead. So the only difference is the surface finish. One is glass the other is aluminum. But both of them have glassy surfaces their considered as the no significant difference to affect the experimental results. The source used for tracking purpose should have long half life and best have single energy. For multiple particles tracking system the energies of the sources should have big enough difference for information analysis. When the energies are too close to each other in a spectrum the system may fail in identifying the different sources. The Summary of the modeling PBR is organized into table 4.1:

Table 4.1 Nature of the Problem for modeling PBR:

Vessel Diameter (D)	30 cm
Height of the cylindrical portion of pebble bed (H)	30 cm
Base cone Angle measure from the horizontal (θ)	$25°$
Pebble diameter (d)	$1.20 \pm .15$ cm
Bed inventory, defined as the total number of pebbles in the bed (N)	21000
Density of the pebbles	$2.3 \pm 0.1\ g/cm^3$
Outlet orifice diameter	3.5cm

5. EXPERIMENTS AND RESULTS I

5.1 Benchmark experimental results

A benchmark experiment was designed to verify the accuracy of the system in tracking single particle. A radioactive particle was moved in a preset trajectory by independent stepper motor with an independent controlling program. So that the time trajectory of the particle is pre-known, and the particle location was programmed in advance. There for, a comparison can be established in Figure 5.1 between the deduced particle's positions by the tracking system and those pre-known positions:

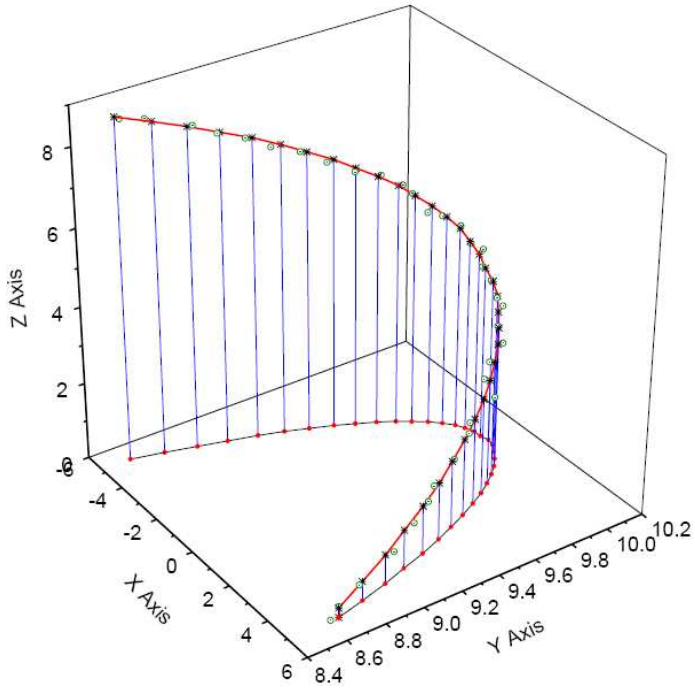

Figure 5.1 A comparison of the predetermined and measured positions

The absolute errors through this benchmark experiment are less than 0.07 cm in X and Y coordinates, and less than 0.10 cm in Z coordinate. These values indicate the uncertainty of this system. For the modeling PBR in a scale of 30cm this accuracy is good enough. But this benchmark experiment can only be carried out in the air, when induce the modeling PBR and pebbles the scattering factor of the materials between the source and the detectors should obscured the maximum counting rate peak and the absolute error should be higher.

5.2 Experimental results with PBR

As a benchmark measurement result, the collimated detectors system is an important

tool to make the un-collimated system work accurately, and will be used to achieve the positions of the tracer particles in the later part of "Experiments and Results II" in comparison with the results from the un-collimated detectors system. A stop and go mode is used to tracking a single Cs137 (0.662Mev) tagged tracer in the modeling PBR is shown in the Figure 5.2:

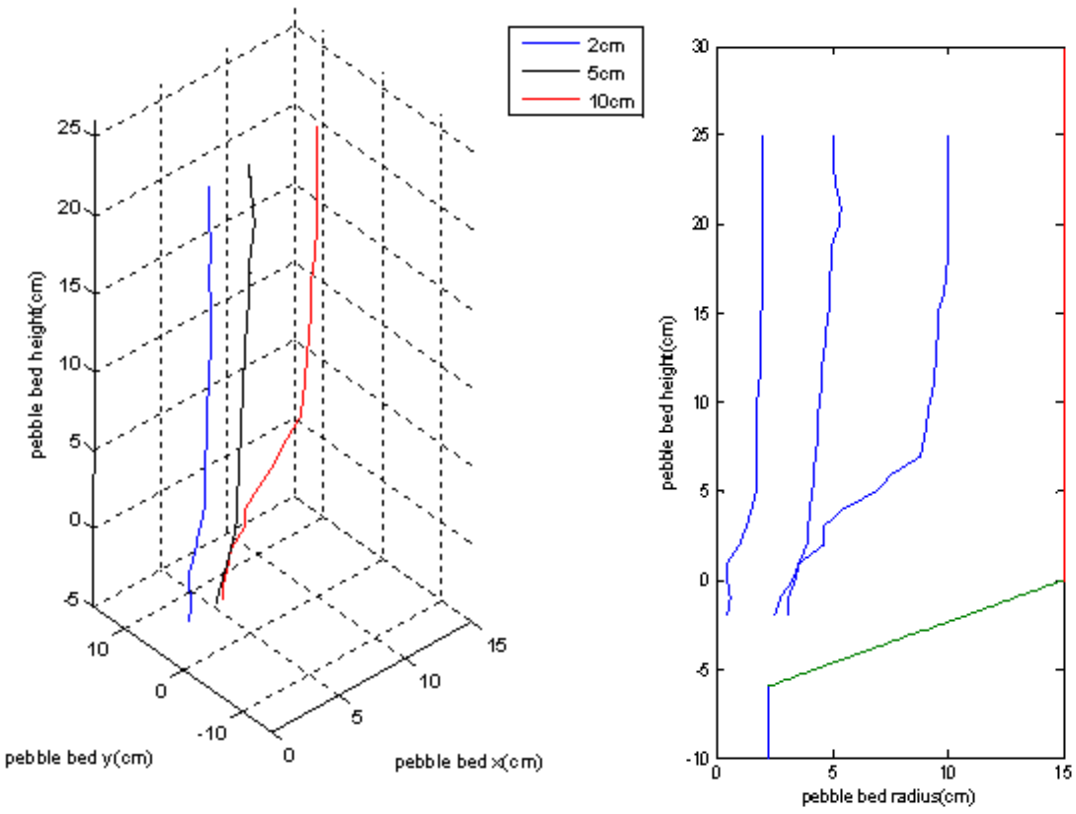

Figure 5.2 Single particle tracking with collimated detectors system

The source is put on the top of the PBR with pebbles loaded at the initial position off the axis at 2cm, 5cm and 10cm respectively. The tracer is initially arranged in 5cm depth in the core, and then loaded pebbles to reach the top of the core, in order to avoid the

incoming pebbles from the top of the core directly hit the tracer to change the position dramatically unexpected. Let around 500 pebbles flow out of the outlet of the core, then stop the flow, measure the new position of the tracer, refill the pebbles from the top of core and organize the input pebbles as the same as the starting point of the pebbles flow. Repeat this process until the tracer discharges from the core.

The results show that the motion of the pebble is focus on an X-Z plane, which means, viewing from the top of the core, the motion focus on r direction without significant motion of rotation. In the region of Z>10cm the pebble motion has a streamline through the Z coordinate.

6. UN-COLLIMATED DETECTORS SYSTEM

6.1 Overview

The un-collimated detectors system was designed for multiple particles tracking simultaneously. It is a totally different approach comparing with the collimated detectors system. The author initially applied the Monte Carlo Library Least Squares approach in particles tracking. Other than analyze the counting rate in the detector, this method analyze the whole spectrum response in the detector. There should be more information than that of counting rate measurement only in the collimated detectors system. When a photon travels from the source through the materials, there are three major types of interactions play important roles in the radiation measurements: Photoelectric absorption, Compton scattering, and Pair production. All these processes lead to the partial or complete transfer of the gamma-ray photon energy to the electron energy, and then through the electrons the incident photon deposits its energy.

In the photoelectric absorption process, a photon interacts with an absorber atom. The

photon transfers its energy completely to the atom and disappears. Then an energetic photoelectron is ejected by the atom from one of its bound shells. In the Compton scattering, the incoming gamma-ray photon is deflected through an angle with respect to its original direction. The photon transfers a portion of its energy to the electron, which is known as a recoil electron. Because all angles of scattering are possible, the energy transferred to the electron can vary from zero to a largest fraction of the gamma ray energy when a backscatter happens. It means that the photon reflected in a direction opposite to its incoming direction. If the gamma ray exceeds twice the energy of an electron (1.02Mev), the process of pair production is energetically possible. In this interaction, the gamma ray photon disappears and is replaced by an electron-positron pair. All the excess energy of the photon above 1.02 Mev required to create the pair goes into kinetic energy shared by the positron and electron. The positron will subsequently annihilate after slowing down in the absorbing medium, and two annihilation photons are normally produced as secondly products of the interaction. But the possibility of this interaction remains very low until the gamma ray energy approaches several Mev.

When a gamma ray source is put into the modeling PBR, at different positions, the source will travel through different paths and consequently different interaction processes will go on before the photons reach the detectors outside the PBR. This difference is significant depended on the energy of the gamma ray and the materials between the detectors and source. For example, in our modeling PBR, marble is used, which is

majorly Silicon and Oxygen. For silicon the mass attenuation coefficient is shown:

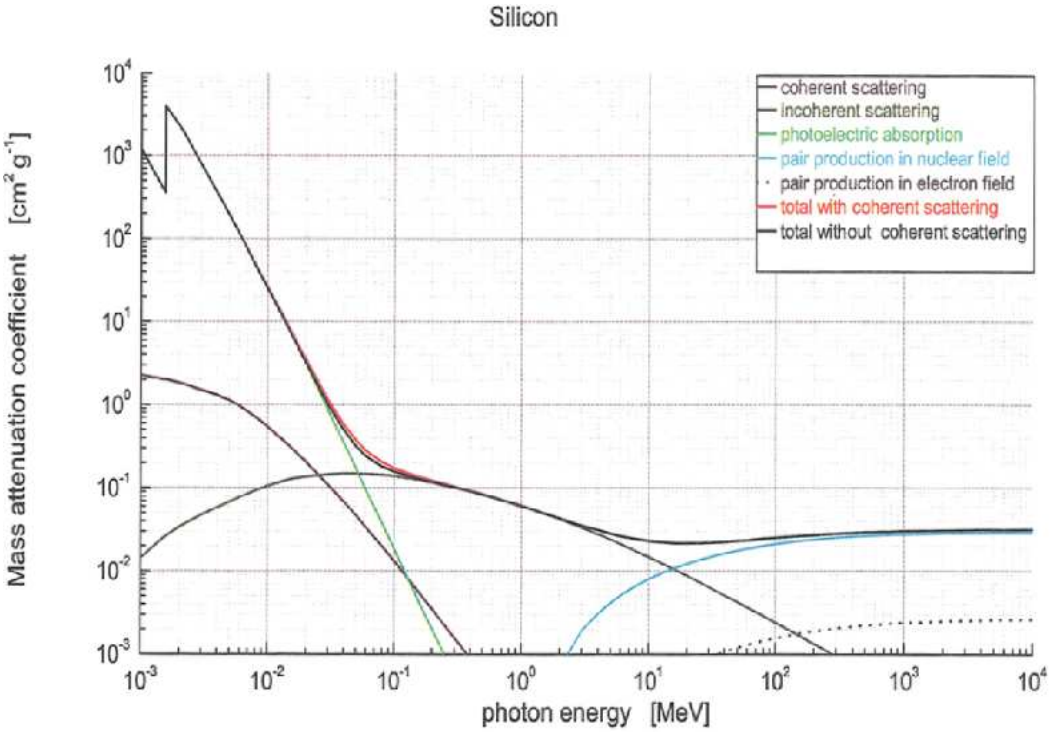

Figure 6.1 Mass attenuation for Si (Berger, Hubbell, seltzer, coursey and Zucker, 1999)

Note: Coherent scattering is a Compton scattering without exciting or ionizing the atom, and the gamma ray retains its original energy after the scattering.

The gamma ray travels through the marbles and the aluminum wall of the modeling PBR, and finally reaches the detectors outside of the PBR. The detection measured by the detectors should carry the information of the source position in two aspects: the intensity difference of the gamma ray due to the attenuation of the medium thickness variation; the scattering difference due to variation of the medium surrounding the source. These differences caused by the position effect project into the spectrum measured by the

detector with Multiple Channel Analyzer (MCA) would behave as the absolute counts differences in each channel and the ratio of the full energy peak to the scatter peak.

The difference of the spectra can be measured with reference positions of the source. But in an application for accurately estimated the positions of the source, the reference measurements are too many and too time consuming. It is infeasible in this case with a large volume of interest. Therefore Monte Carlo simulations can act as an alternative. A tool called Detector Response Function's (DRF's) is used for efficiently obtaining these reference spectra-libraries.

There are two ways to achieve the Detector Response Functions (DRF's) in a certain arrangement. One is experimentally (Heath, 1964) measured by actual experiments. Another is calculated by simulation. A Monte Carlo code G03 developed by Peplow, Gardner, and Verghese (1994) used relatively simple electron transport, which did treat photon transport fairly rigorously, it considered the loss of electrons from the detector surface via a simple straight line electron range relationship, and it accounted for the production of Bremsstrahlung photons along the electron path in a very simplified way. The code gave relative good results compared to more rigorous Monte Carlo simulation such as those by Berger and Seltzer (1972) and to experimental results. Based on this code, Gardner and Sood (2004) improved the by adding NaI nonlinearity and the variable flat continua part of the DRF's for better accuracy.

The applications of DRF's are successful indicated in the Monte Carlo Library Least

Squares (MCLLS) approach for the inverse elemental analysis of Prompt Gamma-ray Neutron Activation Analysis (PGNAA) (Shyu, Gardner, and Verghese, 1993) and Energy Dispersive X-ray Fluorescence (EDXRF) analyzers (He, Gardner, and Verghese, 1993). The author initially applies this approach into radioactive particles tracking in PBR.

6.2 Development of DRF's in MCNP5

The G03 code can be used to generate scintillation detector's DRF's with bare crystal or with simple known geometry arrangement. When develop the Monte Carlo codes for DRF's for scintillation detector two major improvements have been considered: One is the detector's Non-linearity scintillation efficiency when deposits electrons' energies; One is the flat continua adjustment applied for spectrum accuracy.

The inherent nonlinearity of NaI detectors for Gamma-ray spectroscopy allocation had been known for many years and was treated by several early researchers including Zerby et al.(1961), Kaiser et al. (1962), Collinson and Hill (1963), and Heath (1964). It appears that the inherent nonlinearity with deposited electrons occurs at energies below 3 Mev and the relative scintillation efficiency asymptotically approaches a constant at higher electron energies. Assuming that this is true, Gardner and Sood (2004) proposed the following relationship for relative NaI scintillation efficiency with deposited electron energy:

$$S(E_e) = 1 + k_1 \exp[-(\ln E_e - k_2)^2 / k_3] \qquad E_e \geq 10kev$$

$$S(E_e) = 1 + k_1 \exp[-(\ln E_e - k_2)^2 / k_4] \qquad E_e \leq 10kev \qquad (5\text{-}1)$$

where E_e is the electron energy in Kev, k_1 is 0.245, k_2 is $\ln 10 = 2.30258$, k_4 k_3 is 7.1635, and k_4 is 5.1946.

A plot of the model compared to the data of Zerby (1961) is shown in figure 6.2. The correspondence is quite good above 1 Kev which is probably the range of practical interest:

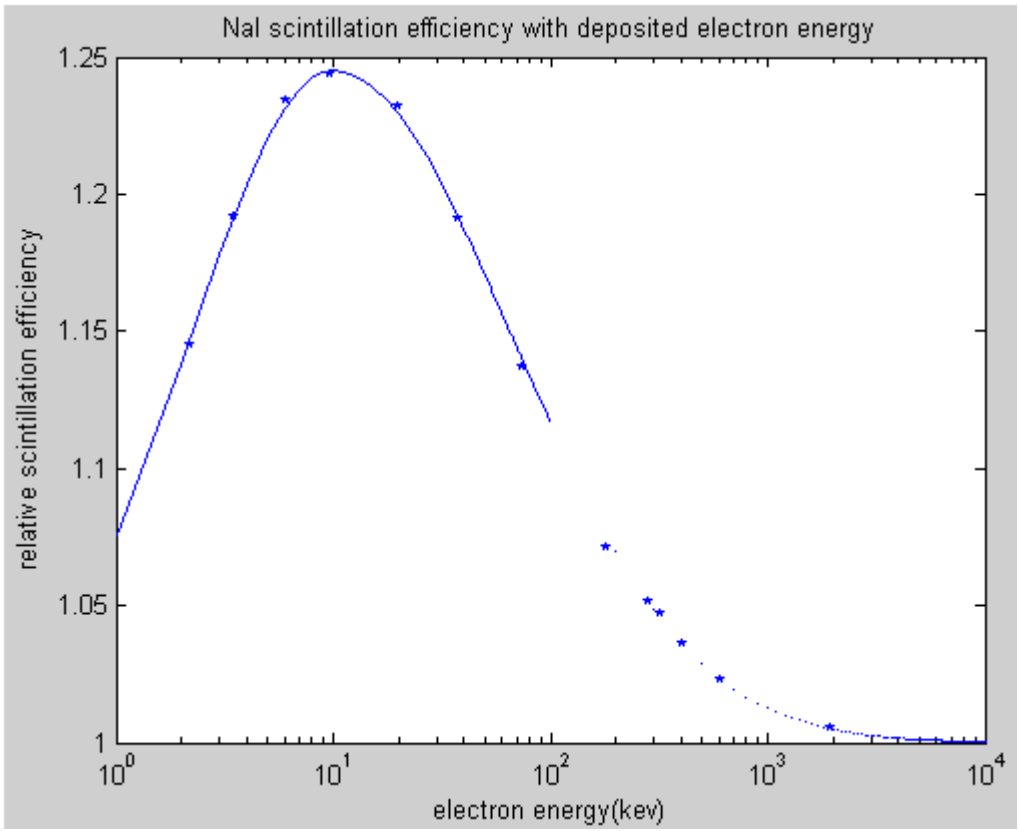

Figure 6.2 NaI scintillation efficiency nonlinearity

There are several parts of DRF's that cannot be simulated exactly by Monte Carlo when one uses the basic principles that utilize the normal exact geometrical description of the detector and the exact physics of the photon and electron transport. This includes the detector resolution or the standard deviation of the Gaussian distribution of the pulse-height distribution, the low-energy exponential tail on the low-energy side of the full energy peak. The flat continua part of the DRF's can be generated by assuming that it is due to the photon interactions that produce electrons that subsequently escape the detector surface before depositing all of their energy. Gardner and Sood (2004) suggested that this maybe due to either the detector imperfections that trap many of the electrons for a period long enough that they are lost from a given photon interaction sequence or electron channeling from the crystal material feature of the detector. In this work a simple code call G03 was developed to generate DRF's in considerate accuracy with high speed. But this code can only work for simple geometry situation and applied a very simple electron transport process.

MCNP is a general-purpose Monte Carlo N-Particle code that can be used for neutron, photon, electron, or couple neutron/photon/electron transport. The code treats an arbitrary three-dimensional configuration of materials in geometric cells bounded by surfaces. The most important features for DRF's in MCNP are its versatile geometry, flexible tally structure, extensive collection of cross-section data and a rich collection of variance reduction techniques.

A modification version of MCNP5 code has been developed for generating the DRF's for NaI detectors, which takes care of the NaI scintillation efficiency nonlinearity and flat continua part of the DRF's. The results were first benchmarked with the Heath (1964) experimental results for 3"X3" NaI detector. Figure 6.3 is used to show how this code works when the source is Cs137, with Gamma rays energies of 0.032, 0.037 and 0.662 Mev. The Blue line is the result of Heath experimental, the green line is the simulation result with the original MCNP5, and the red line is the simulation result from the Modified MCNP5. The difference between the blue and green is a significant example of flat continua inaccurate problem. The modified MCNP5 shows a significant improvement compared with the original MCNP5.

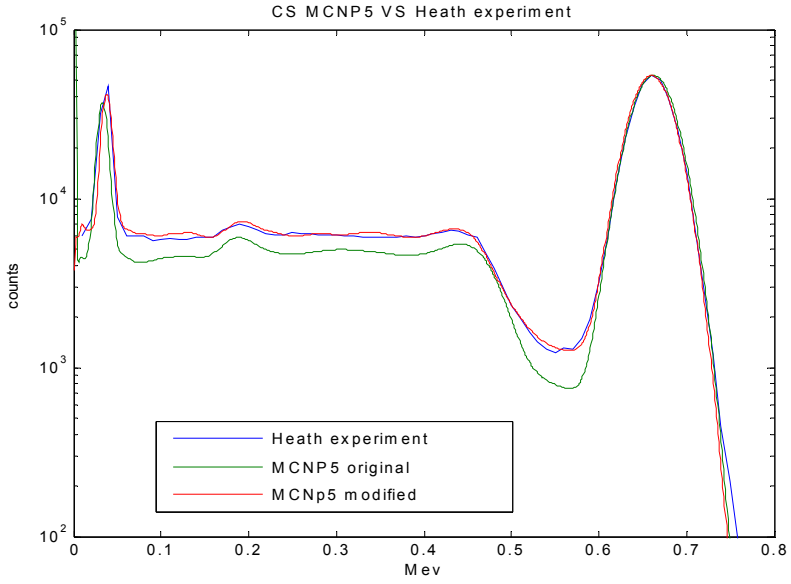

Figure 6.3 Cs137 Benchmark Results

In the modification, the electrons channeling effect (the author agrees with this assumption more) or imperfection effect of the detector crystal phenomenon is simulated by a modification of the electron cross section in the detector crystal. An empirical factor is used in the electron transport process in the detector crystal only. With the available experimental results from Heath experiments, this factor is studied to a range of energy up 3.13 Mev (the source energy of Sulfur-37). Table 6.1 Electron cross section factors:

Table 6.1 The flat continua factors

Energy (Mev)	factors
0.14	0.080
0.16	0.100
0.25	0.020
0.31	0.030
0.50	0.045
0.66	0.055
0.74	0.055
0.85	0.060
0.93	0.070
1.46	0.073

3.13	0.080

In the modified MCNP5, the non-linearity for NaI has a peak at around 10 keV that is about 1.25 times the minimum efficiency. Utilizing this factor, the deposited energy of multiple electrons is obtained as a simple bookkeeping process by:

$$E'_{dep} = S(E_{in}) \times E_{in} - \sum S(E_{esc}) \times E_{esc} \qquad (6\text{-}2)$$

Instead of:

$$E_{dep} = E_{in} - E_{esc} \qquad (6\text{-}3)$$

where S is the non-linear scintillation efficiency factor, E_{in} is the incident electron energy and E_{esc} is the escape electron energy from the detector surfaces. The nonlinearity effect is a little more significant with higher energy source. The Na24 with energy of 2.754Mev is used to demonstrate this effect in Figure 6.4, note that the flat continua adjustment is added. The blue line is the heath experimental result and the Dotted black is the simulation result from original MCNP5 and the red line is the modified MCNP5 simulation result. The modified MCNP5 matches the experimental result much better in the first and second escape peaks than the original MCNP5 dose, shown in Figure 6.4:

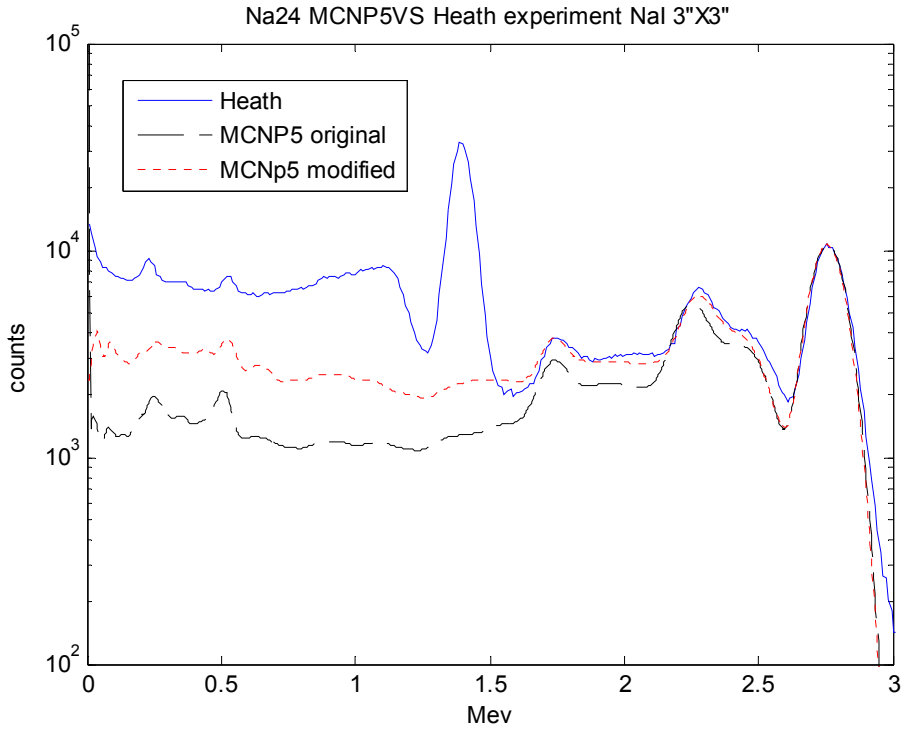

Figure 6.4 S37 for nonlinearity benchmark results

One thing has to be pointed out that the simulation results are accurately used the exact geometry arrangement of the 3"X3" NaI detector experiments described by Heath (1964). If the geometry in the simulation is different from the experiment arrangement this verification will not be validate. And it was found that the detector can is very critical geometric factor that affect the detector's response, because it is very close to the NaI crystal. The experimental arrangement of Heath experiment is shown in Figure 6.5. The simulation geometry is shown in Figure 6.6 correspondingly:

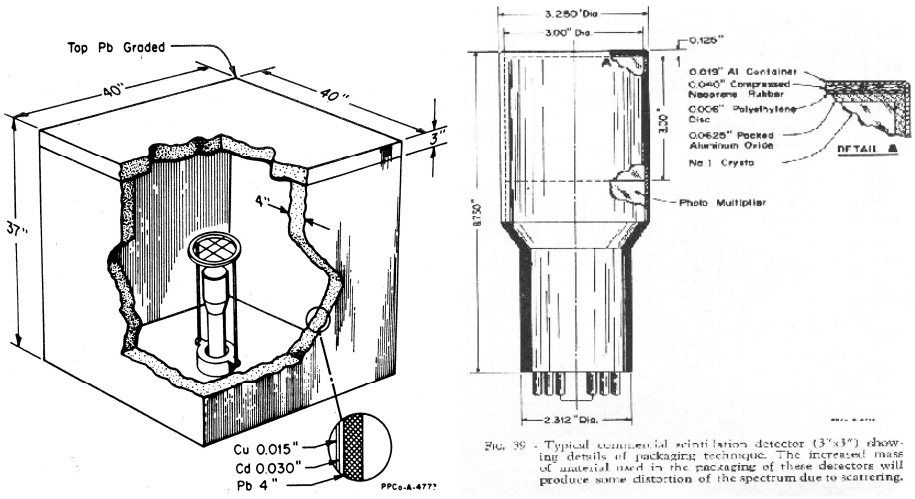

Figure 6.5 Heath Experimental arrangements

The geometry arrangements can exact simulated in MCNP5 look like:

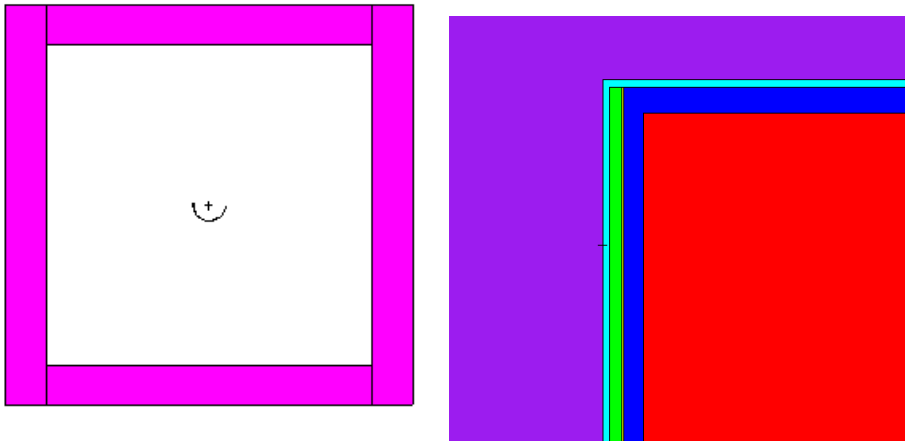

Figure 6.6 Geometrical in put in MCNP5 for Heath experiments (left: the shielding cave; right: the detector sections view)

The modified MCNP5 code has been extended to other sizes of the NaI detectors from 3"X3" to 6"X6", 2"X2" and 2"X4"X16" box-shape, and other kind of scintillation

detector like BGO.

Comparing with the simple DRF's generating code G03, the modified MCNP5 can be used in very complex geometries and treat the electron transport very detail. But in the same time it sacrifices the generating efficiency by a factor of 100 in calculating time consuming. Most of the time consuming in MCNP5 for generating DRF's is the process of electron transport. The algorithms in MCNP for electron interaction are the Goudsmit-Saunderson theory for sampling the deflection angular, the Landau theory for energy-loss fluctuations sampling and the Blunck-Leisegang enhancement of the Landau theory (MCNP5 Manual I). These theories intend to use fundamental cross sections and the statistical nature of the transport process to predict probability distributions for energy loss and angular deflection. In order to do that, MCNP sorts the electrons into group with energy and works in a way of sampling data from pre-calculated tables: bremsstrahlung production probabilities, photon energy distributions, photon angular distributions, etc. In order to simplify the electron transport process in MCNP we investigated:

1) Weighting the importance of electron transport.

For a complex geometry case, following the details of the electron in some cells far away from the detector is not necessary affecting the final spectrum significantly. For example the shielding box in Heath experiments. According to the importance affecting the detector, weighting the cells in electron transport can save simulation time

significantly. The more complex geometry case saves more time with this method. This method can be detailed by using weight windows in the MCNP5 simulations

2) Cutting down the number of major steps and sub-steps.

MCNP treats the electron into energy groups and steps tracking the electron until it loses its energy.

$$E_{n-1} - E_n = -\int_{s_{n-1}}^{s_n} \frac{dE}{ds} ds \qquad (6\text{-}4)$$

where Sn, En, are total path length and energy at the end of n step. MCNP sets:

$$\frac{E_n}{E_{n-1}} = k == 2^{-1/8} \qquad (6\text{-}5)$$

Eq (6-4) and (6-5) decide the major steps, which defaults with the data table preset. To cut off the major steps to simplify the electron transport will involve a rearrangement of those data tables, which is possible only if we have sufficient data. Another way to simplify is to cut off the sub-steps. Sub-step is used to break the major steps into m sub-steps for accuracy in electron transport (each sub-step path length S/m).

3) Reducing the physics complexity of electron transport

In MCNP5, the electron process not only tracking the electron, but also produce secondary particles through the electron transport process. And a process tracking the new particles is added when one is generated. Only follow the energy loss of the electron in the transport process, automatically take the loss energy of the electron as the energy that is absorbed by the medium. Actually, this is very close to the true pattern that a big size scintillation detector will result in electron transport process, because most the secondary particles from the electron will finally deposit their energies into the detector through big enough volume of tracking.

These three methods were used to simulate heath experimental arrangement. The results of them have no significant difference between the spectra, shown in Figure 6.7. The spectrum of cut off sub-steps method is not shown, because sub-steps modifications do not affect the calculating speed significantly. For example, sub-steps in 9 to 90, the running time almost the same with one million histories.

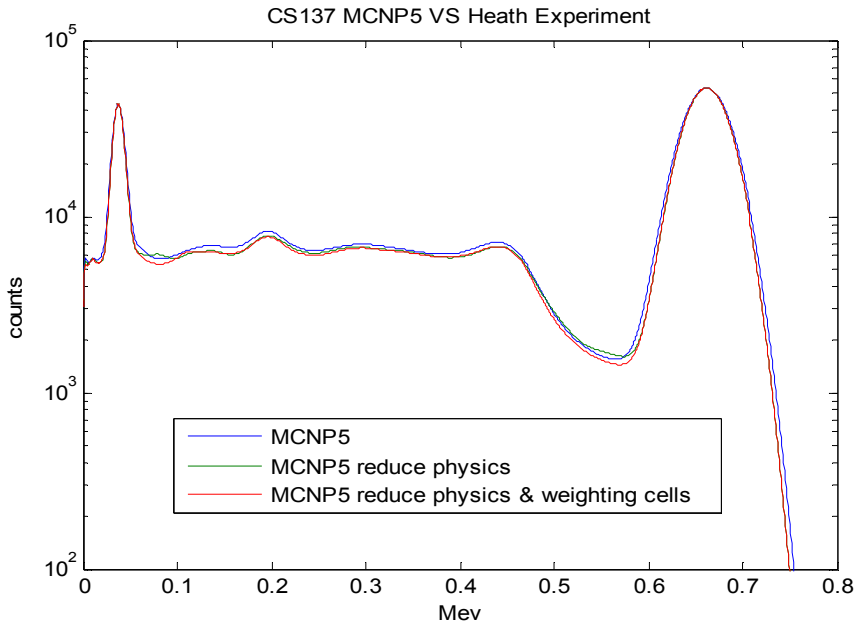

Figure 6.7 the Cs137 for efficiency in MCNP5

Table 6.2 Speed-up methods efficiency

Methods	Run Time (1million history.) (minutes)		factors	Combined factor
Modify MCNP5 for DRFs	189.76		1.0	
With Weighting cells	2.24	Combined 0.88	88.7	215.6
With Simplifying physics	39.94		4.97	
With Cutting substeps	190.21		1.0	

As mentioned before that the detector's can (the layers of materials used to protest

the detector crystal) has strong effect on spectrum, especially the front face cell. In table 6.2 we weighted the detector including the whole can with heavy weight 1.0, but light the shielding box's weight 0.0. The weighting cell method has the highest effect in speed. The combination of weighting cell and simplifying physics method can achieve a factor of about 200 times fast than ordinary run.

The Monte Carlo generated pulse –height spectrum need to perform a Gaussian spread to compare with the experimental spectrum results. A semi-empirical relationship is used between the Gaussian standard deviation for the full energy peak and the incident gamma-ray energy that produces that peak:

$$\delta_T(E_I) = aE_I^{\,b} \;\; \delta_T(E_I) = aE_I^{\,b} \tag{6.6}$$

where $\delta_T(E_I)$ is the total standard deviation required to Gaussian spread the NaI detector response, E_I is the incident gamma-ray energy in Mev, and 'a' and 'b' are the constants for a given detector. For different sizes NaI detectors has different the constants.

6.3 Monte Carlo Library Least Squares Approach

The un-collimated detectors system for multiple radioactive particles tracking consists of five parts: radioactive sources, the modeling PBR, the detectors and associated electronics, Multiple Channel Analyzers (MCA) and associated electronics, and computer with analysis software to perform spectrum analysis for the positions of the sources. The main goal of this system is to determine the positions of the sources. The sources are selected, so the energies of the sources are known. But in different positions, the gamma-ray travels different path of the materials and have different interaction, resulting in different spectra in the detectors. If the detectors are sensitive enough to the position, the system can provide an excellent solution to this problem. With the accurate DRF's from modified MCNP5 discussed in the previous section, a pre-calculated library spectral response can be prepared with Monte Carlo simulations. Case without the limitation, in a general 3-D condition, shown in Figure 6.8:

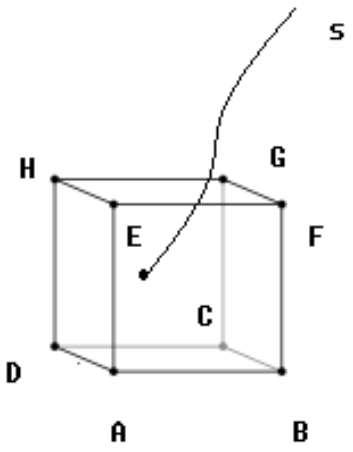

Figure 6.8 Cubic cells Library

This approach uses the gamma-ray spectra at points A, B, C, D, E, F, G, and H as reference libraries to predict the unknown position of the gamma-ray source inside the cubic cell. When the cell is small enough to satisfy the linear assumption, the spectrum at "s" can be a linear combination of those libraries.

$$Ysi = \sum_{j=1}^{m} a_{ij} X_j + E_i, i = 1, n; m = 8 \qquad (6.7)$$

where the 'Ys' is the spectrum at s, Xj's are library spectra. This linear fit can be obtained by minimizing the reduced chi-square:

$$\chi_v^2 = (1/v) \sum_{i=1}^{n} E_i^2 / \sigma_i^2 \qquad (6.8)$$

For multiple sources this process will be repeated for every source in an order from the high to the low energy. In MCLLS approach, it implies that DRF's is required to transform the simulation results into "real" pulse height spectra. Due to the resolution of the detectors, the energies of sources must be different enough, it means there is significant part without overlap in spectra between any pair of the sources, so that the information of the sources can be separated and recognized.

From the experimental spectrum peaks and intensities of each peak, one can tell

roughly where the sources are located through inspecting the peak to total ratio. For each source a library package is preset, and the full energy peak to scatter peak total ratio are pre-calculated as well. An initial guess of the positions of the source can be estimated with known sources and this pre-calculated information.

The main components of MCLLS approach basically include: (1) A reproducible experimental configuration, (2) corrections of simulation geometry and materials density with benchmark experiments, (3) generation of DRF's for spectra libraries based on positions and their peak to total ratio, (4) measurement of the experimental spectra for unknown positions of the sources, (5) initial guess of the position of the highest energy of the sources based on the peak to total ratio of the spectrum. And least squares fit for the position of this source's position, (6) spectrum stripping reduces this source information from the total spectrum, (7) repeat step 5 and 6 until the positions of all sources are analyzed. The process from step 5 is demonstrated in Figure 6.9 with four different sources of K40, Kr 85, Cr51 and Cs137:

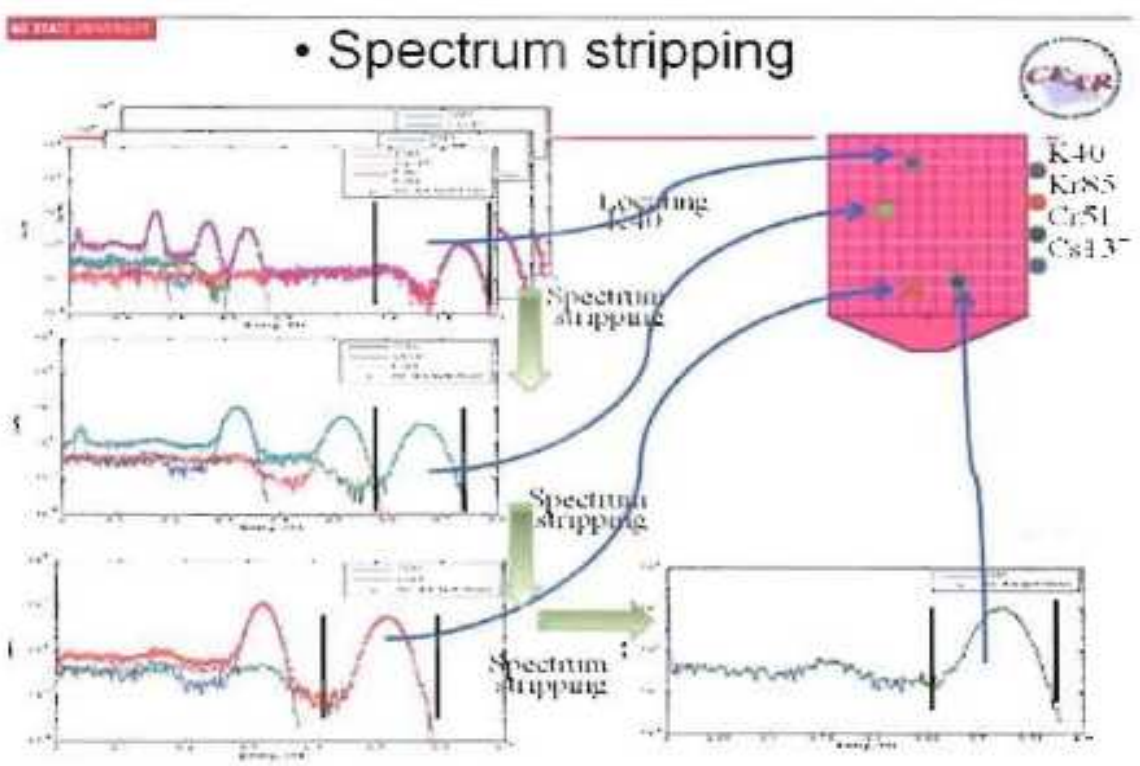

Figure 6.9 Illustration of the spectrum stripping deconvolution of multiple radioactive particles

Differential Operators (DO's) is a method very powerful for measurement sensitivity study and system optimization. The Monte Carlo Differential Operator Library Least Squares approach was successful implemented for simulation differential responses of both sample and elemental library spectra for variations of elemental concentration by in EDXRF (Gardner, R.P., F. Li and W. Guo, 2006). By using the Taylor series expansion, these differential responses can be used for spectrum adjustment. This is potentially a very accurate approach for taking into account of the nonlinear response due to interested factor like the positions of the sources.

The Taylor Series Expansion behind differential operators is shown as:

$$R(\varpi_{1,x},\varpi_{2,x},...\varpi_{n,x}) = R(\varpi_{1,0},\varpi_{2,0},...\varpi_{n,0}) + \sum_i \frac{\partial R}{\partial \varpi}(\varpi_{i,x} - \varpi_{i,,0}) + O(\varpi_x - \varpi_0)^2 \quad (6.9)$$

where $R(\varpi_{1,x},\varpi_{2,x},...\varpi_{n,x})$ is the detector response or called spectrum for the position x, and $R(\varpi_{1,0},\varpi_{2,0},...\varpi_{n,0})$ is the spectrum for reference position of x=0. With a pre-calculated differential operator, we can predict the response in x with the response at position x=0.

A technique called Inverse DO's (IDO's) is also proposed for real-time multiple radioactive particles tracking. The principle is using the changing of the spectra in different positions to predict the changed positions. Derived from Eq6.9 for each channel:

$$\frac{R_{i,x} - R_{i,x_0}}{\frac{\partial R}{\partial \varpi_{i,x}}} + x_0 = X_i \quad (6.10)$$

And then the target position for x will be average of all channels' predictions:

$$x = \overline{X_i} \quad (6.11)$$

This method required:

1) Accurate pre-calculated DO's.

2) Accurate measurement of the changing of the spectra.

But it will not involve any fitting actions any more. And only simple mathematical treatments are applied. These features will make real-time particles tracking possible. The MCNP simulations indicate this method works pretty well only with six un-collimated 2"X2" NaI detectors. But in this dissertation, the author will only focus on the general MCLLS approach.

6.4 Un-collimated detectors system arrangement

6.4.1 Detectors and configurations

Since was found in 1948, the NaI (TI) detector had become one of the most used scintillation detectors. The noblest property of NaI is its excellent light yield. It has come to be accepted as the standard scintillation material for routine gamma-ray spectroscopy and can be machined into a wide assortment of sizes and shapes. A research of optimal detector for flow mapping in opaque reactor reveals that NaI does have advantage over the BGO detector (Roy, Larachi, Al-Dahhan and Dudukovic, 2002). They drew the conclusion after comparing the resolution and sensitivity of the two types of detectors with the same size, where resolution refers to the sphere of uncertainty around the exact particle position and sensitivity refers the fractional change in detection with small

change in tracer's position:

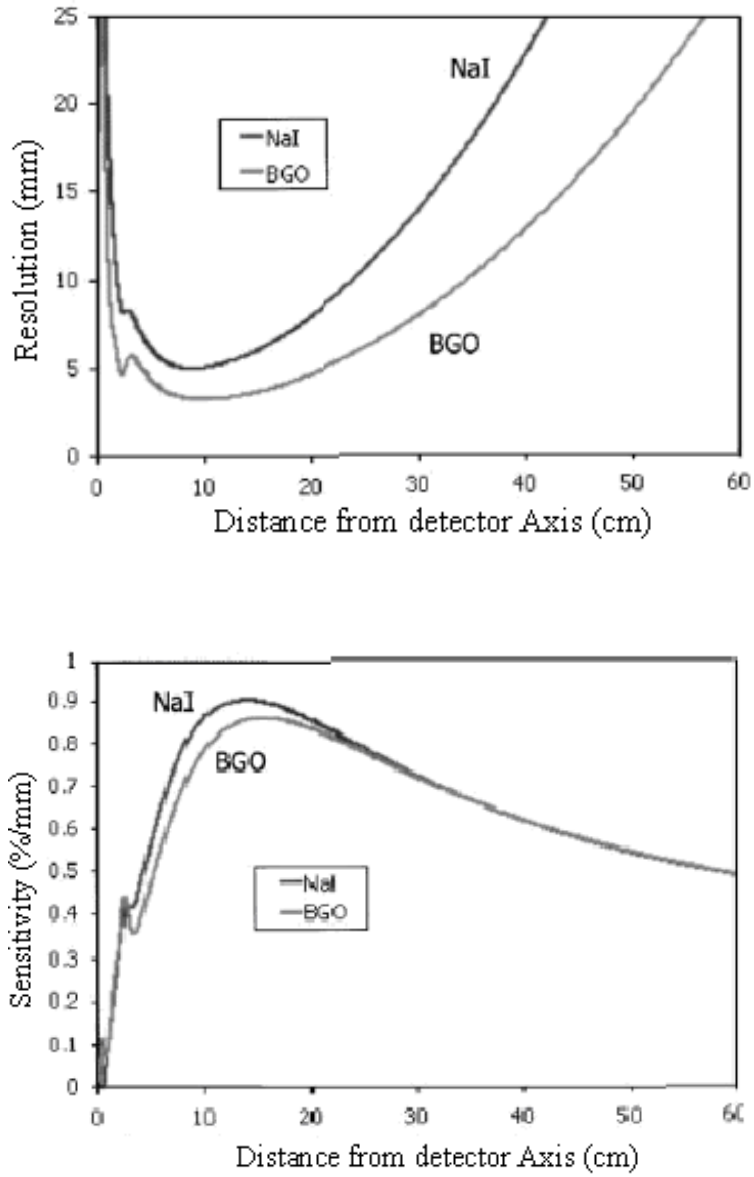

Figure 6.10 Comparison for NaI and BGO for Resolution (top) and Sensitivity (bottom)

Figure 6.10 shows that the NaI has over all better behaviors for resolution and sensitivity property against BGO detector, which is a popular alternative scintillation

material, $Bi_4Ge_3O_{12}$ (BGO) is commercially available as crystals as well.

The detector size is also an important parameter for resolution and sensitivity. Large detector have higher detection efficiency, but with lower resolution and sensitivity, shown in Figure 6.11.

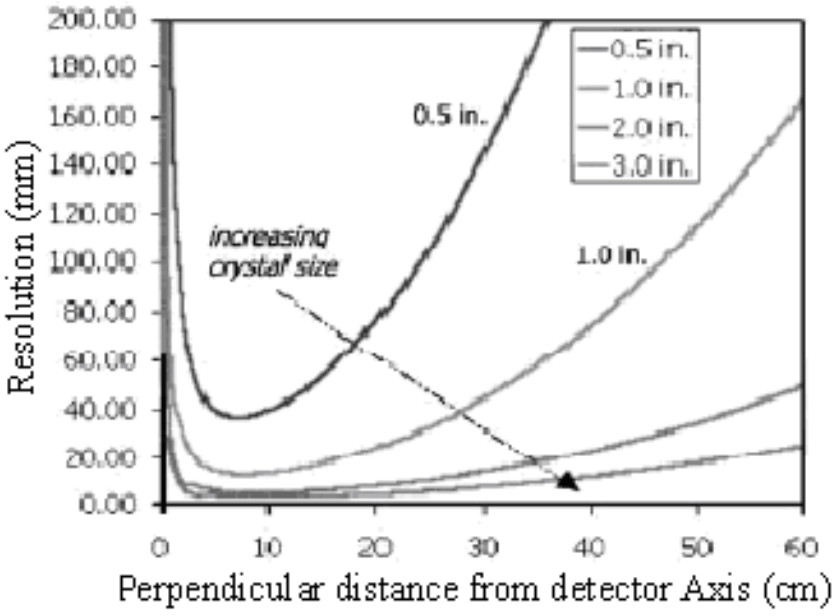

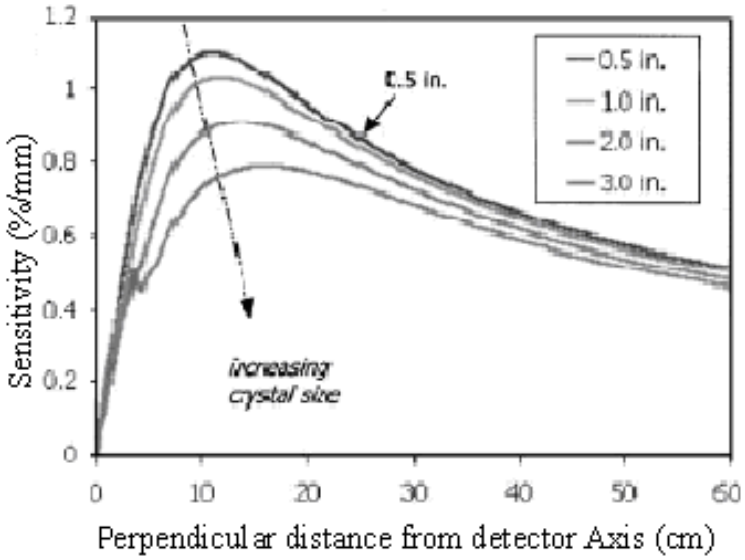

Figure 6.11 Effect of Size of Resolution (top) and Sensitivity (bottom)

It indicates that the smaller size detector has better capability in position tracking applications. But the smaller detector has lower detection efficiency, for example, has lower peak efficiency (Knoll 2000):

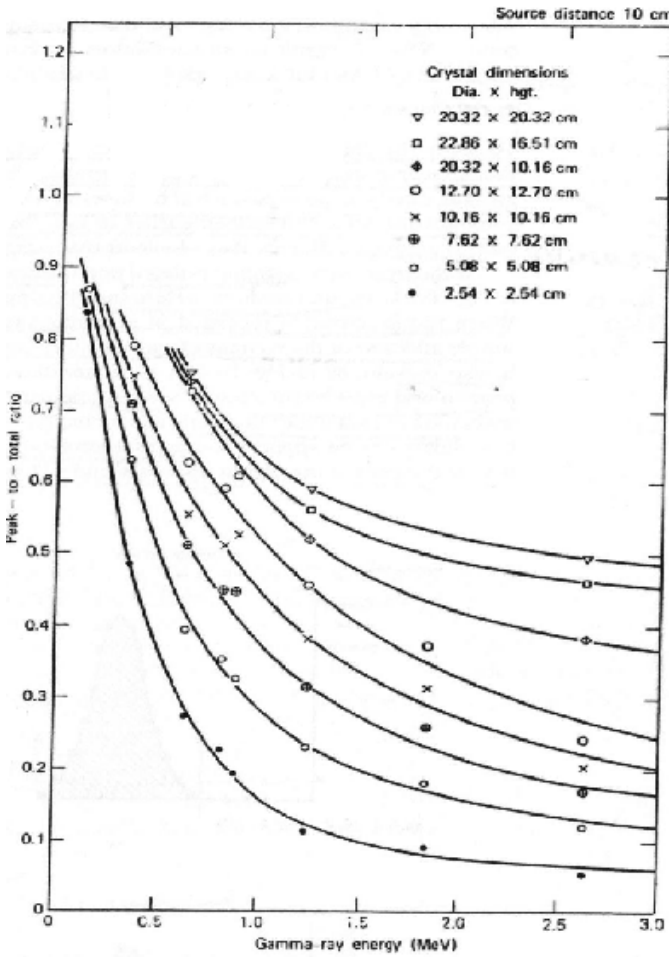

Figure 6.12 Peak-to-total Ratio for Various Sizes Detectors

It is a trade off problem between detection time and detection accuracy, in our case with a 30 cm X 30 modeling PBR, 2 inches (5.08 cm) right detector is a good compromise for multiple detectors space, detection yield, and considerate resolution and sensitivity. Some other factors also affect the detection efficiency. In our case the size of the modeling PBR, the intensity of the source and distance of the detectors from the PBR can all affect the detecting time for a good statistical uncertainty. In a case of Cs-137 source with 15μCi in the center of the 30 cm diameter modeling PBR, a 2"X2" NaI

detector needs around two hours to have a confident spectrum for MCLLS analysis.

Configuration of the Detectors:

Our interested area is shown in Figure 6.12, as the whole are of the modeling PBR. For plane interested for tracking a typical arrangement of the detectors is that the detectors are uniformly position around the plane (Larachi, Chaouki and Kennedy 1995) is the optimal solution. And obviously, more detectors can provide more information and can increase our confidence in the final result. As a result from the collimated detector system of the single particle tracking, the pebble motion is focus on the a plane cross the axis of the bed, if we neglect the motion out of this plane, we can use less detectors and focus on the tracking problem in this 2-D plane ABCDEF in the Figure 6.13:

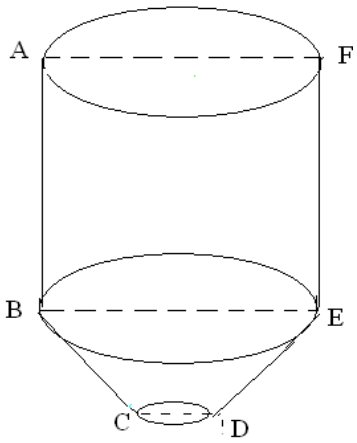

Figure 6.13 Motion plane ABCDEF

For optimal solution the detectors should be uniformly distributed around this plane. A symmetrical arrangement of six 2"X2" NaI detectors is adapted in this case. The

configuration of the system is shown in Figure 6.14:

Figure 6.14 Un-collimated detectors tracking system

6.4.2 Electronics and software II

The MCLLS method is an application analyzing the spectrum other than total counts. Each detector in the system obtains a spectrum with a Multiple Channel Analyzer (MCA). A 900 V high voltage is added to the 2"X2" NaI detector from the power supplier. The detector output signals are connected to a linear amplifier; the output is then connected to a 7072 dual channel Analog –to- Digital-Converter (ADC); the output signals then connected to a Multi-Parameter Analyzer (MPA) system - eight Single Parameter Analyzers (SPA) are available in our system; and finally the signals from the six detectors are connected from the MPA to the host computer and controlled by a Labview program. The electronic set up is shown in Figure 6.15:

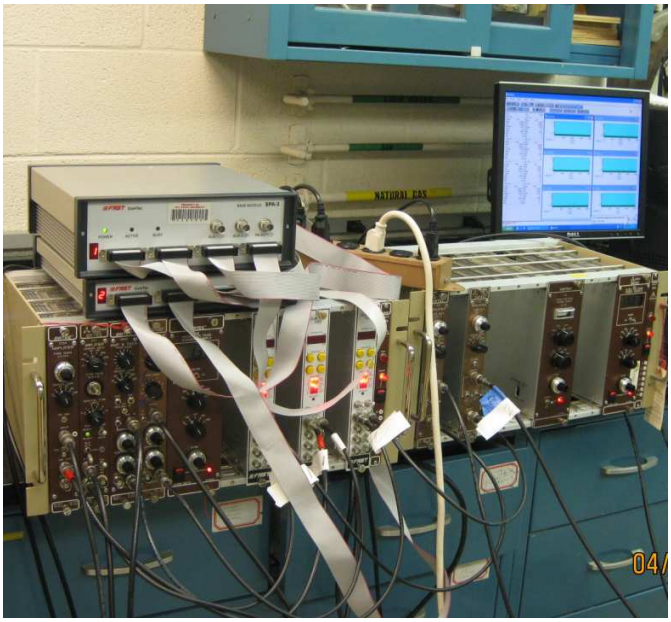

Figure 6.15 Electronics set up for un-collimated detectors system

The connection logic for each branch of the six detector system is shown in flow chart in Figure 6.16:

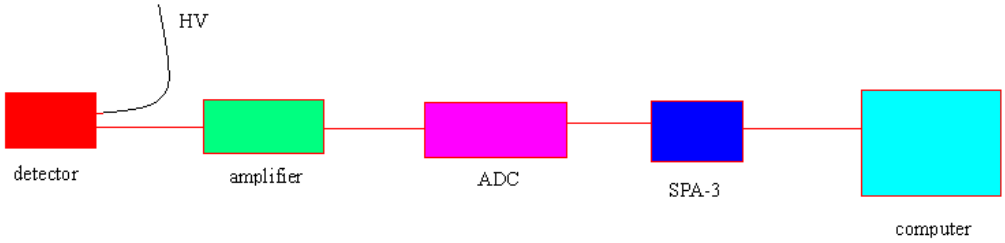

Figure 6.16 Electronics flow chart in un-collimated detectors system

7 . EXPERIMENTS AND RESULTS II

Benchmark experiments are very important in Monte Carlo simulation codes design and application. In the case of using MCNP5 to generate the libraries, there are two

aspects of benchmark experiments. The first one is to verify the accuracy of the DRF's. The second one is to verify the correction of the geometry input of the problem in the simulations.

Single and multiple radioactive particles tracking applications of the un-collimated detectors system with pebbles tagged with Cs137 and Co60 respectively in the modeling PBR is demonstrated. The Collimated detector system is used for benchmark purpose in the same time.

7.1 Benchmark experimental results

In a cave similar to the Heath (1964) experiment, a 2"X2" NaI detector is put into it with around 2 inches lead shield on five sides, except the top. The detail geometry of the experiment is simulated in the MCNP5, Shown in Figure 7.1.

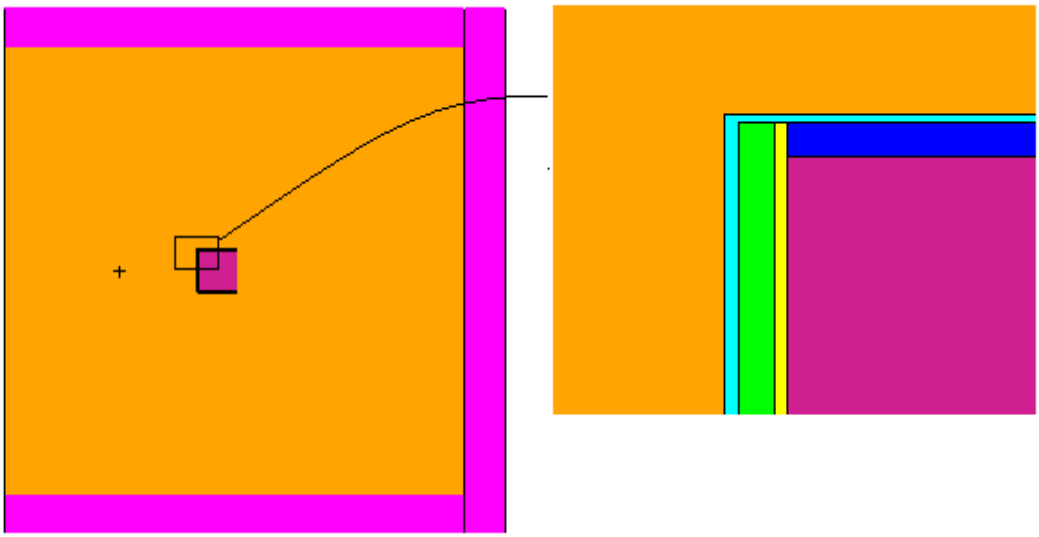

Figure 7.1 the lead shielding cave with detector (Left); the details of the 2"X2"NaI detector (right)

A Cs137 Source is placed 10 cm to the detector surface on the top on the axis. The simulating from the Modified MCNP5 and experimental results are compared in Figure 7.2. Note the MCNP5 has different version as through the year of it development. In this cast we used a cluster base installed MCNP5.1.51. The Original modified MCNP5 for DRF's is developed in a single PC with version MCNP5.1.14. They have a slight different behavior with the flat continua factors. As we adapted the cluster built in CEAR in Nuclear Engineering Department of NCSU, we benchmarked this code with this version.

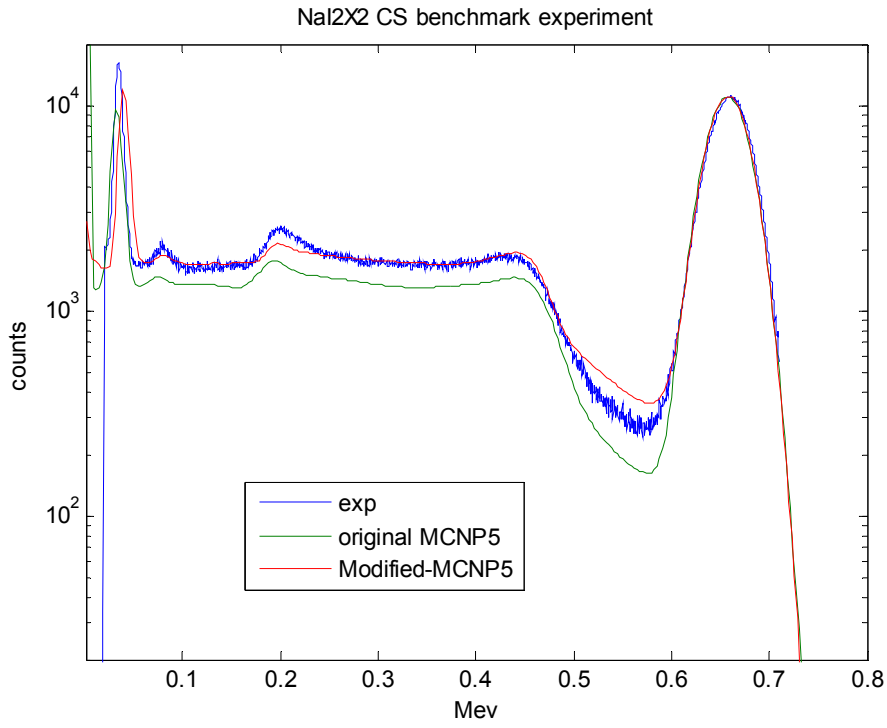

Figure 7.2 Cs137 benchmark experiment for 2"X2 NaI in Cave

The modified MCNP5 code shows higher accuracy in the overall spectrum comparing with the original MCNP5. The flat continua part is strongly affected by the electron cross section correction in the code and a very good understanding of the detector geometry arrangement. The thickness and composition information of the aluminum can and reflection materials between the can and the NaI crystal is directly acquired from the detector manufacturer. The biggest difference between the Modified MCNP5 simulation result and experimental result is the valley part, but where the count is one magnitude lower than the count in the flat continua part, and two magnitudes lower than the count in the full energy peak.

Another aspect of benchmark is important for any real application arrangements, unless you have accurate information before hand. According to the un-collimated detectors system arrangements in Figure 6.14, a serial of simulations are carried out and compared with the experimental results. The real experimental configuration is simulated as shown in Figure 7.3. Note the collimated detectors system is used for the position of source for benchmark purpose.

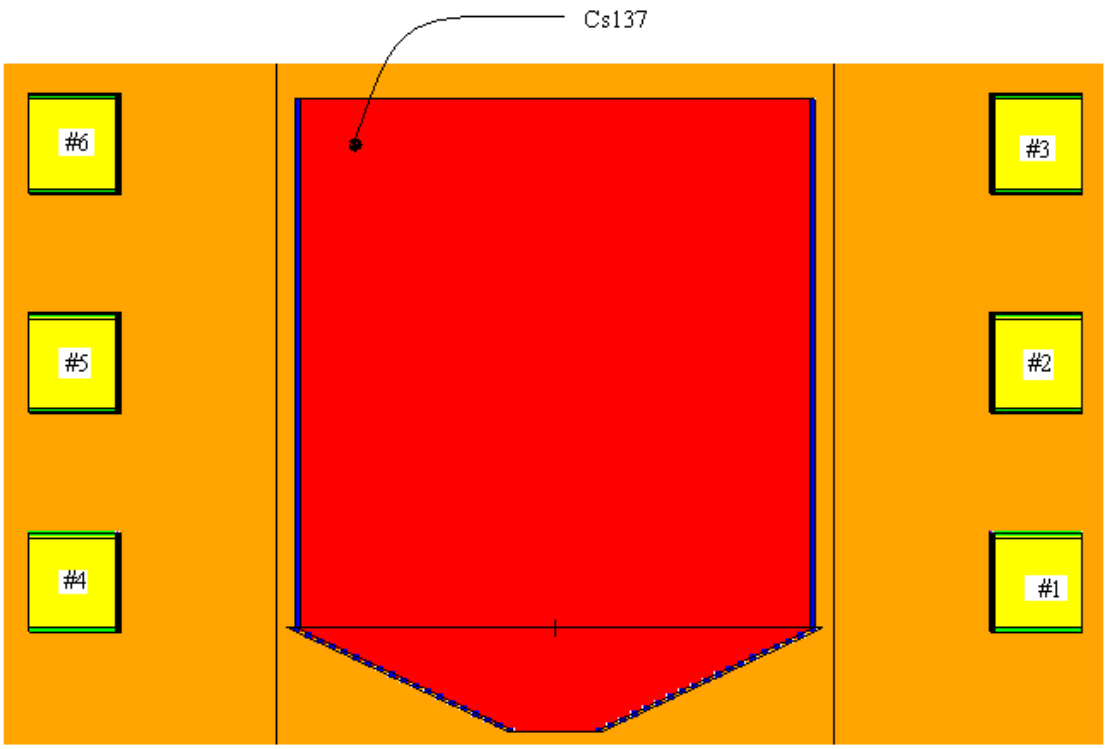

Figure 7.3 The MCNP5 input plot in simulation

A Cs137 (15u Ci) source tagged pebble is put in to the modeling PBR in a position of

(-12, 0, 28)-located with the collimated detectors system. A measurement for two hours with the un-collimated detector system is used to acquire the net spectrum in the six detectors simultaneously. The benchmark experiments in this step are to confirm the geometry configuration of the system and the densities of the materials are used in the simulations.

As the modeling PBR is designed and manufactured in our lab, the geometry can also be confirmed by measurement. The geometry in-correction is not a significant factor to be concerned. The modeling PBR walls are made of 2 mm aluminum metal. The thickness of the wall is small compared with the 30 cm diameter of the whole modeling PBR. And the aluminum density is well known as $2.7\, g/cm^3$. As the pebbles are mimicked with marbles, the density of glass can vary from 2.4-2.8 g/cm^3. And most importantly the pebble void faction is uncertain with a random packing style as we used in our case. This benchmark experiment can be used to verify the density of the pebbles area (the red part in the figure 7.4). Because the source is closer to the detector #6 (see Figure 7.4), the spectrum from this detector has best statistical fluctuation

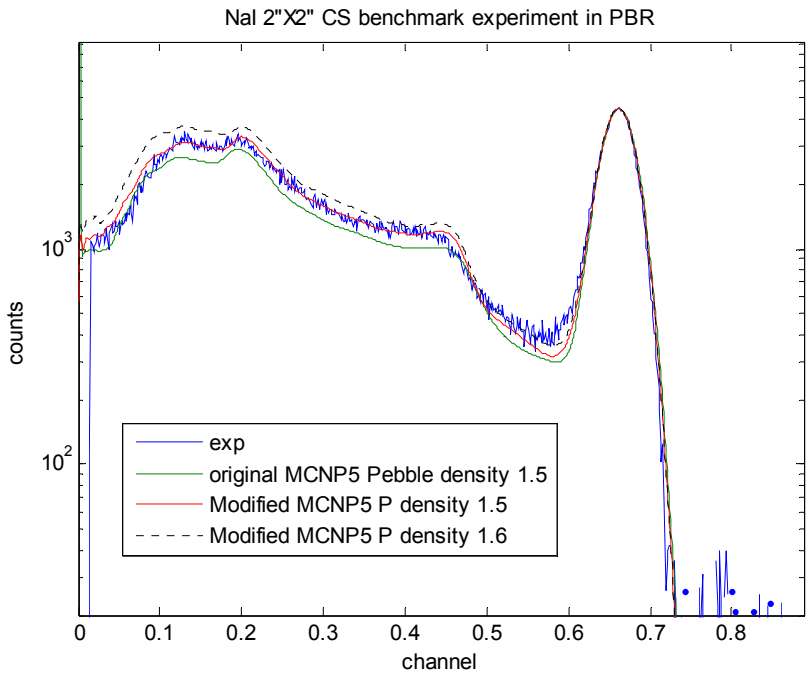

Figure 7.4 Cs 137 benchmark experiment in PBR

The benchmark experiment shows that the density of 1.5 g/cm^3 is the best parameter for detector #6. When the density is not correct, for example the black dot line in the figure 7.5, the spectrum will not match the experimental results. When the density is over estimated, the Compton scatter part of the spectrum will be higher in the simulation than the experimental results, and lower density results in the opposite. The result is based on an assumption that the position of the source is very accurately estimated by the collimated detectors system. But the two systems are set into two coordinate systems, and these two systems must be coordinated exactly. The source in different positions, the spectra different response is the basic idea of MCLLS method for particles tracking. In this benchmark process, the density of the pebble volume and the

position of the source both can affect the spectrum. If the position of the source has been estimated mistakenly, the density will also be estimated wrongly in the same time. But the advantage of this system is that there are six detectors, if we can benchmark the sex detectors with the simulations of all the six detectors with the same estimated position and pebble volume density, then these two estimated parameters can be corrected in the same time.

The plots for benchmark results for detectors #4 and #5 are shown below in Figure 7.5:

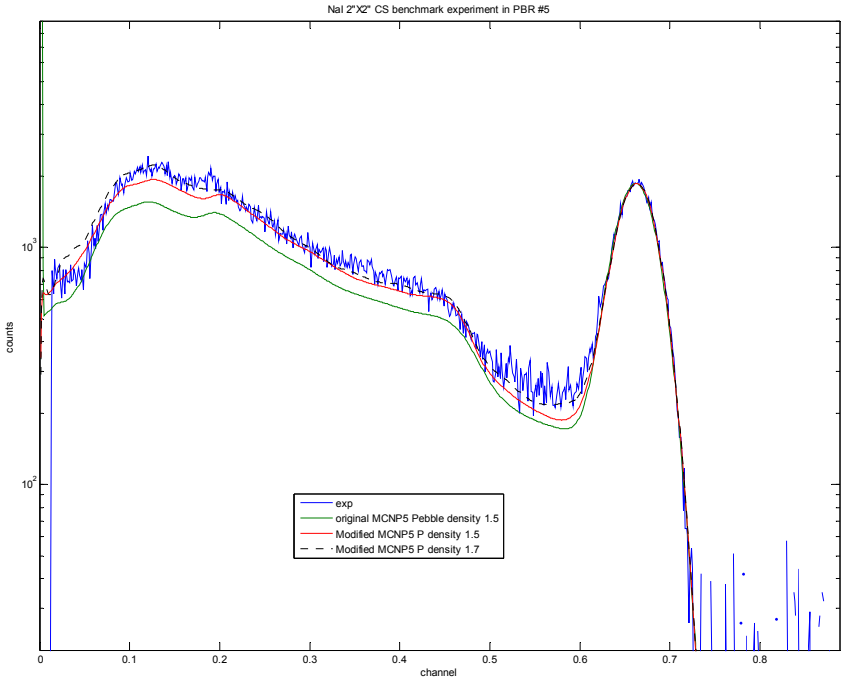

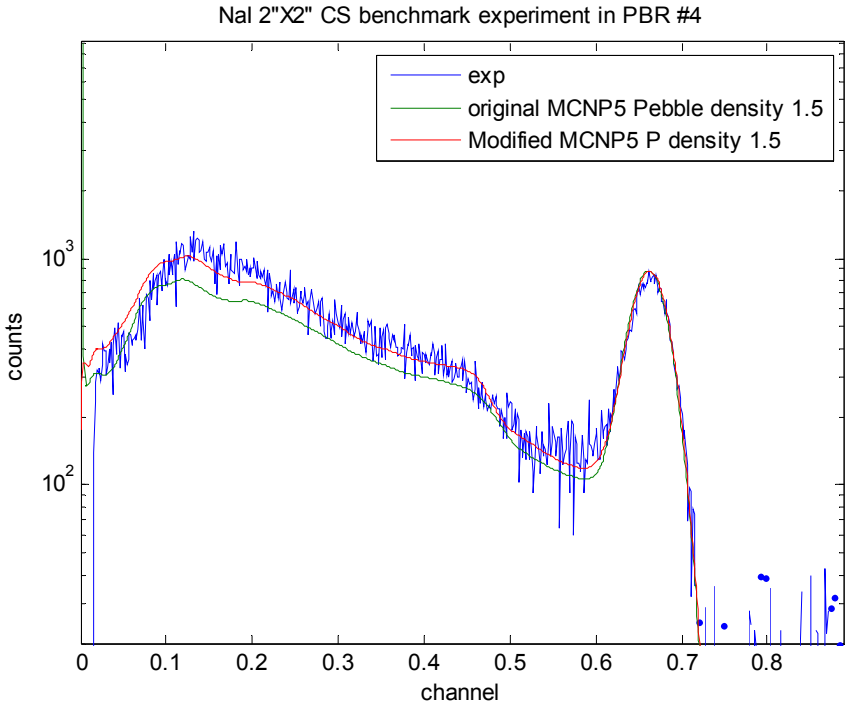

Figure 7.5 Benchmark results for detectors #4 (bottom) and #5 (top)

The benchmark results show that both simulation results from #4 and #5 detectors are fitting well with the experimental results. But as the detector distance to the source increasing, the spectrum statistic fluctuation goes worse dramatically. The results of detectors of #1 to #3 are not used for benchmark purpose in this process, because the statistics in these spectra are too bad, which are out of the certainty confidence.

7.2 Particle tracking testing results

As mentioned in section 6.3, after we accurately benchmark the Monte Carlo simulation code- Modified MCNP5 with correct geometry configuration and materials densities, the next step is using all these information to set up the library package of all the sources that will be used in the later tracking process.

A spatially based library must be set up for position tracking purpose. An issue rises immediately: what is the optimal way to set up the library in the interested space? There are two criterions to be compromised: one is the efficiency of the library; another is the accuracy requirement. Basically, the library package contains the fewer libraries with the higher efficiency; and the space more detail cut into libraries the system can reach higher accuracy. There is an optimal point for this problem: set up the elements small enough where the spectrum change can reach the linear assumption.

The simplest elemental set up method for this problem is square elements, which set

up the libraries into square elements:

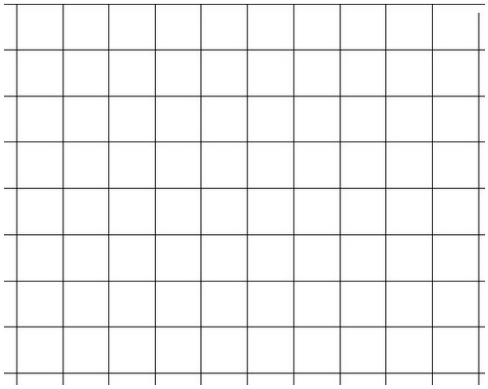

Figure 7.6 Square elements for libraries

Each node in the Figure 7.6 presents a library. The side length is critical for the two criterions mentioned above. Larger side length means higher efficiency but less accuracy. A series of simulations with MCNP5 is carried out to find the optimal length with 5cm, 2cm and 1cm respectively. The results show that when the length reach 1cm the prediction position can be confident with the true position.

Table 7.1 The side length of square elements:

Cells	Libraries nodes (x,z),y=0(cm)	True position	Predicted position &errors
5cmX5cm	(-5,10),(-5,15) (-10,10),(-10,15)	(-6,12)	(-6.196,13.829) (3.26%, 15.24%)
2cmX2cm	(-4, 15),(-4.14) (-3,15),(-3,14)	(-3.9,14.2)	(-3.525, 14.501) (9.62%, 4.27%)
1cmX1cm	(-5,10),(-5,11) (-6,10),(-6,11)	(-5.5,10.4)	(-5.492,10.402) (0.14%, 0.014%)

The results in the table7.1 show that the side length of the square elements is safe for

accuracy with 1cm. This parameter actually is highly depended on the pebble volume density, the higher density need smaller side length to reach the linear assumption of the spectrum change.

The MCLLS method uses the libraries equally important. But in the square element ABCD shown in Figure 7.7, the four libraries A, B, C and D are not equally important. There are six relationships among these four libraries: AB, BC, CD, AD, AC and BD, the previous four relationships are equally important in a spatial point of view. But the AC and BD are $\sqrt{2}$ of the previous ones in spatial point of view.

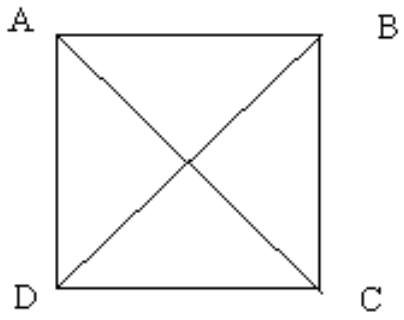

Figure 7.7 Square element libraries relationship

A solution for this problem is using triangular elements:

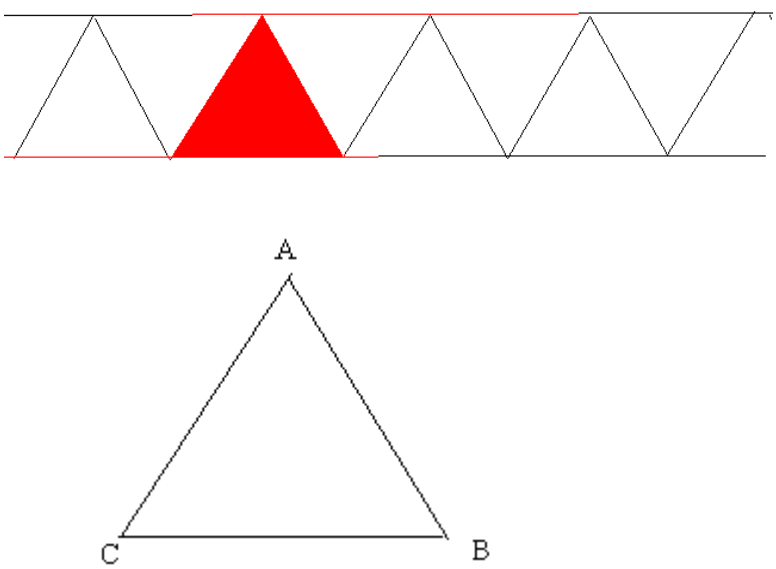

Figure 7.8 Triangular elements

In this scenario the libraries A, B and C have all equal importance in spatial point of view. And each fit only includes three libraries. As the fitting process sweep through the interested area search for minimum Chi-square, each time of sweeping will include less library substitution that makes the sweeping process faster than the square elements scenario, but with a much more complicate configuration and searching process.

7.2.1 The testing experimental results for single particle:

This innovative tracking method was tested in our lab condition with the collimated detectors system. Two aspects of tracking ability of this method have been tested: one is the ability to locate a single source position in the modeling PBR; another is the

capability of locating multiple (at least two) radioactive particles in the modeling PBR.

With a Cs137 tagged pebble in a known position-result from the collimated detectors system, a process of fitting search for minimum Chi-square is used for the position of the source. The process is reported into table 7.2:

Table 7.2 the search of the minimum Chi-square

Element#	Chi-squares	Sum area	Estimated position
1	1.096	97.5%	
2	0.931	98.7%	
3	0.980	98.1%	
4	0.766	98.8%	(4.70,21.52)
5	0.809	98.4%	
6	0.769	98.8%	
7*	0.871	98.3%	

The elements spatial relationship is shown below:

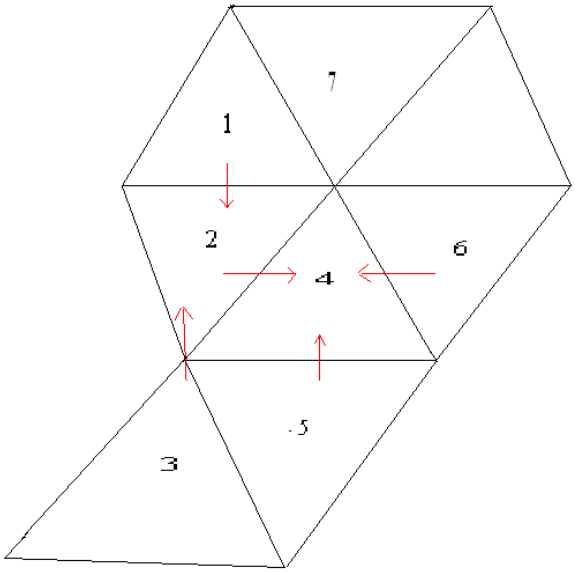

Figure 7.9 Elements in testing experiment

In this case, the initial guess position of the source is in the region of element #1 in Figure 7.9. The MCLLS method is first used to fit with the three libraries of this cell, and report and store a result Chi-square of 1.096. A sweeping search is in a direction from the top to the bottom, and then from the left to the right, because the pebble in the core is going from the top of the reactor and down exit from the outlet at the center bottom of the core. In a case of using the previous position of the source as an initial guess to stop a new search for new position of the source this search direction is the most efficient one. If the initial guess is the start point, and estimating the position of the source too low, then the down-ward search will reach an increasing Chi-square immediately, and only in this scenario an-up ward search process is necessary. A so called “Chi-square Flow” searching direction is defined as searching from the higher Chi-square to lower Chi-square. When sweeping down, the fitting in # 2 cell reported a decreased Chi-square 0.931. So, it will

continue sweeping down to #3 cell and reach a increased Chi-square of 0.98. The sweeping process will restart from #2 cell and sweep from left to right, reach the #4 cell with a Chi-square value of 0.766. The similar process goes on the sweeping was reflected back to #4 cell from #5 and #6 cell with increasing Chi-square 0.809 and 0.769 respectively. A cell #7 is also reported as reference, but the sweeping process will not go through it. Totally five fitting process is demonstrated in this searching to locate the source position at (4.70, 21.52). Comparing with the benchmark position report by the collimated detectors system at (4.50, 21.5), the result is considered good. The Sum area in the table indicates how well the fitting result spectrum matches the experimental spectrum.

A similar process is used to test whether the original MCNP5 has the capability of locating the position of the source. The same searching process with the libraries generated from the original MCNP5, reports a position of (3.40, 18.06); the minimum Chi-square value 25.6; and Sum area 86%. First of all the estimated position of the source is difference from the result of the modified MCNP5. And more importantly, the Chi-square value is too high, and the fitting is not good with a Sum area result 86%. The results show that the modification of the MCNP5 in this method is necessary. The results are shown in table 7.3:

Table 7.3 The searching results with original MCNP5”

Elem#		Sum area	estimated
1	25.90	85.3%	
2	25.70	86%	
3	25.70	86.%	
4	25.70	86%	
5	25.50	86%	(3.40,18.06)
6	26.40	84%	

7.2.2 The testing experimental results for two particles:

Two sources Cs137 (0.662Mev) and Co60 (1.173, and 1.332Mev) tagged pebble were put into the modeling PBR in location (-6.2, 25.0) and (7.5, 24.0) respectively. The total spectra are shown in Figure 7.10:

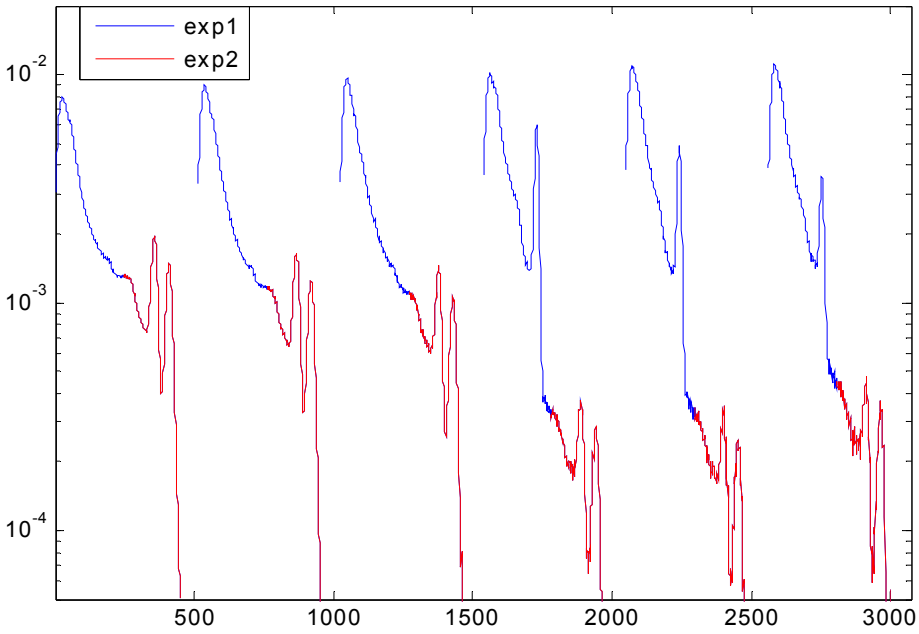

Figure 7.10 Multiple Source spectra with Cs137 and Co60

In this case, spectrum in each detector has 500 channels. The channels from 251 to 500 are used to analyze the information of Co60 source pebble, and channels from 1 to 250 are used to analyze the information for Cs137 source pebble. For each single spectrum the spectrum is cut into two parts into process of locating the positions of the particles:

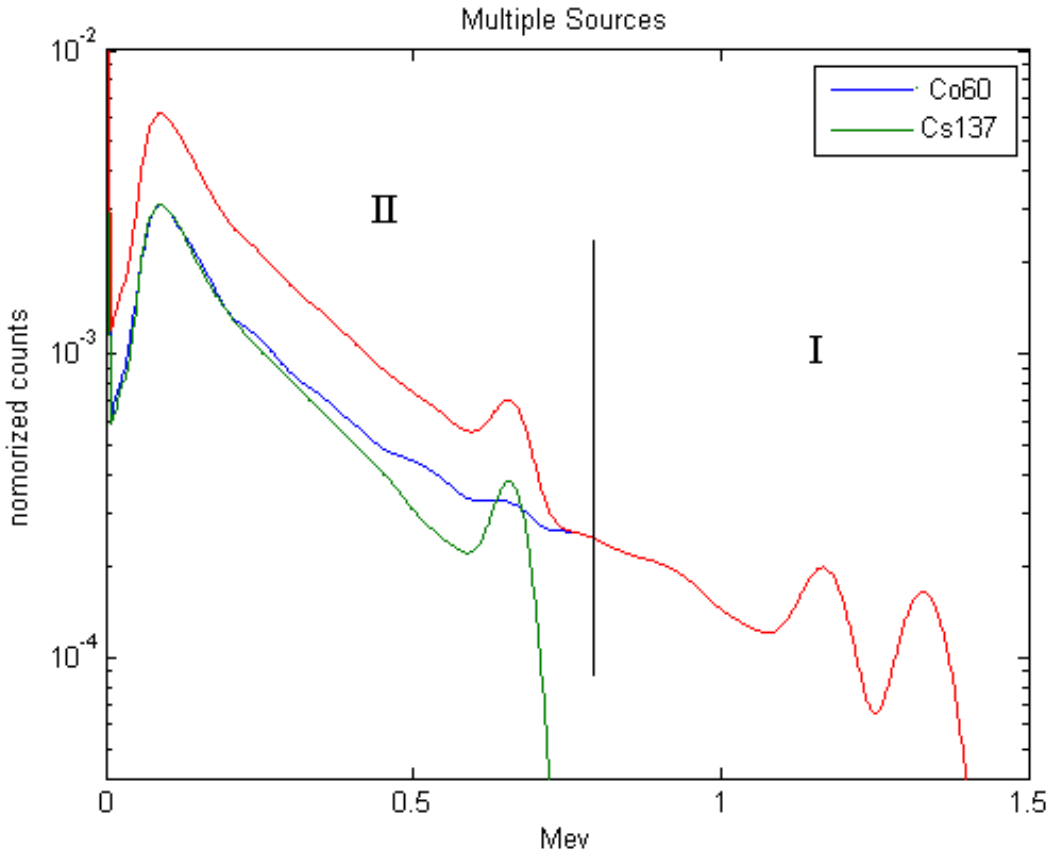

Figure 7.11 Spectrum for multiple source treating process

Showing in Figure 7.11, the spectrum in region I is used to fit for a minimum Chi-square for locating the position of Co60. A Chi-square value of 1.07 is reported with an estimated position of (7.39, 23.86), the Sum area is very good, with a value at 99.7%. This means we can fit the unknown spectrum very well with only 0.3% error caused by fitting process. This error will be propagated to the next process of fitting for the position of source Cs137. When using the original MCNP5 for this tracking purpose, with a Sum area of 86%, the error propagated to the next step will be overwhelming, and may make the tracking process impossible for multiple particles.

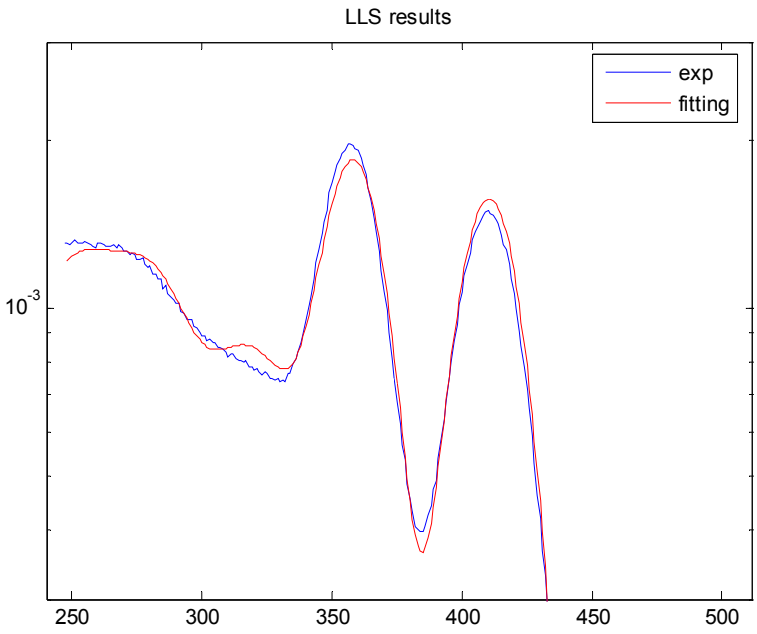

Figure 7.12 The fitting results of Co60

A process of spectrum stripping is used after the fitting for the Co60. In Figure 7.12, the fitting results for Co60 (blue line) is subtracted from the total spectrum (red line). The results end up as the net spectrum for the Cs137 (green line in Figure 7.11). The net spectrum of Cs137 is then used to perform another MCLLS process to locate the position of the Cs137 pebble and report (-6.08, 24.86) with a Chi-square of 5.71, and Sum area of 93.0%.

The results show a good capability of locating the positions of the sources in modeling PBR. Note: in this test the history applied to generate the libraries is only 2 million, if we increase the simulation history the Chi-square and Sum area can result with

a better value.

7.3 Particle tracking experiments and results

The experiment includes three major steps: unknown spectra measurements; library package arrangements; and the analysis for positions of the tracer pebbles with MCLLS method.

7.3.1 Experiment description:

The un-collimated detectors system is set to let the Cs137 (0.662Mev) full energy peak appear at round the channel of 500 and a total channel number is set to be 2048 and the Co60 (1.332 Mev) full energy peak is at around 1000 channel as a result. So the measurement can cover a to an energy range of 2.711Mev for potential more radioactive tracers to be added. The peak position is set by adjusting the magnitude of the amplifier, and total channel number is set by the program in the host computer.

For each unknown spectrum, it includes a measurement of the total spectrum with the radioactive tracers and a measurement of the background without the radioactive tracers. As the time between the measurements is close enough, the background can be assumed to be stable enough to be the same for all unknown spectra, so one measurement is

applied to all.

A single Cs137 tagged tracer is used in the modeling PBR for tracking purpose. As the pebble motion pattern is mostly depended on the position off the axis, the source tagged pebble is initially put in different off axis positions to study the whole region in the PBR. In order to achieve a good statistics of the spectra in measurement, with a Cs137 source at around 15μCi it requires one hour for Multiple Channels Analyzer (MCA) to measure. Of course increase the source intensity can short the measurement time, but in lab condition for safety purpose we increase the measurement time instead. But even with one hour measurement the detector far away from the source tagged particle still does not has appreciate statistics. For example a measurement with Cs source off the axis in 13 cm the first measurement "1301" spectra process in Figure 7.13.

Figure 7.13 Measurement examples for “Cs1301” The total view (top); the zoom in view for spectrum of detector one in the left hand side square (middle); the zoom in view for spectrum of detector six in the right hand side square (button):

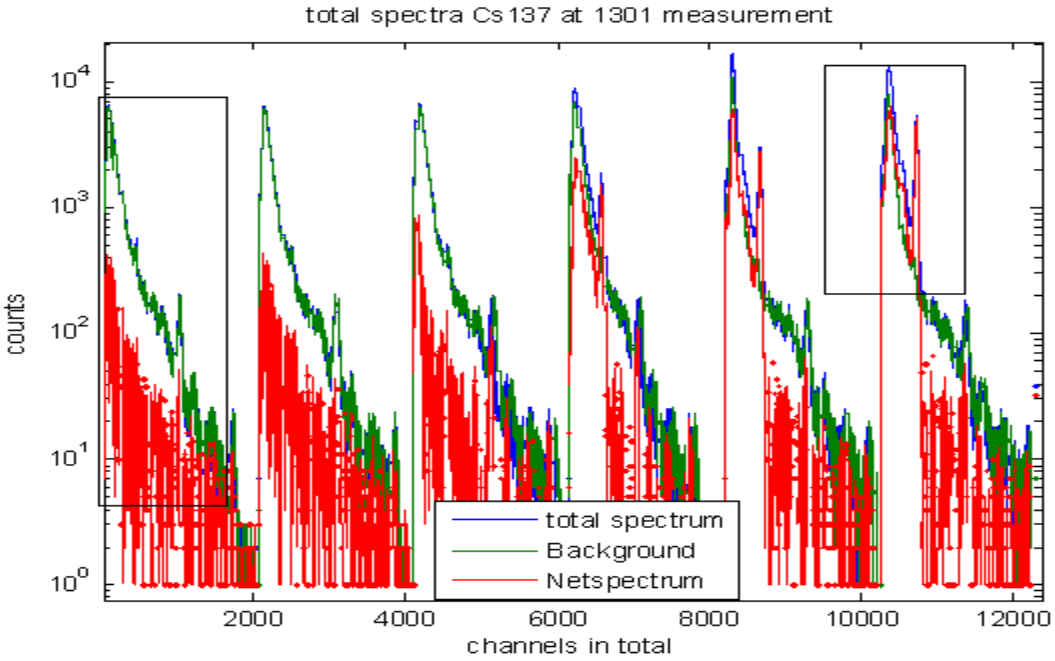

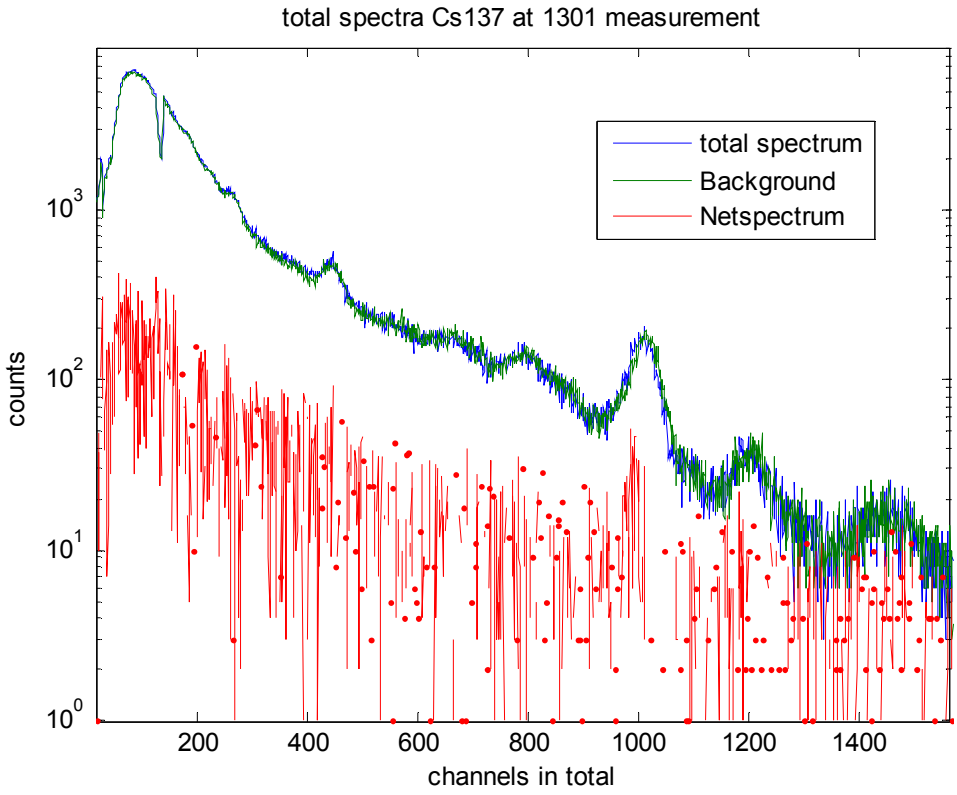

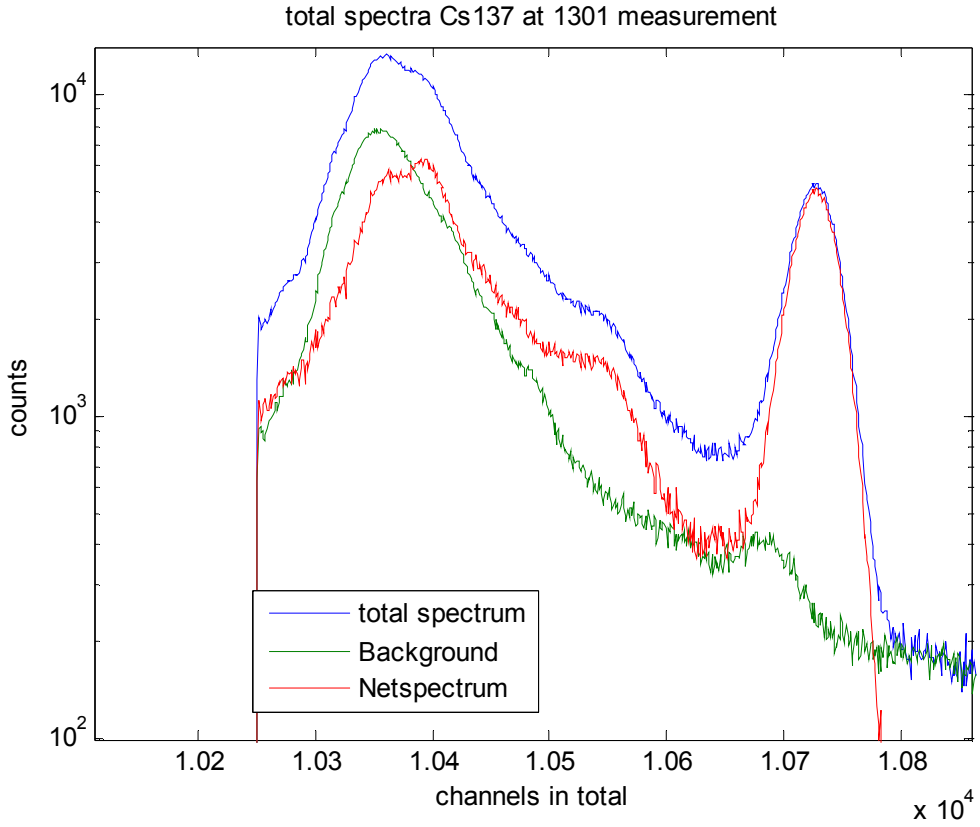

In the Figure 7.13, as the detector #1 is far always from the tracer, the Net spectrum is almost un-visible as a Cs source's response, but the detector #6 has a pretty good spectrum of typical Cs response with reasonable statistics errors. It means first of all, to achieve good statistics in all detectors may require very long time in measurement especially when the tracer pebble is far away from some of the detectors; secondly, use all the spectra in the six detectors to analyze the positions of the sources will induce too large errors if some of them have relative high statistic errors. Multiple detectors in this point of view, is to ensure that tracer pebbles can be measured with some detectors in any region inside the modeling PBR. And in the analysis process, only those detectors with low enough statistics errors will be used for MCLLS fitting, those far away detectors can be weighted out.

As the spectra capturing is time consuming, a stop-and-go mode is used to study the pebble motion in the modeling PBR. Every around 1000 pebbles discharging from the outlet of the modeling PBR, the pebble flow is stopped and measurement system is started for a measurement for one hour. Repeat this process until the radioactive tracer is discharged from the modeling PBR. For multiple particles tracking this process will stop when all tracers are discharged and the previously discharged radioactive tracer should be removed from the lab.

Table 7.4 shows how much iteration is needed for different initial positions off the

axis:

Table 7.4 iterations depended on off axis position for Cs137:

Initial off axis positions in X (cm)	Iterations(900 pebble/step)
1	7
3	13
5	14
7	14
9	13
11	15
13	19

It is indicated in table 7.4 that the pebble motion in modeling PBR has a stable region between 3 cm to 11 cm off the axis. A fast region is probably within 3 cm and a slow region around and beyond 13 cm off axis.

7.3.2 The arrangement of the library packages

In the triangle elements scenario the interested region in the modeling PBR is divided into spatial point for source position to run by Monte Carlo simulation to acquire the library package for each tracer source. With a length of 1.0 cm in the spatial element, the configuration is shown in Figure 7.14:

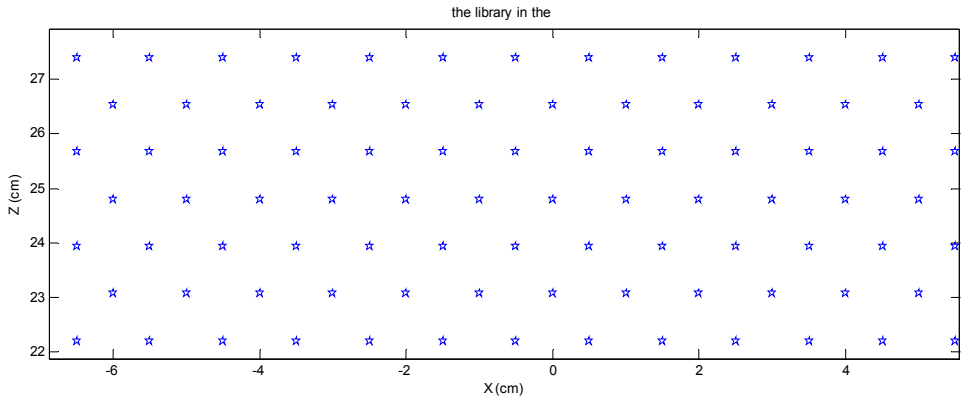

Figure 7.14 Spatial configuration of library

To cover the whole region of the modeling PBR, it needs 1092 libraries for each detector. For sex detectors totally is 6552 libraries. If the one library runs averagely need 5 minutes, then 23 days is required to prepare these packages for one source. And as the energy of the radioactive tracer source increase the running time will be longer, as expected. For example Co60 (1.332Mev) is around 50% increase in the running time compared with Cs137 (0.662Mev) for the same statistics error level.

As the libraries are thousands, group process is necessary for input files preparation, the running of the input files, output files treatments, library spectra preparations, and libraries arrangements into a package. The major process and supporting codes or scripts are described as below:

A “Perl” script adapted from MCNP5 parameter study is used to generate the input file for MCNP5 simulations, the variable here is the position of the source according to Figure 7.15. The series input files then performed a continue run into the cluster one by

one. The output files contain all other information of each run, including running time, interactions in cells. The simulation spectra in the output files are collected with another script written in “Matlab”. “Matlab” is used majorly in the data process for its powerful visible tool. The simulation spectra have to be performed a Gaussian Broadening and a source intensity adjustment.

The library package must be well arranged according to the positions of the source in order for the next step application: MCLLS analysis for the positions of sources.

7.3.3 The analysis for the positions of the sources

A code adapted from original MCLLS analysis code in “Fortran” is used for position analysis purpose. The original MCLLS code carries one time MCLLS fitting to analyze the unknown spectrum with the known libraries, and then report the fractions of each library. In the un-collimated detectors particles tracking system process is dynamic. The MCLLS fitting is iterated until it reaches the minimum Chi-square value. And then based on this minimum fitting result, a position is reported according to the libraries involved and the fractions they hold.

The searching for the minimum Chi-square method is critical in this method. A failure of reaching the real minimum Chi-square will result in a wrong position report and

cause a system error within the code. Of course, trying all the possible combinations (still adjacent required) of the library is the most secure pattern. But as the library is in thousands and the possible combinations will be thousands as well. And most importantly, an empirical result can be used to speed up the search process. In the PBR core, the pebbles always travel into two directions down ward to the outlet and to axis of the core. In a view as shown in Figure 7.15, for example, when the tracer particles are in the left hand side of the core. There are only four reaching schemes:

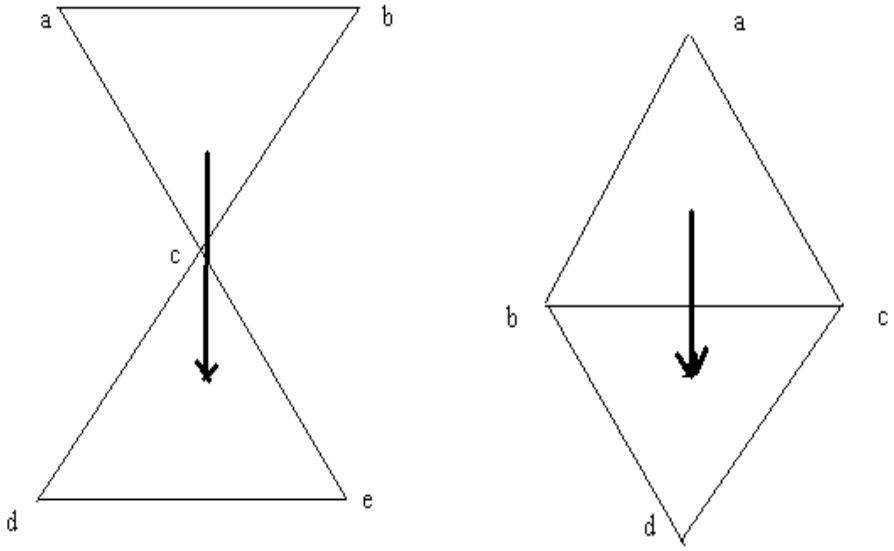

Figure 7.15 down ward searching schemes

In the left hand side the libraries “a” and “b” will be substituted by “a” and “e” simultaneously, while on the right hand side a will be substituted by “d”. Another two different schemes are similar to these two schemes but scans to from right to left in libraries substitutions. The reaching will start from down ward searching first, which has

been described in details in previous section 7.2.

7.3.4 The experimental results:

As the position searching process with Library Least Square (LLS) is relative fast, the initial guess of the first position of the source can be set higher and further to the axis than the real position of the source, shown in Figure 7.16. But the initial guess of the position of the source must be higher and further than the real position, or the reported results can not be trusted. And except the first position, the later search will use the output position from the previous fitting to make a reasonable initial guess. Considering the possible error, and boundary condition, the new initial guess uses previous position plus 1 to the further direction of the convergence without getting out of the PBR, shown in Figure 7.16:.

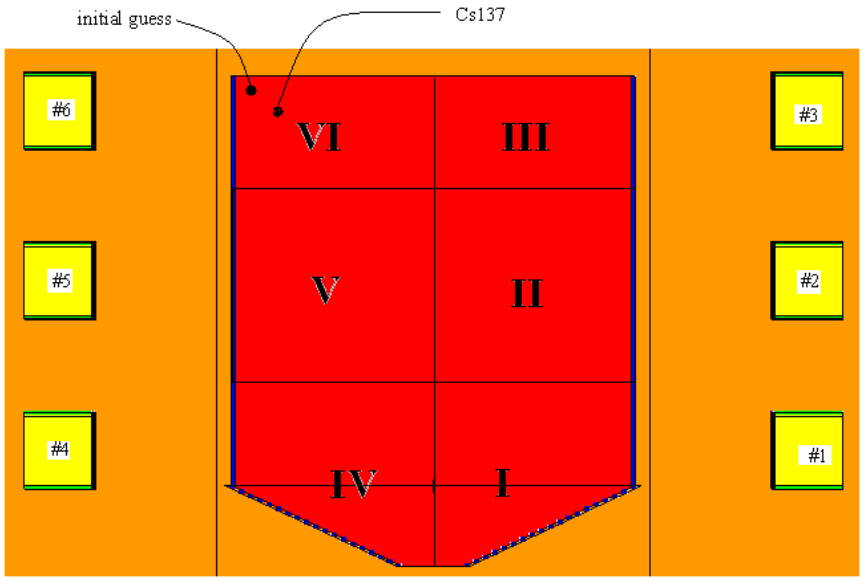

Figure 7.16 Initial guess and regions

The time consuming in the un-collimated detectors system comes from the measurement process. As pointed out in section 7.3.1, in a limited time of measurement and source intensity, the interested region is further divided into six areas according to the library and detectors arrangements. The searching process in the area would use the corresponding detector's library and measured spectra only.

A typical output of the fitting process is shown below in Figure 7.17 and interpreted in table 7.5:

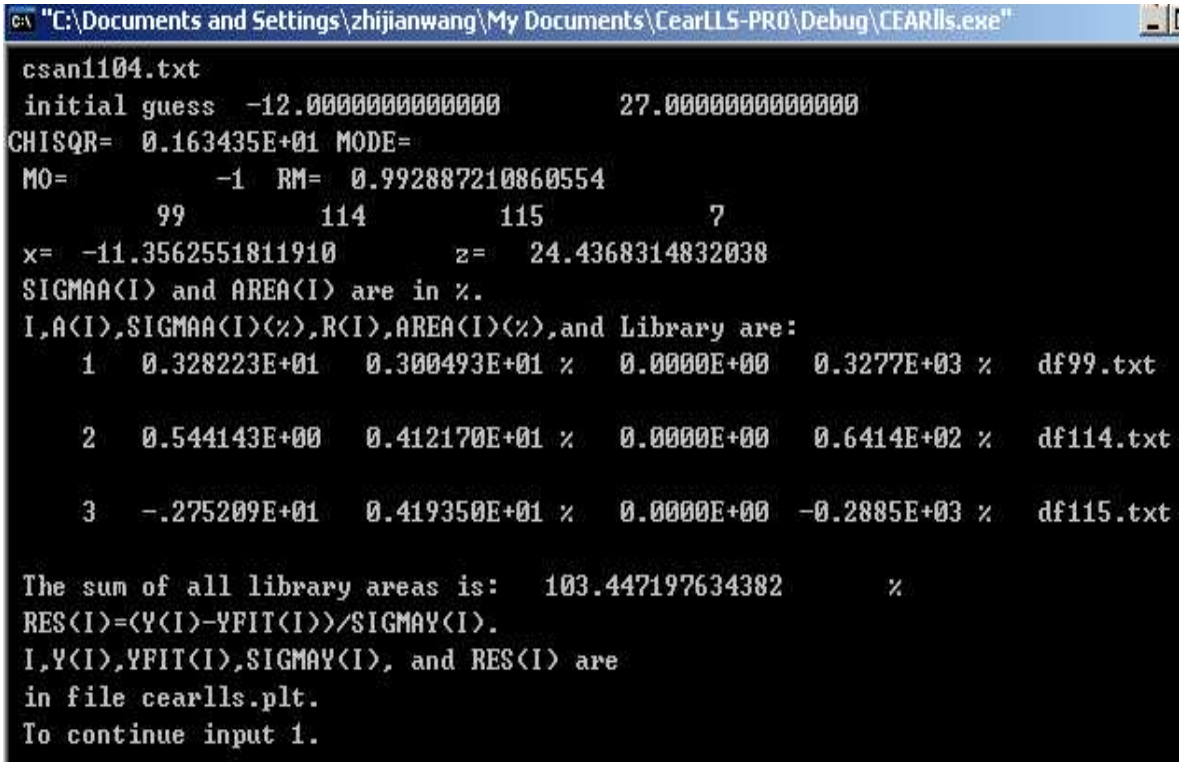

Figure 7.17 Output information for position search

Table 7.5 the interpretation of the output:

Items	Values
Measured spectrum	Csan1104.txt
Initial guess (x,z) (cm)	(-12,27)
Minimum Chi-Square	1.63435
Standard deviation mode	-1 (for Poisson distribution)
Multiple linear correlation Coef. Rm	0.99289
Final elements for position of the source	“df99.txt”,”df114.txt”,”df115.txt”
Fitting iteration times	7
Position of the source (x,z) (cm)	(-11.356,24.437)
Libraries fractions	(3.28223,0.54414,2.75209)
Sum of library area	103.447%

The output results show a pretty good fitting in the final element of the search with a Chi-square of 1.63435, and Sum area of 103.447%. The fitting spectrum is compared with the measured spectrum in Figure 7.18 and residuals plot in Figure 7.19:

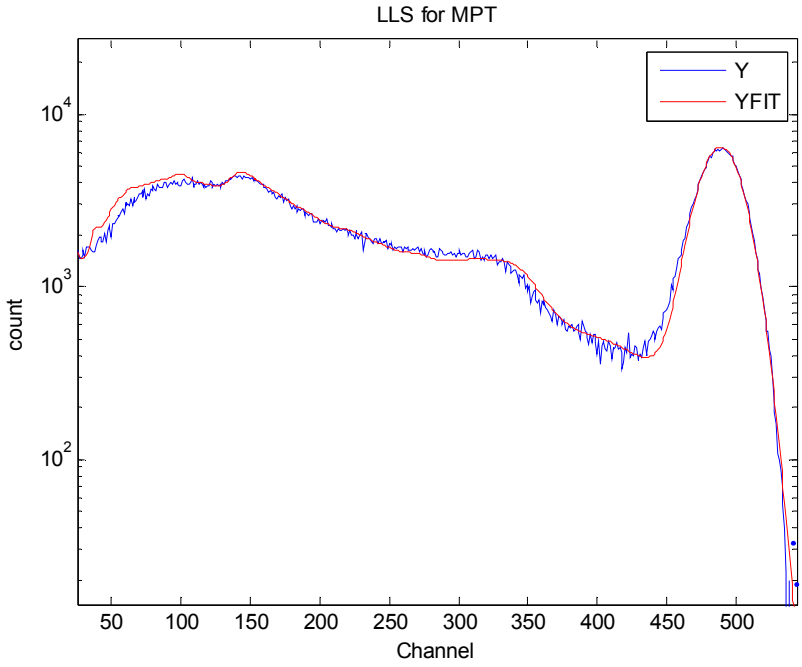

Figure 7.18 Fitting results Vs measured spectrum

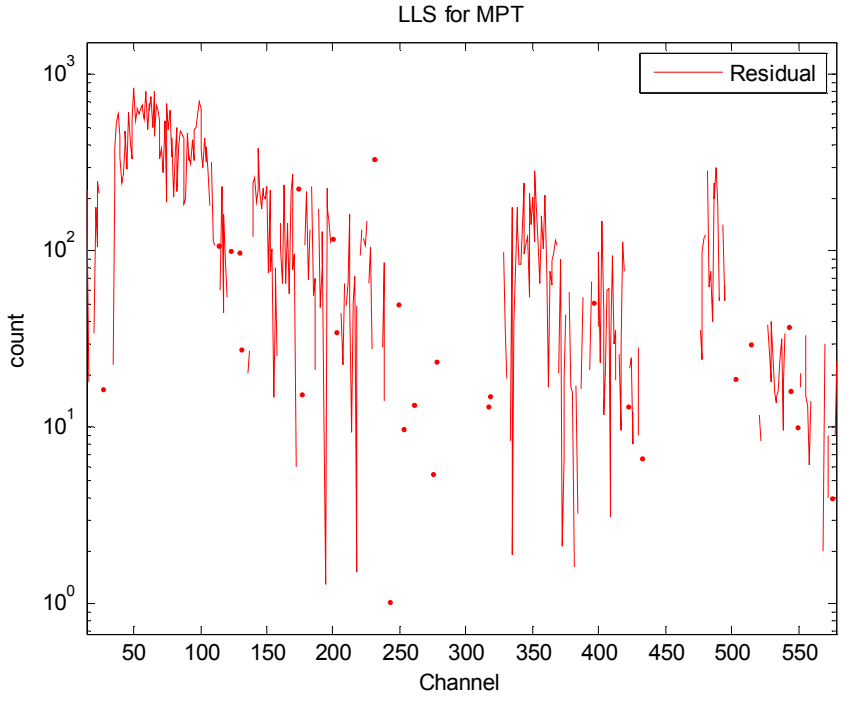

Figure 7.19 Residual plot of fitting

The overall fitting spectrum is matched the measured spectrum pretty well in whole range. The residual in the scatter peak is a little high at around 800 for a count in channel of around 4000 in 20% level. A channels weighting out is used for channel from 1 to 150, and of course for the channels in the high energy end from 531 to 2048, to reduce the errors in fitting process.

A plot of the fitting results for the experiments described in table 7.4 is shown in Figure 7.20:

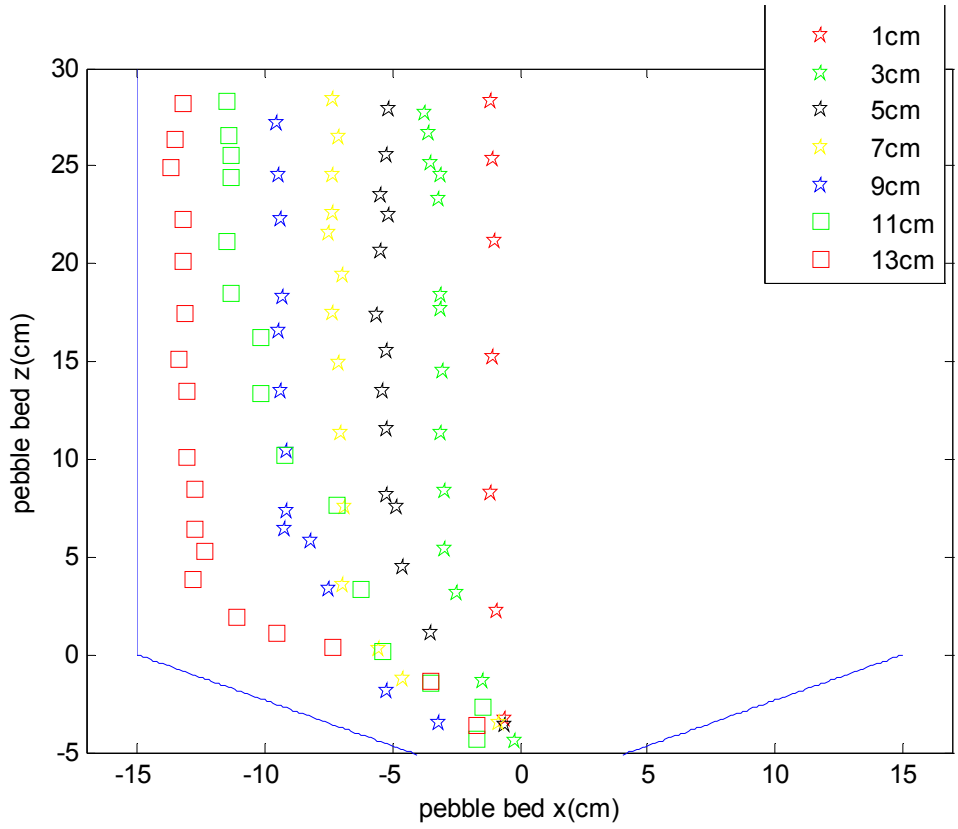

Figure 7.20 Pebble paths plot

The un-collimated detectors system shows good capability in pebble tracking in the PBR. As the measurements time for each step is long, the measurement for one tracking particle to go through the PBR may need more than two days. In this period, the spectrum may have a drift effect in the peak due to the insatiability of the electronics or temperature of the environment. The pebble tracking at around 11 cm original position observed a cross line to the 9 cm original position. This phenomenon may due to the suddenly void space available in the flow process of the pebbles.

The multiple particles tracking experiments used One Cs137 tagged pebble and one Co60 tagged pebble from the different side of the axis the results is shown in Figure 7.21:

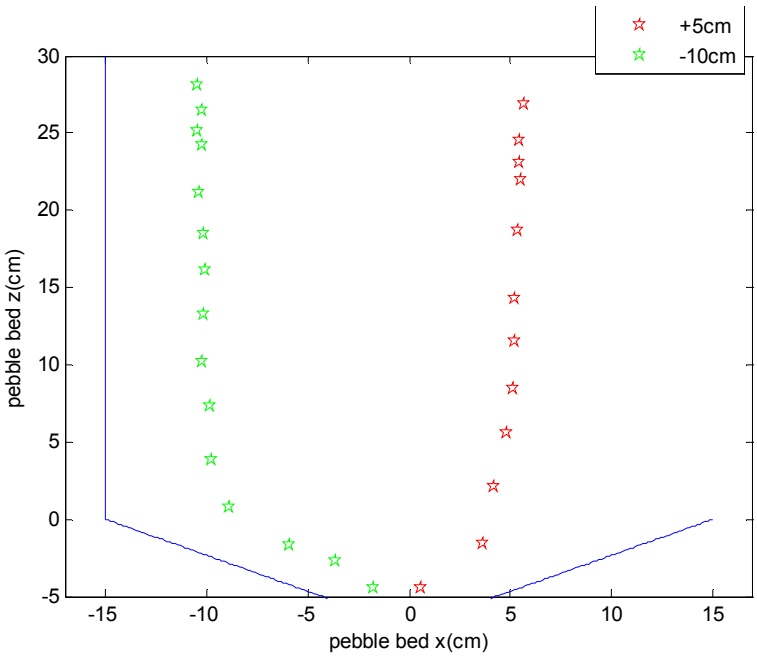

Figure 7.21 Multiple tracking with Cs137 and Co60

The first fitting for Co60 positions the code report sum areas are around 99% and the

second fitting for Cs137 have sum areas around 93%. The results show good potential for more pebbles tracking in the same time.

A comparison between the collimated detectors system and the un-collimated detectors system for around the same initial starting position of the tracking is shown in Figure 7.22 (left). In this Figure (right), the results from the Gatt's experiments with initial starting positions at 5cm and 10cm is also plotted for comparison:

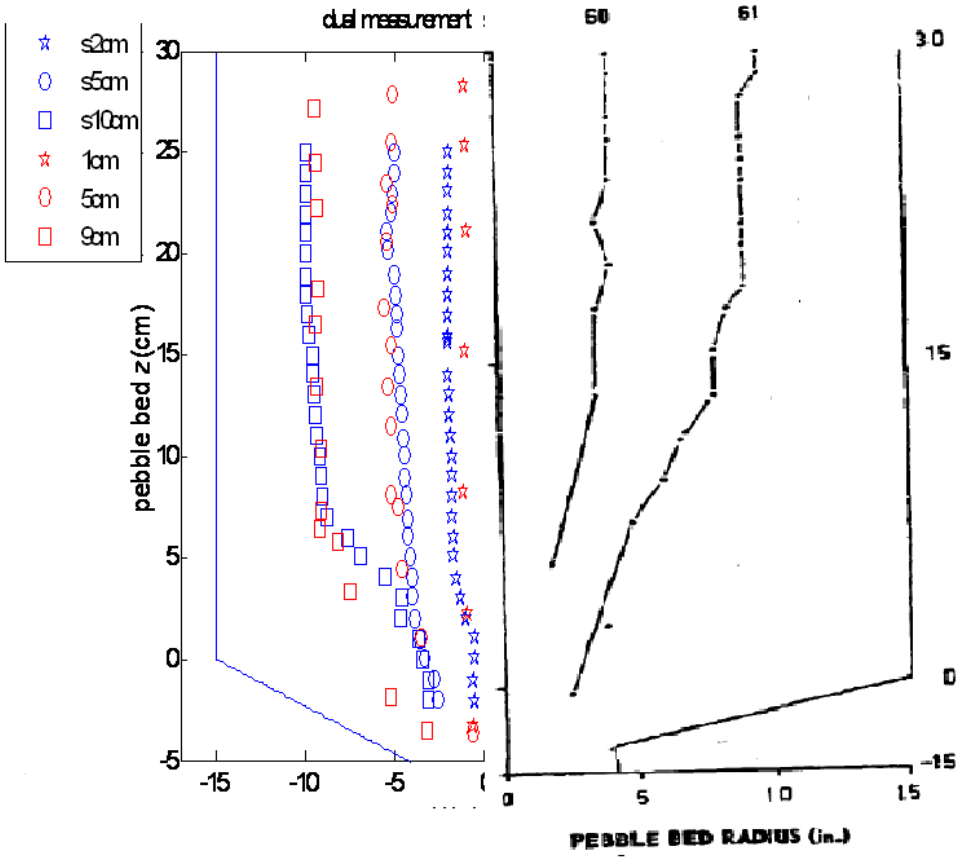

Figure 7.22 Dual measurement system comparisons (left: within the two measurement systems; right: Gatt's experimental results)

The results show good matches with each other in shape. Note the Gatt's experiment has almost the same geometry arrangement of the modeling PBR in sizes ratio in pebble to core (1:30), but double in the height from 30 to 60 in ratio.

A series measurements were repeated at initial positions around -11cm off the axis to find out the fluctuation of the pebble motions with the un-collimated detectors system. The results are shown in Figure 7.23:

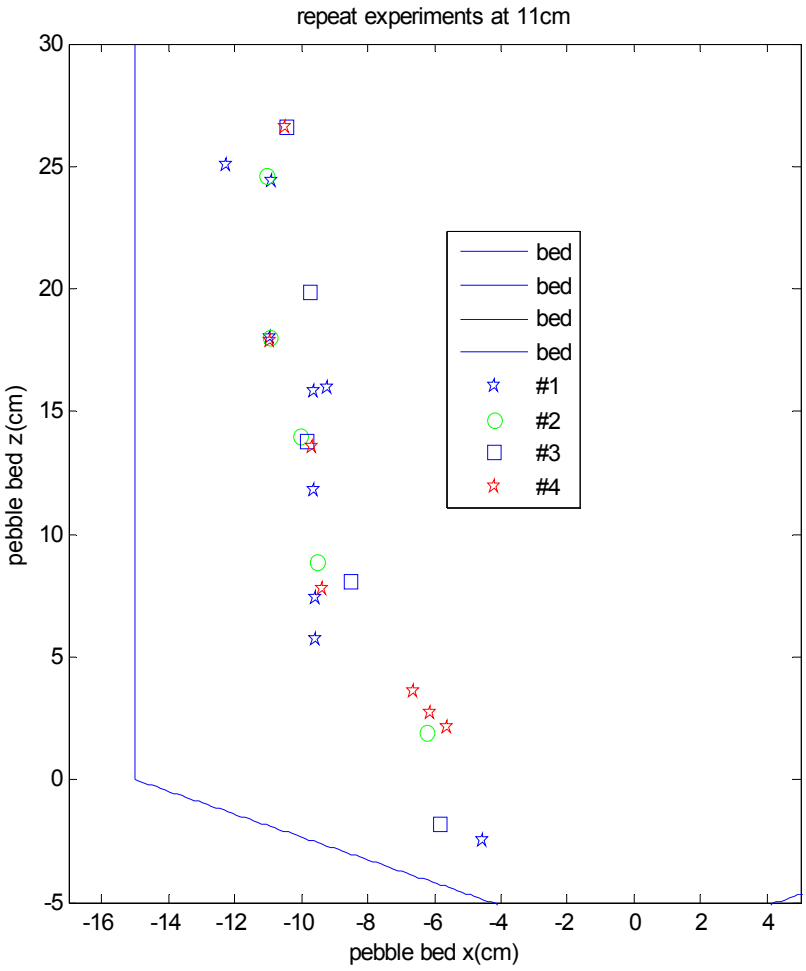

Figure 7.23 The motion fluctuation at -11cm off axis

The fluctuation of the pebble motion is getting bigger when the pebble enter the height under 5cm in the modeling PBR. But basically a constant shape is shown as well.

7.4 Summary

The un-collimated detectors system worked pretty well in tracking radioactive particles in the modeling PBR, in both single and multiple particles cases. But the results shown previously, are based on a lot of try of failures. Several things are critical in the application of this dual measurement system. Firstly, the benchmark experiments are very important both for DRF's generating code-Modified MCNP5 and the geometry of the system correction in simulation. One of them fail to be benchmarked very well will cause severe error and the tracking process will fail as well. The benchmark measurements with the collimated detectors system can be very critical from this point of view. Secondly, to hold the system as stable as possible in the measurement process is important too. For example, the detectors can loose because gravity effect on the detector. If the detectors' positions change a little bit, especial in rotation of the angle, the system can also fall into fatal errors; the measured spectra will not match the preset libraries any more. A slight rotation effect is shown in Figure 7.22:

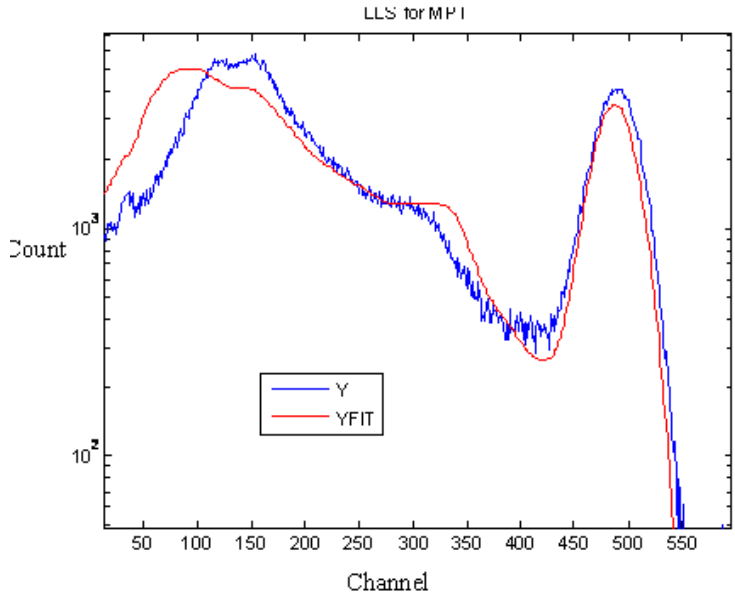

Figure 7.24 The rotation effect of the detector

And if the simulation libraries result in high statistic errors, the fitting results will look like Figure 7.25:

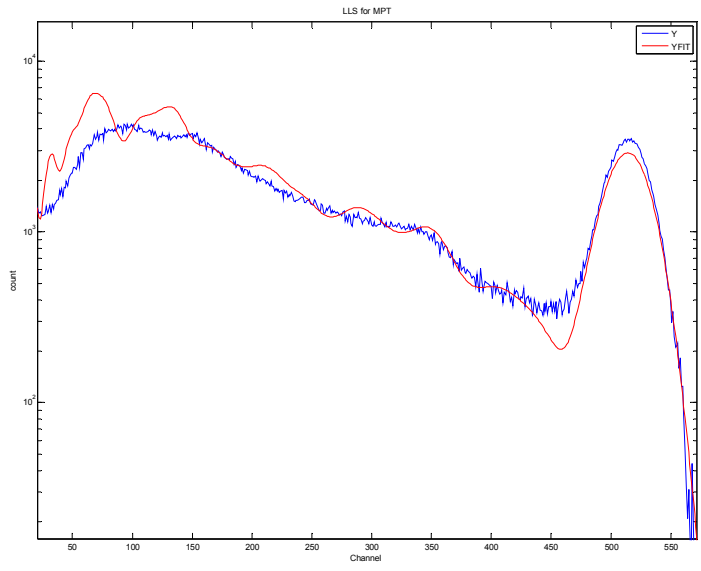

Figure 7.25 Library error effect

Thirdly, the peak drifting effect in a long period of time is also need to be taken into account in the fitting process. The most sensitive fitting error is from those parts of the spectrum that have highest counting rate: the peaks. The little drifting of the peaks can cause big errors in the fitting process.

8. RELATED CRITICAL TOPICS

8.1 The safety feature of PBR

Anxiety about nuclear safety is at a high, as Japan struggles to bring radiation emissions under control at its Fukushima nuclear plant. The plant was badly damaged by the devastating earthquake and tsunami in the northeastern Japan in March, 2011. The explosion in Fukushima triggered the explosion of the safety concerns about nuclear plant in the public and scientists as well.

The PBR power plant combines a gas-cooled core and a novel packaging of the fuel that dramatically reduces the complexity while improving safety.

When the nuclear fuel increases temperature, the rapid motion of the atoms in the fuel causes an effect known as Doppler broadening. The neutron speeds would spread into a wider range. U^{238}, which forms the bulk of the uranium in the reactor, is more sensitive to absorb fast or epithermal neutrons at higher temperatures. This reduces the number of neutrons available to cause fission, and reduces the power of the reactor. Therefore the Doppler broadening creates a negative feedback because the increasing temperature of the fuel. All reactors have reactivity feedback mechanisms, but the pebble bed reactor is designed so that this effect is very strong and doses not depend on any kind of machinery or moving parts. Because of this, the passive cooling, and because the

pebble bed reactor is designed for higher temperatures, the pebble bed reactor can passively reduce to a safe power level in an accident scenario. This is the unique safety feature of PBR comparing with the conventional light water reactors which require active safety controls.

The reactor is cooled by inert, fireproof gas. The coolant has no phase transitions, which remains as gas in the whole cooling process. Similarly, the moderator solid carbon involves no phase transition either. In the conventional reactor the coolant and moderator light water performs phase transitions between liquid and gas, which can have a steam explosion.

Thus the PBR with a scenario that supporting machinery fail, the reactor will not crack, melt, explore or spew hazardous wastes. It simply goes up to a designed “idle” temperature, and stays there. In this state, the reactor vessel radiates heat, but vessel and fuel spheres remain intact and undamaged. These safety features were tested with the German AVR reactor.

PBRs are intentionally operated above the 250 C annealing temperature of graphite, so that Wigner energy (energy stored as crystalline dislocations in the graphite) is not accumulated. This solves a problem discovered in an infamous accident, the Windscale fire.

The design and reliability of the pebbles is crucial to the reactor's simplicity and safety. It takes 380,000 to fuel a reactor of 120 MWe. The continuous refueling means that is no excess reactivity in the core. Continuous refueling also permits continuous inspection of the fuel elements. A well understanding of the pebbles motion in the black box of the core is also crucial in core design and analysis for safety.

8.2 Spectrum stripping

MCLLS method used in this dissertation is a relatively complex analytical process. The Monte Carlo simulation libraries are used to analyze the experimental spectra. As a matter of fact, the experimental spectrum is strongly depended on the intensity of the source, while the simulation one is normalized. The normalized simulation results can be interpreted into the same magnitude with the experimental ones by multiplying the source intensity. This multiplier can be found with the benchmark experiments described in section7.1. Actually, in the process of fitting this value does not have to be very accurate. But in the process of benchmarking the DRF's generating code this value is critical.

But if the libraries have a several magnitudes different from the measured spectra, the fitting process can potentially induce an unexpected error by extremely over estimate some of the libraries used in the fitting process. In the fitting process we estimate for the

Cs137 source in the time the measurement were carried out, the intensity of the source is: I=1.7E+5 photons for two hours measurement. Co60 had an intensity at around I=2.014E+6 photons for two hours measurement.

All spectra from gamma ray sources can be considered as a set of monoenergetic gamma spectra. It is possible to eliminate the large comprehensive library of all possible contributing radioactive radio nuclides providing two assumption hold true, (1) That the complex spectra may be made up of a linear summation of the monoenergetic gamma ray spectra and (2) that gamma rays of very nearly the same energy will yield interchangeable pulse height spectra (Furr, Robinson and Robins, 1968). In the intensity of the sources used in our case in PBR is compared low to have significant pulse pile up or sum effects of different sources. The monoenergetic library can be combined as nuclides library with known sources. In this case, the spectra stripping technique is valid.

For multiple radioactive particles tracking in the PBR, the measured spectra contain two or more gamma ray sources. It is necessary to use spectra stripping technique to resolve the separate contributions and use them as individual spectra. In our process, actually two kind of spectrum stripping techniques are used: (1) Strip the measured background spectra from the measured total spectra to achieve to net spectra of the sources. (2) Strip the individual spectra from the total spectra or total residual spectra. In the second one, the individual spectra are the fitting results from the libraries. The difference between these two processes is from statistics. The first seems with no any

problem, because when strip the spectra channel by channel, as both background and total spectra can be considered approximately two Poisson distributions (Knoll, 2000) in each channel, where the predicted standard deviation is just the square root of the count number in each channel:

$$\delta = \sqrt{N} \tag{8.1}$$

The standard deviation of the net spectra in channel after the stripping will be:

$$\delta_n = \sqrt{T + G} \tag{8.2}$$

where T is the Total spectra count in the channel, G is the backGround spectra count in the channel.

The second spectra stripping process induce a Poisson distribution and the fitting spectra with propagated errors from the simulation statistic error and fitting errors. In this process, we assume that the residual total spectra are still Poisson distribution in each channel after the stripping. The standard deviation of the residual total spectra in channel will be estimated by:

$$\sigma = \sqrt{\delta_T^2 + \delta_s^2 + \delta_f^2} \tag{8.3}$$

where δ_T^2 is from the total spectra before the stripping; δ_s^2 is from the Simulation statistics errors; and δ_f^2 is from the Fitting errors.

Equation 8.3 indicates that the errors propagate must faster then the Equation 8.2 does. Treatments to reduce the errors in all three aspects in the Eq 8.3 must be concerned for accuracy when the tracking particles number goes up.

8.3 Dead Time

To almost all detector systems, there will be a minimum amount of time that must separate two events in order that they can be recognized be the detector systems as two separate pulses. The limiting time can come from the detector capability, and may arise in the associated electronics. This minimum limit of time is usually called dead time of the counting system. Because of the random nature of the radioactive decay of nuclides sources, there is always some probability that a true event will be lost because it occurs too quickly followed a preceding event.

In the un-collimated detectors system there are two things will cause severe dead time losses. One is the intensity of the sources, high intensity of the sources can have high counting rate which can short the measuring time and speed the tracking process and reduce the statistics error in the spectra. But in the same time, too high intensity sources

can result in a very high dead time measurement. Another is the amplifier magnitude, too high magnitude of the amplifier can also result in a high dead time losses.

In our measurements, for the background the dead time to real time ratio is around 1.2% and for total spectra the ratio is around 1.3%.

8.4 Peak analysis by PEAKSI

When the DRF's generator developed from MCNP5, a modification of the NaI scintillation efficiency nonlinearity was added in the code. The simulation results always have a shift to the high energy end with the peaks:

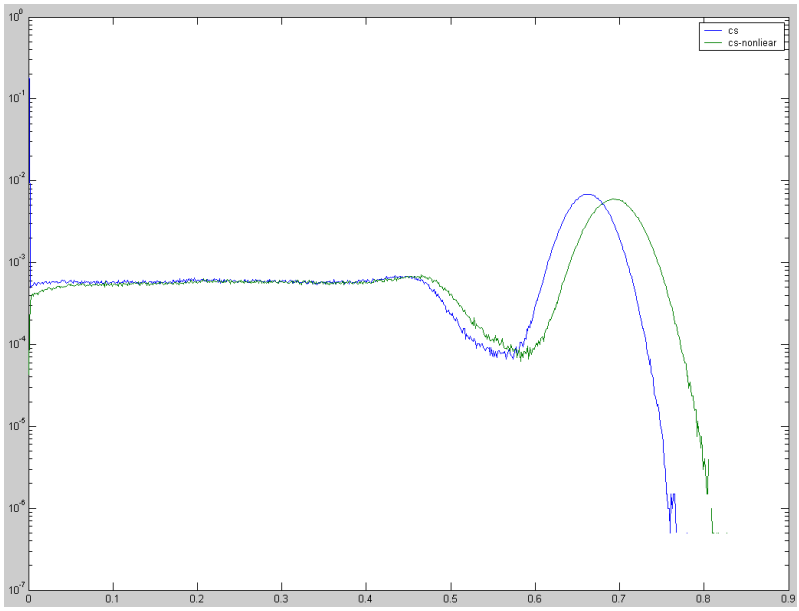

Figure 8.1 Peak behaviors with nonlinearity with Cs137

where the modified MCNP5 results (green) shifts to the right of the original MCNP5 (blue) results, according to the relationship shown in Figure 6.2, it is predicted. In order to calibrate the measured spectra with the simulated spectra, first of all, find the exact peaks channel positions with known energy is critical.

One simple method is to zoom and search the maximum count value among the data of the peak region. But this method is not always accurate, especially when the measure statistics of the spectra is poor. Another method is adopted from PEASI, which is developed by CEAR and used to obtain a least squares fit with experimental data for either a single resolved Gaussian peak model or two unresolved Gaussian peaks model plus a constant, linear, or quadratic background. These two approaches results can have different results which are shown in Figure 8.2:

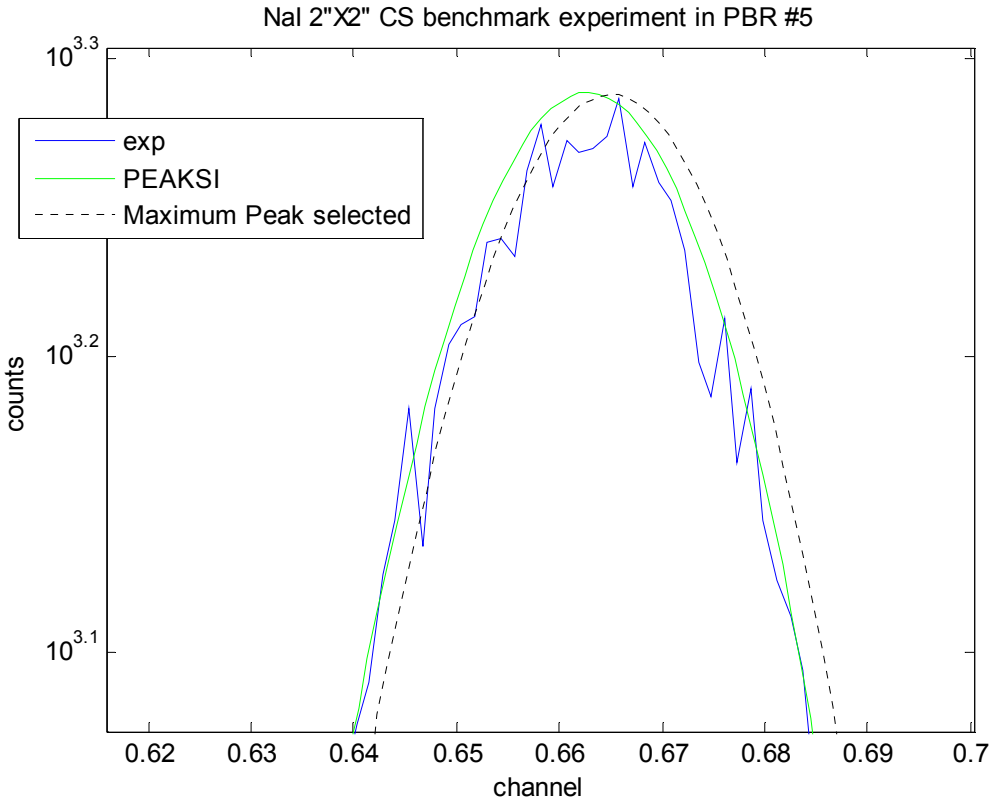

Figure 8.2 PEAKSI and maximum point for peak channel with Cs137

After accurately define the peak channels of the spectra from the experiments, each detector due to slightly different in amplifier magnifications, has different peak channels, but they are all around 500 channel for 0.662 (Cs137) and 1.332 around (1000) by preset. These peak channels will be used in the later library generation process to set the simulation peak into the experimental channels, respectively.

8.5 Variance reduction techniques

In the MCLLS methods, mentioned in the Eq 8.3, there are three kinds of errors have to be concerned: (1) the measurement errors; (2) the simulation errors; and (3) the fitting errors. For the second one, in order to make a Monte Carlo Simulation statistically efficient, i.e. to achieve greater precision and smaller confidence intervals for the output spectra, variance reduction techniques can be used. It is a procedure used to increase the counting statistics in library spectra for a give number of history.

As the interested area in the PBR is large comparing with the library step in 1cm. With a cluster for 41 nodes and speed up features in the modified code, to generate the library for the six detectors in all area is still very time consuming. There are several techniques used for variance reduction purpose:

8.5.1 Weight window

The weight window is a method used to provide an alternative means to importance and energy splitting for specifying space and energy importance function. The weight windows provide (1) an importance function in pace and time or space and energy; (2) control particle weights (MCNP5 manual, 2003). The independence of the important mesh structure and the physical geometry results in simplicity and accuracy.

When the modeling PBR go bigger and more closely in size to the real PBRs weight

windows will be more critical in variance reduction. It will provide an easy way to generate global distribution information: the regular particle flux into each mesh, contribution flux into each mesh, and the adjoin flux into each mesh. Especially, the contribution current distribution shows how particles from the source travel inside medium and reach the detector, and provides the physical insight analysis.

8.5.2 Energy cut off

The modified MCNP5 must use a mode of "P E". It means that the electron process transport is required, that is because we use the electron cross modification for the flat continua adjustment. Energy cut offs for photon and electron are both default as 1Kev. Increase the cut off energy of both of photon or electron can save computing time per history since it is unnecessary to track the photon or electron below certain energy without losing accuracy significantly. The effects are shown in Figure 8.3:

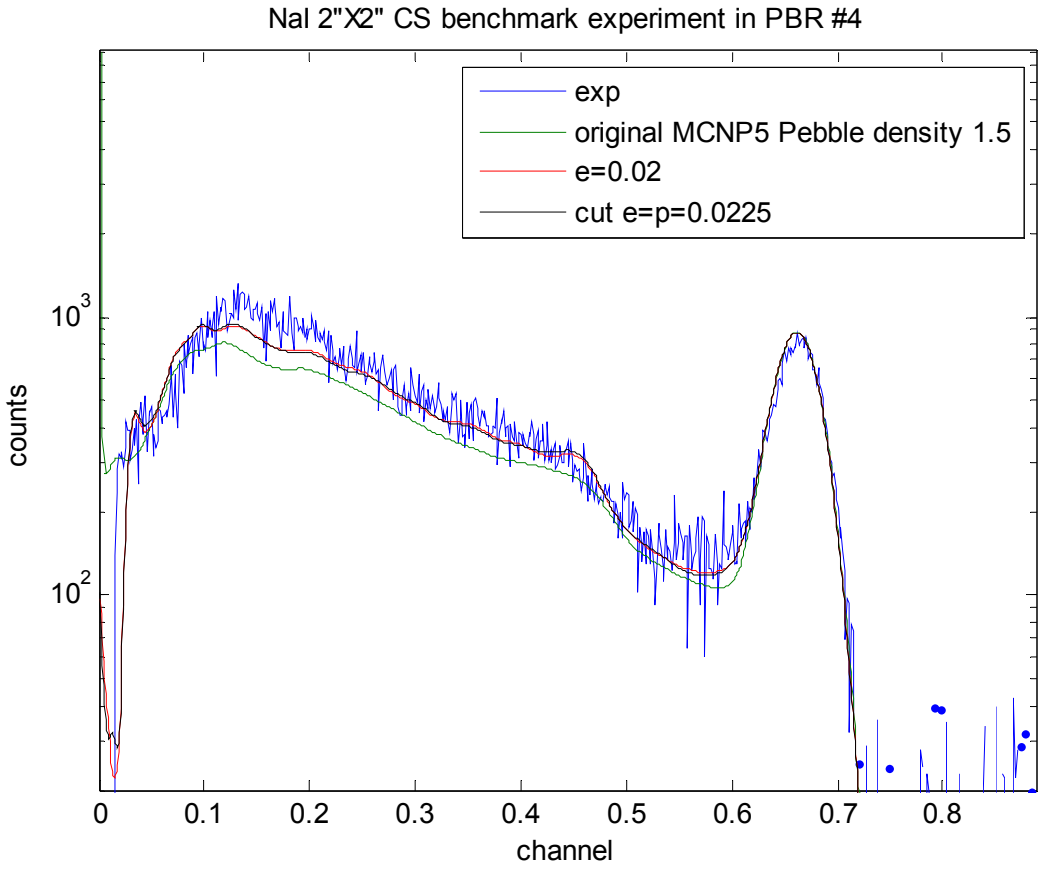

Figure 8.3 The Energy cut off effects Cs137 in detector #4

When the energy cut off of photon and electron reach 0.0225 Mev the computing time will save around 15%.

8.5.3 Correlated sampling

Consider the task of computing the integral

$$\Delta I = I_1 - I_2, \tag{8.4}$$

where:

$$I_1 = \int dx g_1(x) f_1(x), \tag{8.5}$$

And

$$I_2 = \int dx g_2(x) f_2(x). \tag{8.6}$$

The procedure for correlated sampling can be described as follows:

Step (1) Sample random configurations x_j by using the sampling function $f_1(x)$ and evaluate the function g_1 for each of these configurations to obtain $g_1(x_j)$. In addition, sample random configurations y_j by using the sampling function $f_2(y)$ and evaluate the function g_2 for each of these configurations to obtain $g_2(y_j)$. Step (2) Estimate ΔI according to

$$\Delta I = \frac{1}{N}\sum_{j=1}^{N} g_1(x_j) - g_2(y_j).$$

(8.7)

The variance of ΔI is

$$\sigma^2 = \frac{1}{N}\sum_{j=1}^{N}\left(g_1(x_j) - g_2(y_j) - (I_1 - I_2)\right)^2,$$

(8.8)

$$\sigma^2 = \frac{1}{N}\sum_{j=1}^{N}\left(g_1(x_j) - I_1\right)^2 + \frac{1}{N}\sum_{j=1}^{N}\left(g_2(y_j) - I_1\right)^2 - 2\frac{1}{N}\sum_{j=1}^{N}\left(g_1(x_j) - I_1\right)\left(g_2(y_j) - I_2\right),$$

(8.9)

where the first two terms on the right hand side of Eq. above are the variances δ_1^2 and δ_2^2 of the random variables g_1 and g_2, respectively, and the third term is the covariance cov(g1,g2) of the two random variables. Note that when x_j and y_j are statistically independent then the cov(g1,g2) =0 and

$$\sigma^2 = \sigma_1^2 + \sigma_2^2.$$

(8.10)

However, if the random variables are positively correlated then the cov(g1, g2)>0 and the variance σ^2 is reduced.

The key to reduce the variance is thus to insure positive correlation between g_1 and g_2. This could be achieved by using the same sequence of random numbers for sampling both sets of random configurations x_j and y_j.

The correlated sampling technique is a partially deterministic method in Monte Carlo simulation application. It is accomplished by making the normal simulation on a reference sample and then forcing the same particle path in a number of correlated samples that contain test samples with different weight fractions and densities of the component, when the purpose is study the known components in the samples (Gardner et al., 1989). Appropriate weight adjusts are made for the distance to next collision site and the collision element. This implies that these correlated samples must contain the same elements in the reference sample. If not, user must include very small pseudo amount of the element or elements in question. The additional computation time required to simulated comparison samples is pretty small, typically in the order of 20% for twenty correlated samples (Lee et al., 2001)

The correlated sampling technique in case of particles tracking in PBR is a little different. The position is used as reference for correlated position close to it. All the compositions and densities of the materials in the simulation are the same, the only parameter changes is the position of one coordinate one time. The position is the

correlating factor other than the weight fractions and densities of the components.

8.6 Computer Cluster

Even including all the variance reduction techniques mentioned above, as the libraries in un-collimated detectors system for MCLLS method is huge about 4392 with triangle element scenario for six detectors cover the whole interested area. The Modeling PBR in our lab is relatively small, when used graphite pebbles with higher density and larger scale, more libraries may be required and each longer computing time due to density effect for the same statistics standard deviation.

A computer cluster with paralleled processes is set in CEAR of NCSU. The cluster has 144 processes with a network file system. The MCNP5 runs can be submitted with remote computer for sequel runs process. It is faster than the normal PC. For case of Heath experiments With Cs137 (0.662 Mev) 2 millions histories a dual-cores PC takes 27 minutes and 52 seconds, in the cluster it is about 1 minute and 56 seconds, with a factor about 14.4. This factor is affected by the complexity of the problem and the number of the histories.

9. CONCLUSIONS AND DISCUSSION

In this dissertation, a feasible scaled down modeling PBR was designed and used to

mimic the pebble motions in the PBR. Both collimated and un-collimated detectors system were developed and tested working properly in the modeling PBR. Until now, the very high temperature pebble bed reactors were run and tested in a mode of black box. These two methods are used in the same system as one benchmarks another, which is the first time closest to the real PBR working mode. We provided data of the pebbles motion in a modeling PBR, and our target is to use this system to provide more data in a scaled down modeling PBR more closely designed like the real PBR.

For the un-collimated detectors system, the modified MCNP5 code for gamma-ray DRF's generating has been proved to have much better accuracy and much faster simulation speed capability. This code can be easily adapted into other scintillation detectors with all sizes. Actually, we had applied it for BGO detector and box-shape NaI detectors. The improvement of accuracy and speed just make some complicate system inverse analysis with MCLLS method possible. For case of the detector response is very sensitive to the unknown parameters, the detail simulations of the problem can be achieved.

The dual measurement methods in the system have their own advantages and disadvantages. The collimated detectors system is slow and can track only one particle per time, but with a straight forward arrangement and relatively simple analysis process. The un-collimated detectors system can do off line fast analysis and multiple particles

tracking, which is important for pebbles interactions study, but the system arrangement is complicate and a lot of measurement and analysis techniques are required.

The accuracy of the system is highly depended on the benchmark experiments. And there are two levels of benchmark experiments. One is the benchmark for the accuracy of the code. Basing on the satisfied accuracy of the code in the previous benchmark results the benchmark for the accuracy of the geometry surrounding materials and the accurate benchmark position is critical in the later application of the system accuracy.

10. FUTURE WORKS

As the pebble motion in the PBR is in a statistical nature, the motion flow should be measured multiple times for confidently understanding the pebble flow. More experiments will be used for uncertainty study of the pebble motion, and especially in the

possible dead zones in the PBR.

More radioactive tracers will be used in the same time for tracking in the PBR to study the possible correlation motions and bulks motion of the pebbles in the PBR. And this multiple tracking method can be used in other non-invasive system in the industry. If not for the position of the tracers, it can be used to study other parameters in interest.

A proposed future work with this dual measurement system was submitted to the 2011 Nuclear Energy University Programs (NEUP) for a further research in PBR. We proposed to use this system in a condition closer to the real PBR in materials, sizes and operating temperature, which will be cooperated with INL. In this proposal graphite pebbles will be used, a size of 1-3 meters in diameter core will be used as a modeling PBR, and the operating temperature in the core can be up to hundreds degrees to find out the temperature effect of the pebble motion. The major process of the future in this program is: 1) design the new scaled PBR based on maximum capability of the dual measurement system; 2) benchmark experiments with the new scaled modeling PBR; 3) codes may need to be developed for exactly used in this case and new Monte Carlo simulations should be required; 4) new analysis tool may need to be upgraded in this more complicated situation from the one we already have in this dissertation.

If with sufficient fund, we can go 3-D tracking if it is necessary with more detectors

and more complicate inverse analysis process. Basically, all the techniques required for the purpose of tracking the radioactive tracers in a PBR we already have. The next step is to used them more efficiently and exactly to the points that important.

11. References

AGE (1990), "AVR- Experimental High Temperature Reactor:21 Years of Successful Operation for a Future Energy Technology", the society for Energy Technologies, Dusseldorf.

Ashraf Shehata, H. C. and Robin P. Gardner (2006), "A New Method for Single

Radioactive Particle", 5th World Congress on Industrial Process Tomography, Bergen, Norway.

Ashraf, Shehata, H, C. (2005), "A New Method for Single Radioactive Particle," Ph.D thesis 2005, Department of Nuclear Engineering, NCSU.

Berger, M.J., Hubbell, J.H, Seltzer, S.M., Coursey, J.S. and Zucker, D.S. (1999), XCOM: Photon Cross Section Database (Version 1.2), National Institute of Standards and Technology, Gaithersburg, MD.

Berger, M.J. and S.M. Seltzer (1972), "Response Functions for Sodium Iodide Scintillation Detectors," Nucl. Instn. Meth., 104, pp.3317-3322.

BOTZEM, W., J.WÖRNER (NUKEM Nuklear GmbH, Alzenau, Germany) (2001-06-14).

Carlsmith, R. S. (1962), "Fuel cycles for an 800 Mw(t) pebble-bed reactor" ORNL-TM-314, Aug. 8, 1962.

Collinson, A.J.L. And R. Hill (1963). "The Fluorescent Response of NaI(TI) and CsI(TI) to x Rays and γrays," Proc. Phys. Soc. 81, pp.883-892.

Deutsh, G. P. (1967), "Investigation of Flow Mechanism of Balls in a Container," Departmental Report No. 14 Department of Civil Engineering, Uni. Of Melboume.

Edwards, M (1965) "Experimental work on effect on transit number of variations in pebble extraction rate". AAEC unpublished report

Furr, A.K., E. L. Robinson and C. H. Robins (1968). "A spectrum stripping technique for qualitative activation analysis using monoenergetic gamma spectra", Nul. Instr. And Meth. 63 (1968) pp.205-209.

Gardner, R.P. and Ely, R. L., "Radioisotope Measurement Applications in Engineering", Reinhold Publishing Corporation, New York, 1967.

Gardner, R.P. and A. Sood (2004), "A Monte Carlo Simulation approach for generating NaI detector response functions (DRF's) that accounts for nonlinearity and variable flat continua," Nucl. Instr. Meth. Phys. Res. Section B: Beam interact. Mater. Atoms, 213:87-99.

Gardner, R.P, F. Li and W. Guo (2006), " Use of the Monte Carlo Simulation code CEARXRF for the EDXRF Inverse Problem", JCPDS International Centre of Diff. dada

2006 ISSN 1097-0002.

Gardner, R. P., M. W. Mickael, and K. verghese, (1989). “Complete composition and density correlated sampling in the specific purpose Mont Carlo codes McPNL and McDNL for simulating Pulse Neutron porosity logging Tools”, Nucl., Geo., Vol. 3, No. 3, pp.157-165.

Gatt, F. C. (1970, 1972, 1973), “Flow of Spheres and Near Spheres in Cylindrical Vessels Part II – Pebble Transit in Circulated Random Packing.

Han, Xiaogang and Robin P. Gardner (2006), “CEARCPG: A Monte Carlo Simulation for Normal and Coincidence Prompt Gamma-ray Neutron Activation Analysis (PGNAA). Transactions of the ANS, Vol. 95, pp.512-522, 2006.

Heath, R. L. (1964), “Scintillation Spectrometry Gamma-Ray Spectrum Catalogue”, IDO-16880-1, AEC and Development Report, Physics, TID-4500

He¸T., R. P. Gardner, and K. Verghese (1993), “The Monte Carlo Library Squares Approach for Energy Dispersive X-ray Fluorescence Analysis”, Applied Radiation and Isotopes, Vol. 44, No. 10/11, pp.1381-1388.

IAEA (2000), International Atomic Energy Agency,

Kadak, Andrew C. (2004), "A Future for Nuclear Energy- Pebble Bed Reactors" Apr. 25.

Kadak, Andrew C. and Martin Z. Bazant (2004), "Pebble flow experiments for Pebble Bed Reactors," 2nd International Topical meeting on High Temperature Reactor Technology," Sept. 22-24,2004.

Kaiser, W.C. S.I. Baker, A.J. MacKay, and I.S. Sherman (1962). "Response of NaI(TI) to X-rays and Low Energy Gamma Rays", IRE Trans. Nucl. Sci. NS-9, No. 3, pp. 22-27.

Knoll, Glenn F. (2000), Radiation Detection and Measurement. Third Edition, 2000 John Wiley & Sons, Inc.

Koster, A, Matzie, R., and Matner, D. (2004), "Pebble-bed modular reactor: a generation IV high-temperature gas-cooled reactor", Proc. Instn. Mech. Engrs. Vol.218 Part A: J. Power and Energy.

Larachi, F., Jamal Chaouki and Gregory Kennedy (1995), "3-D Mapping of Solid Flow Field in Multiphase Reactors with RPT," AICHE, Feb., 1995 Vol. 41, No.2

Lee, S.H., R.P. Gardner, and A.C. Todd. (2001), "Preliminary studies on combining the K and L XRF methods for in vivo bone lead measurement", Applied Radiation and Isotopes, 54, pp.893-904.

Leesment, H. And L. P. Stephenson (1964), "Design and Preliminary Results of PBR Ball Flow Rig 1. (AAEC)

Li, Fusheng, (2008), "Monte Carlo Simulation of energy-dispersive x-ray fluorescence and application". Ph.D thesis, 2008, Department of Nuclear Engineering, NCSU.

MCNP5 manual Vols. I, II and III, LA-UR-04-2506, Los Alamos National Lab

Peplow, D.E., R.P. Gardner, and K. Verghese (1994), "Sodium Iodide Detector Response Function Using Simplified Monte Carlo Simulation and Principal Components:, Nuclear Geophysics, Vol. 8, No. 3, pp.430-438.

Roy, Shantanu, F. Larahi, M.H. Al-Dahhan, and M.P. Dudukovic (2002), "Optimal Design of Radioactive Particle Tracking Experiments for Flow Mapping in Opaque Multiphase Reactors," Applied Radiation and Isotopes 56 (2002) pp.485-503.

Shyu, C.m., R.P. Gadner, and K. Verghese (1993), "Development of the Monte Carlo Library Least Squares Method of the Analysis for Neutron Capture Prompt Gamma-ray

Analyzers", Nuclear Geophysics, Vol. 7, No.2, pp.241-268.

Szomanski, E. and G. A. Tingate (1967), "Investigation of the flow and Structure of Spherical Particles in Packed Bed," Australian Chemical Engineering, 8, N8, Aug. 1967, pp.21-27.

Sun, Yuliang (2007), "Status of the HTR Program in China," IAEA TWG-GCR, 15-17 Jan. VIC Vienna.

Takizuka, Takakazu (2005), "Reactor Technology Development under the HTTR Project," Progress in Nuclear Energy, Vol.47, No.1-4, pp.283-291.

Wang, Zhijian, Daniel P. Speaker and Robin P. Gardner (2008), "Two Monte Carlo Approaches for Generation of Scintillation Detector Response Functions (DRF's)," Transaction of ANS, Vol.198, pp.585-586,2008.